1-1-2012

Multifunctional bioreducible nanoparticles for gene therapy

Jing Li
Wayne State University,

MULTIFUNCTIONAL BIOREDUCIBLE NANOPARTICLES FOR GENE THERAPY

by

JING LI

DISSERTATION

Submitted to the Graduate School

of Wayne State University,

Detroit, Michigan

in partial fulfillment of the requirements

for the degree of

DOCTOR OF PHILOSOPHY

2012

MAJOR: PHARMACEUTICAL SCIENCES

Approved by:

_____

Advisor Date

_____

_____

_____

ACKNOWLEDGEMENTS

I would like to express my most profound and sincere thanks to my advisor and mentor, Prof. David Oupický for all his guidance, encouragement, patience and support during my incredible five-year journey as his PhD student. His unlimited passion and dedication to science, impressive talent and innovation have inspired me since day one and I couldn't have asked for a better PhD mentor.

I would also like to thank my committee members, Profs. Steve Firestine, Joshua Reineke and Jing Li (Karmanos Cancer Institute and Department of Pharmacology, School of Medicine) for their professional suggestions and continuous guidance.

My sincere gratitude also goes to Prof. Hirata and Ms. Aiko Hirata for all the kind help with the molecular biology-related work. I thank Dr. Chunying Li from the Department of Biochemistry and Molecular Biology, School of Medicine and his group members for their advice and help with the CXCR4-related studies. I thank all my former and current labmates, especially Dr. Devika S. Manickam, whose hard work and continuous kind help have always encouraged me. Special thank goes to Yu Zhu, who has always been supportive in and out of the lab. I thank DLAR for all the help and training with the animal studies. I thank Dr. Lisa Polin from the Karmanos Cancer Institute for the systematic training with establishing murine tumor models.

I thank the Department of Pharmaceutical Sciences, Wayne State University for this great opportunity and learning experience in the wonderful

graduate program.

Last but not least, I would like to thank my family for their unconditional love and support, and all my friends for their company and encouragement along the way.

TABLE OF CONTENTS

LIST OF TABLES

LIST OF FIGURES

LIST OF SCHEMES

CHAPTER 1

INTRODUCTION

Please note that part of this chapter was taken from a book chapter titled "Intracellular Delivery Considerations for RNAi Therapeutics" to be published in *RNA Interference from Biology to Therapeutics*, K. A. Howard, Ed., Springer, New York, 2012 (in press). The authors of the book chapter include Yu Zhu, Prof. David Oupicky, and me. All the authors agreed with including their work in this dissertation.

1.1 Gene Therapy

Gene therapy is the introduction of genetic materials into an individual's cells and tissues to treat or prevent a disease. Gene therapy was first regarded as best-suited for treating inherited disorders caused by single gene defects such as cystic fibrosis. However, during the past three decades, the definition and scope of gene therapy evolved to include diseases caused by multiple gene mutations such as cancer, immunodeficiencies, or Parkinson's disease. Common strategies for gene therapy include (i) replacing a gene that causes the disease with a healthy, functional copy; (ii) silencing a mutated gene or knocking-down an overexpressed gene; (iii) introducing a new therapeutic gene for treating the disease (Stoff-Khalili, Dall et al. 2006).

Viral vectors and synthetic vectors are two major classes of delivery systems used for gene therapy. Viral vectors utilize the virus infection pathway to

introduce their genetic material into the host cells as part of their replication cycle. The viral genetic material is usually engineered by deleting the coding regions of the viral genome, replacing them with therapeutic genes, and leaving sequences required for virus packaging and integration. Viral vectors exhibit advantages of high transfection efficiency and capability to transduce non-dividing cells, however, the arising immunogenicity and tumorigenicity concerns make non-viral gene delivery vectors preferred alternative. Despite all the efforts devoted to the design and development of non-viral vectors their transfection efficiency remains low and not comparable with viral vectors. As a result, only a small number of non-viral products are mature enough for clinical trials, compared with the large number of clinical trials in the past 20 years that utilize viral vectors.

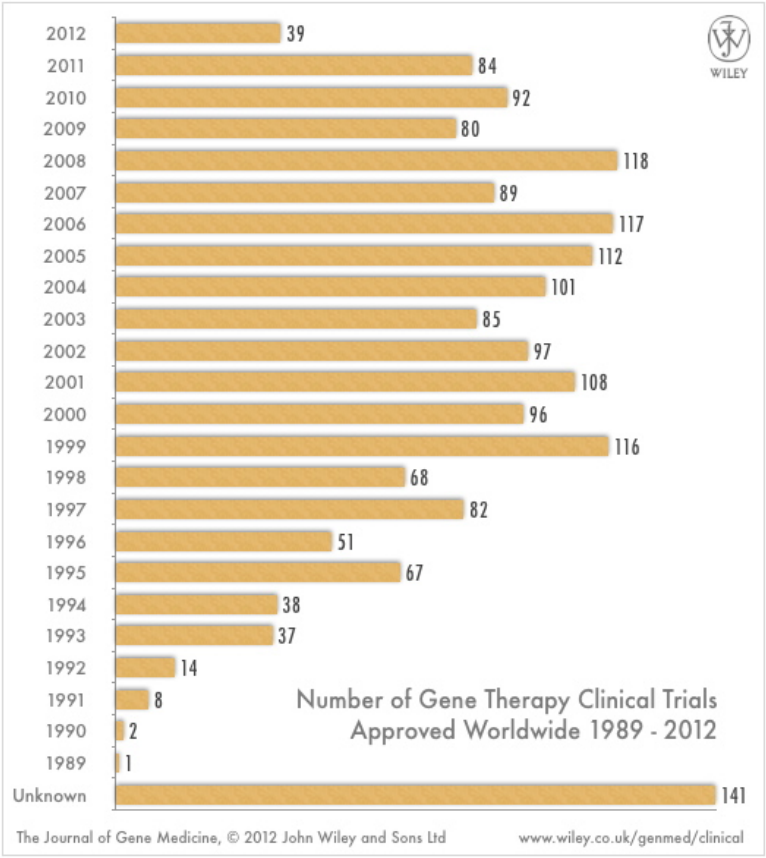

Figure 1. Number of gene therapy clinical trials approved worldwide from 1989 to 2012. (Source: The Journal of Gene Medicine)

Ever since the approval of the first human gene therapy clinical trial for treating severe combined immunodeficiency (SCID) in 1990 (Blaese, Culver et al. 1995), the total number of clinical trials for gene therapy worldwide has increased rapidly (Figure 1). Impressive progress has been made during the past years, including the first gene therapy drug entering the market in China. However, during this period, there were also times when incidents during clinical trials set gene therapy field back because of the reported serious adverse effects.

The overview of gene therapy clinical trials since 1989 compiled by the Journal of Gene Medicine reveals some interesting facts about the gene therapy

field worldwide (Figure 2). Concerning the indications addressed by the clinical trials throughout the years, the majority of the trials are aimed at treating cancer (64.4%), followed by monogenic diseases (8.7%) and cardiovascular diseases (8.4%). Among the hundreds of different genes that have been introduced into humans during gene therapy clinical trials, around 60% of the genes are related to cancer treatment. Although non-viral vectors have become more popular in the area of basic research, viral vectors continue to dominate the clinical trials so far. The interest in using naked DNA as the simplest non-viral vector has increased to 18.3%, followed by the second most popular non-viral vectors, cationic lipids, at 5.9%. The vast majority of gene therapy clinical trials are still in phase I or II (a total of 95.3%) and only 0.1% has ever moved to phase IV. The number of countries that have participated in performing gene therapy clinical trials has increased to 31 from 28 in 2007. The USA still accounts for most of the trials (63.7%) with a slight but continuous drop compared with 67% in 2004 and 64.2% in 2007.

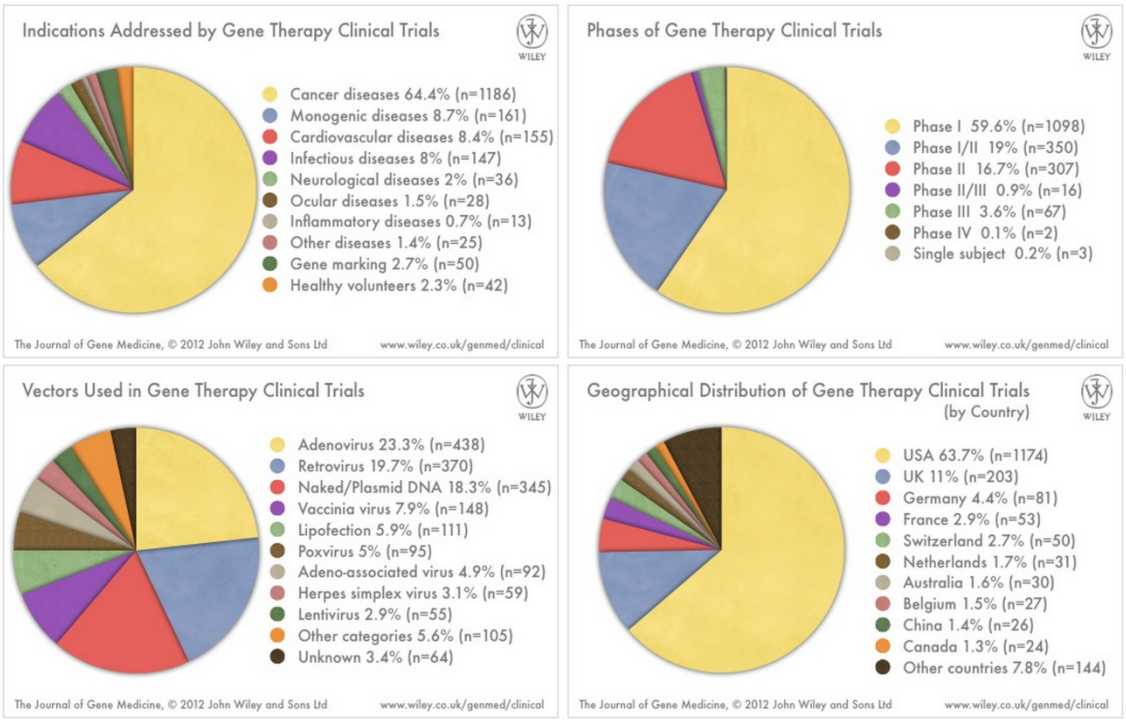

Figure 2. Gene Therapy clinical trials categorized based on disease indication, vector used, clinical trial phase, and geographical distribution by country to 2012. (Source: The Journal of Gene therapy)

Concerns from the researchers as well as the public regarding safety and potential side effects of gene therapy procedures using genetically engineered viruses have never been stopped (Edelstein, Abedi et al. 2007). On September 17, 1999, the first major adverse incident of gene therapy occurred (Raper, Chirmule et al. 2003), which was widely viewed as a major setback of the gene therapy field. 18-year-old Jesse Gelsinger, who was a patient with ornithine transcarbamylase (OTC) deficiency and participated in a clinical trial of adenovirus-based vector, died due to devastating and unexpected immune response to the virus. In January 2000, the US Food and Drug Administration (FDA) put a hold on the trial and several other related trials were also stopped. The final judgment in the Gelsinger case in February 2005 led to $517,000

settlement. FDA also adjusted their research restrictions and guidelines for gene therapy clinical trials, including prolonged observation time for delayed adverse effects. Concerns regarding safety of using retrovirus have been raised after a number of major adverse events in several clinical trials for treating X-linked severe combined immune deficiency (X-SCID) and chronic granulomatous disease (CGD) (Gansbacher 2002; Check 2003; Gansbacher 2003; Kohn and Gansbacher 2003; 2006) and the negative attitude towards virus-based gene therapy from the press cover and the public have dampened the enthusiasm of the field.

Despite the setbacks, numerous promising pre-clinical studies and a large number of successful cases of human gene therapy have shown the great potential of the field, especially for cancer gene therapy and for treating Parkinson's disease (Morgan, Dudley et al. 2006; Edelstein, Abedi et al. 2007). Although there are no current gene therapy products in the United States, China has pushed the approval and marketing of the first gene therapy drug worldwide. Gendicine™ is an adenoviral vector containing recombinant human p53 tumor suppressor gene used as a local injection in the treatment of the head and neck squamous cell carcinoma (HNSCC). The drug was developed by SiBiono GeneTech Co. of Shenzhen and was approved for clinical use by the Chinese State Food and Drug Administration (SFDA) in the fall 2003 and became available on the market in the spring 2004. However, the approval of the drug was achieved without the standard phase III trial data and the quality, safety as well as the efficacy of the treatment have been questioned by several research

groups (Edelstein, Abedi et al. 2007). Despite the issues mentioned above, increasing number cancer patients from around the world has traveled to China and been treated with Gendicine. One can hope that the increasing experience and collected data will be made public to diffuse existing concerns with the treatment.

1.2 Nucleic Acids for Gene Therapy

One of the major advantages of using non-viral gene delivery vectors is the versatility of using different type of therapeutic nucleic acids and the ease of formulation development. This section will focus on different types of nucleic acids that could be used in gene therapy and their current applications.

1.2.1 Plasmid DNA (pDNA)

pDNA is a simple gene therapy vehicle that can be easily designed and produced in vitro from bacteria or bacteria-derived products. This unique circular double-stranded form of engineered nucleic acids could be used to code for a single protein of interest, and not be associated with any other proteins. The gene of interest could be inserted into the plasmid backbone with replication function only in bacteria. pDNA is usually large in size ranging from 2 to 15 kbps. It typically contains three basic elements: (i) an origin of replication which is active in bacteria; (ii) a prokaryotic expression cassette, including prokaryotic promoter and terminator of transcription that codes for an antibiotic-resistance protein; (iii) an eukaryotic expression cassette including eukaryotic promoter,

start codon in Kozak surrounding, coding sequence, stop codon and terminator of transcription for the protein product of interest (Weide, Garbe et al. 2008). pDNA requires delivery to the cell nucleus to reach the transcription machinery and production of mRNA and subsequent translation into protein product. Many studies have reported successful delivery of therapeutic pDNA into animal and human cells. These treatments have improved conditions of the diseases, including various interleukin genes for immunotherapy and tumor suppressor genes and pro-apoptotic genes for cancer treatment (Mahato, Lee et al. 2001; Horton, Lalor et al. 2008; Sun, Zhang et al. 2009; Xu, Zhang et al. 2010; Faham, Herringson et al. 2011; Kawabata, Baoum et al. 2012; Lee, Nguyen et al. 2012).

1.2.2 Messenger RNA (mRNA)

Interest in the use of mRNA as an alternative to pDNA in gene therapy has only grown recently, since mRNA has been regarded as too unstable for practical application (Tavernier, Andries et al. 2011). Structurally, single-stranded mRNA molecules are a few hundreds up to approximately 10 kb in size obtained by in vitro transcription of pDNA. They usually contain three basic elements: (i) a cap structure (methyl-7-guanine followed by three phosphate groups) at the 5′ end; (ii) a coding sequence including the start codon, the coding sequence for protein of interest and the stop codon; (iii) a poly A-tail of around 30 residues at the 3′ end (Weide, Garbe et al. 2008). Despite the instability of mRNA determined by its structure, several research groups have not only proven the feasibility of using mRNA to achieve high transfection efficiency and prolonged

protein expression, but they also have been able to demonstrate major advantages over the use of pDNA (Malone, Felgner et al. 1989; Dwarki, Malone et al. 1993; Van Tendeloo, Ponsaerts et al. 2001; Rejman, Tavernier et al. 2010). The first major advantage is that mRNA does not need to be delivered into the cell nucleus to exert its biological activity. Furthermore, mRNA can only provide a transient protein expression without the risk of integration into the genome, which can be safer and advantageous in some applications. Finally, mRNA lacks CpG motifs (unmethylated cytosine-phosphate-guanine signal present in bacterial and viral DNA triggering immune responses), and thus its use is expected to be less immunogenic than the use of pDNA (Krieg, Yi et al. 1995; Tavernier, Andries et al. 2011). Currently, different delivery techniques and vehicles for mRNA are been exploited and most attention has been paid to vaccine development (Conry, LoBuglio et al. 1995; Jarnjak-Jankovic, Pettersen et al. 2005; Bonehill, Van Nuffel et al. 2009). Other major application areas of mRNA in gene therapy include anti-cancer immunotherapy (Saeboe-Larssen, Fossberg et al. 2002; Ponsaerts, Van Tendeloo et al. 2003; Gilboa and Vieweg 2004; Mu, Kyte et al. 2005; Qiu, Lil et al. 2007), anti-infection immunotherapy (Martinon, Krishnan et al. 1993; Yu, Babiuk et al. 2007; Roesler, Weiss et al. 2009) and relieving hypoxic stress in the brain (Martinon, Krishnan et al. 1993; Yu, Babiuk et al. 2007; Roesler, Weiss et al. 2009).

1.2.3 Antisense Oligonucleotides (AON)

AON are a type of short single-stranded nucleic acids with about 22-28 bases. AON can be used to target a specific complementary (coding or non-coding) mRNA sequence by Watson-Crick base pairing. The formed DNA/RNA hybrid is recognized and degraded by RNase H, therefore inhibiting the expression of a specific mRNA and blocking the genetic transfer from DNA to protein (Dias and Stein 2002; Chan, Lim et al. 2006). AON do not deliver a new gene to the target cells, but rather modulate existing gene products (mRNA) or alter the transcription pathways. A variety of mechanisms mediated by AON could be used for therapeutic purposes. The most important ones include reframing of mRNA transcripts by hiding an exon from the splicing machinery and causing the skipping of exon (Aartsma-Rus and van Ommen 2010); RNase H knockdown of DNA-RNA hybrids (Marwick 1998; Pan and Clawson 2006); immune activation through toll-like receptor 9 (Dorn and Kippenberger 2008); and translation initiation/elongation block (Nasevicius and Ekker 2000; Rayburn and Zhang 2008). Currently, AON are commonly in use not only in the laboratory to study specific functions of a specific gene (loss-of-gene function) and valid therapeutic targets, but also in clinic to be applied as a therapeutic agent to target various diseases including cancer, AIDS, neuromuscular disorders, arthritis etc (Ratajczak, Kant et al. 1992; Kim, Tewari et al. 2009; Aartsma-Rus and van Ommen 2010; Nlend Nlend, Meyer et al. 2010). Fomivirsen has been the first AON to be approved by the FDA (1998) and introduced to the US market for the treatment of cytomegalovirus retinitis.

1.2.4 Small interfering RNA (siRNA) and other RNAi therapeutics

Since RNA interference (RNAi)-based gene silencing by double stranded RNA was first described in 1998 (Fire, Xu et al. 1998), the field of RNAi-mediated gene therapy has been quickly developing. Despite the recent setback of RNAi research and the shutdown of RNAi departments of big pharmaceutical companies, the rationale and potential of RNAi therapeutics are still strong and siRNA delivery remains of great interest. There are three major types of RNAi therapeutics: small interfering RNA (siRNA), microRNA (miRNA) and small hairpin RNA (shRNA). siRNA is a class of double-stranded RNA (dsRNA) molecules with 20-25 nucleotides in length. siRNA performs its silencing function in the cytoplasm by first incorporating into RNA-induced silencing complex (RISC). siRNA duplex then undergoes unwinding and the sense strand is excluded from the RISC. RISC-induced mRNA cleavage, which is facilitated by complementary base pairing with the antisense strand, results in post-transcriptional gene silencing. miRNA is a single strand RNA generated during endogenous transcription (He and Hannon 2004). It is ~ 22 nucleotides in length, firstly transcribed in the nucleus as long primary transcripts (pri-miRNA) with local hairpin structure and then processed into precursor miRNAs (pre-miRNA) by Drosha enzyme, followed by export to the cytoplasm where it is processed to form mature miRNA by Dicer (Lee, Jeon et al. 2002). Unlike siRNA, which forms a perfect duplex with its target mRNA and directs the RISC-mediated mRNA degradation, the action of miRNA depends on the level of complementarity. It

may cause mRNA cleavage or it may bind imperfectly with the untranslated regions of mRNA, leading to translational repression. The endogenous processing pathway of miRNA improves the silencing efficacy and avoids activation of the interferon system associated with externally introduced synthetic siRNA (Boden, Pusch et al. 2004). Depending on the type of miRNA, the desired intracellular site of delivery varies from cytoplasm to the nucleus. shRNA is a class of RNAi agents with tight hairpin turn that can be cleaved by Dicer enzyme to generate siRNA with 21-23 nucleotides. shRNA can be introduced into host cells via plasmid or virus, and further integrated into the host genome. This gives advantage of the silencing effect not necessarily being lost or diluted during cell division. shRNA is used more frequently in the laboratory to achieve permanent knockdown of a specific mRNA. Unlike siRNA, shRNA is usually delivered as the corresponding gene inserted into a plasmid DNA, which undergoes transcription process to form shRNA. Therefore, the sequence encoding for shRNA has to enter the nucleus and the delivery considerations fall into the DNA delivery category (Tokatlian and Segura 2010).

1.3 Gene Delivery by Polyplexes

Non-viral vectors for gene delivery have the advantages of simplicity of use, ease of large-scale production, and possibly a lack of specific immune response. A variety of non-viral delivery systems can be used for gene therapy, including complexes of cationic lipids and nucleic acids called lipoplexes (Felgner, Gadek et al. 1987; Nabel, Nabel et al. 1993; Lee, Marshall et al. 1996;

Wheeler, Felgner et al. 1996), complexes of cationic polymers and nucleic acids called polyplexes (Boussif, Lezoualc'h et al. 1995; Roy, Mao et al. 1999; Oupicky, Konak et al. 2000; Ogris and Wagner 2002), and naked plasmid DNA for use in electroporation, gene gun or hydrodynamic approaches of delivery (Rols, Delteil et al. 1998; Liu, Song et al. 1999; Rizzuto, Cappelletti et al. 1999). This section will focus on the properties and use of polyplexes with emphasis on the intracellular barriers faced by these delivery systems, and possible strategies of vector design to overcome these challenges.

For efficient delivery and transfection of various nucleic acids, polyplexes need to overcome a number of intracellular barriers to successfully deliver and release the gene cargo in the right subcellular locations. In most cases, polyplexes are internalized into the cells via endocytosis. Many studies have shown evidence that multiple endocytic pathways are involved, including clathrin- and caveolae-mediated pathways, macropinocytosis and phagocytosis (Goncalves, Mennesson et al. 2004; Rejman, Bragonzi et al. 2005; Vercauteren, Piest et al. 2011). The relative importance of these different mechanisms of uptake depends on the used cell line. It remains to be seen which of the pathways is most beneficial for effective gene delivery although the dominant view currently favors caveolae pathway as the most favorable. If polyplexes contain specific targeting ligands that bind to cell surface receptors, they could be internalized by receptor-mediated endocytosis. Initial uptake of polyplexes proceeds through a sequence of trafficking vesicles including early endosomes, late endosomes and lysosomes. If polyplexes successfully escape lysosomal

degradation, cytosolically active nucleic acids (siRNA, mRNA) require release in the cytoplasm, while the nuclearly active ones (pDNA, AON, miRNA, shRNA) require further transport to the nucleus for transcription. Nucleic acids released in the cytoplasm can be either degraded by cytosolic nucleases or be further transported to the nucleus as well. Polyplexes that do not disassemble in the cytoplasm are transported into the nucleus either passively by association with nuclear material during breakdown of the nuclear envelope during cell division or actively through nuclear pore complexes. The possibility of active transport of intact polyplexes through the nuclear pore complex remains controversial despite many attempts to confirm it.

Cell uptake is the first and one of the key steps required for successful delivery of polyplexes. Since the cell membrane consists of a hydrophobic phospholipid bilayer embedded with various surface proteins, the physicochemical properties of this biological barrier make direct translocation of hydrophilic nucleic with negative charge very difficult. Complexation of nucleic acids with cationic polymers results in a formation of particles (usually nano-sized) with a net positive charge, which facilitates interaction with the cell membrane and triggers polyplex internalization via endocytosis. Evidence shows that cell uptake of the polyplexes could be improved by modification of the polycations by attaching various targeting ligands to enhance receptor-mediated internalization or other lipophilic moieties such as cholesterol to promote fusion with the cell membrane as well as improve subcellular trafficking (Zidovska, Evans et al. 2009; Filippov, Konak et al. 2010). Various cell-penetrating peptides

(CPPs) like TAT trans-activator protein have also been incorporated into the gene delivery vectors to promote cell uptake and membrane translocation (Soundara Manickam, Bisht et al. 2005; Ishihara, Goto et al. 2009; Nam, Kim et al. 2011).

After polyplexes are internalized into the cell, the intracellular trafficking starts in early endosomes and proceeds through the stage of late endosomes, which are acidified by a vacuolar-type H+ ATPase membrane proton pump (Dominska and Dykxhoorn 2010). Without an endosomal escaping mechanism, free nucleic acids are most likely trapped in the endosomes and are subsequently routed to the lysosomes where they are exposed to lysosomal enzymes and degraded (Di Guglielmo, Le Roy et al. 2003). Hence, endosomal escape is one of the most significant barriers encountered during intracellular gene delivery. Many successful polyplexes utilize the so-called “proton sponge effect” to facilitate breaking out of the endosomes and entrance into the cytoplasm. Polycations with high buffering capacity in the endo/lysosomal pH range (pH 4.5-6) have the capability of absorbing protons and preventing the acidification of the endosomes, ultimately resulting in the release of the polyplexes into the cytoplasm. The proposed mechanism of action relies on elevated influx of the protons to endosomes mediated by the H+-ATPase. The increased concentration of the protons and the counter ions in the endosomal vesicles lead to increasing osmotic pressure, causing endosomal swelling, membrane rupture and finally the release of the polyplexes into the cytosol (Sonawane, Szoka et al. 2003; Dominska and Dykxhoorn 2010). Poly(ethylene

imine) (PEI) was the first and remains the most wildly used polycation based on the proton sponge hypothesis (Baker, Saltik et al. 1997; Zou, Erbacher et al. 2000; Urban-Klein, Werth et al. 2005; Goyal, Tripathi et al. 2012). The mix of primary, secondary, and tertiary amines in the PEI chain not only provide multiple positive charges at physiological conditions to bind with various negatively charged nucleic acids, but they also act as the proton sponge to facilitate the endosomal escape (Goyal, Tripathi et al. 2012). Unfortunately, the high cationic charge density also contributes to high cytotoxicity of PEI, which has impeded its *in vivo* applications (Florea, Meaney et al. 2002; Aravindan, Bicknell et al. 2009; Malek, Merkel et al. 2009). PAMAM dendrimers are another group of polycationic gene delivery vectors with high buffering capacity. These tree-like polymers have highly controlled and defined sizes and architecture with surface primary amines and central tertiary amines. These multiple amino groups provide high buffering capacity and proton absorbing ability, which can improve the endosomal escape of the dendrimers (Bielinska, Kukowska-Latallo et al. 1996; Kukowska-Latallo, Bielinska et al. 1996; Choi, Thomas et al. 2005; Tsutsumi, Hirayama et al. 2007). Alternative approaches have been applied in vector design to improve endosomal escape such as using synthetic fusogenic peptides that mimic the fusion process during virus infection (Oliveira, van Rooy et al. 2007) and introducing membranolytic peptides from viruses with pore-forming ability (Kwon, Bergen et al. 2008).

The mechanism of action of pDNA, miRNA and shRNA requires successful delivery to the cell nucleus. The cytoplasmic environment is

composed of densely packed soluble proteins and cytoskeleton protein structures such as actin filaments and microtubules. This dense packing creates a substantial barrier for trafficking of large delivery vectors because their passive diffusion is severely limited. The trafficking of the delivery vectors, and endosomes containing the vectors, mainly relies on microtubules and kinesin/dynein motor proteins (Leopold, Kreitzer et al. 2000; Kulkarni, Castelino et al. 2006). Disrupting the microtubule network using nocodazole to depolymerize tubulin significantly decreases the cytoplasmic transport of the delivery vectors. In contrast, applying cyclic mechanical stretch to the cells to reorganize and stabilize the microtubules leads to tubulin acetylation and enhanced endosomal trafficking leading to improved transfection efficiency (Geiger, Kaufman et al. 2009).

Early research showed that microinjection of exogenous genes into the nucleus produced strong gene expression while injection into the cytoplasm resulted in poor expression (Capecchi 1980; Graessmann, Menne et al. 1989). These findings clearly demonstrated that the nuclear envelope is a crucial barrier for delivery of nucleic acids to the nucleus. In rapidly dividing cells, delivery vectors have the opportunity to access nucleus during the process of mitosis when the nuclear envelope breaks down and becomes permeable to the material present in the cytoplasm (Dean, Strong et al. 2005). However, in non-dividing cells the nuclear envelope is a major barrier for non-viral delivery vectors. Significant effort has been made in improving nuclear delivery of the polyplexes and one of the most successful strategies is to incorporate nuclear localization

signals (NLS) in the vector to target cell nucleus. The conjugated NLS sequence will guide the polyplexes through the nuclear pore complex into the nucleus leading to enhanced transfection (Ritter, Plank et al. 2003; Manickam and Oupicky 2006; Zhang, Mitin et al. 2009).

In summary, to design efficient and safe gene delivery vectors, each and every intracellular barrier, including cell uptake, endosomal escape, and nuclear entry, should be taken into consideration. Polycationic vectors allow versatile design and modification to overcome these intracellular barriers, therefore representing promising gene delivery vectors not only in *in vitro* studies but also future *in vivo* applications.

1.4 Stimulus-Responsive Polyplexes

Among the different strategies applied in the design of polyplexes, various stimuli were used to trigger the disassembly of the formed particles and the release of the carried genetic materials after entering into the cells. Polyplexes responsive to different stimuli, including pH, hyperthermia, light, and redox-potential gradient, possess great potential for controlled release of the nucleic acids (Read, Logan et al. 2005).

Modification of polymeric vector by introducing pH-sensitive linkers is one of the most common approaches to improve intracellular release and endosomal escape of the polyplexes. 2,4,6-trimethoxybenzylidene-tris(hydroxymethyl)ethane (TMB-THME) hydrophobe as a pH-sensitive linker, has been conjugated to PEI to improve endosomal release of the polyplexes leading to improved transfection

efficiency in Hela cells (Liu, Zheng et al. 2011). Other research groups have also tried to modify the classic PEI polymers with pH-sensitive moieties to improve cell uptake and intracellular release (Wong, Sood et al. 2009). Polyethylene glycol (PEG) could also be conjugated to PEI via pH-sensitive linkers like amine-reactive, endosomal pH cleavable acetal or hydrazone to form bioreversible surface shielding of DNA polyplexes for controlled release (Knorr, Allmendinger et al. 2007; Fella, Walker et al. 2008). Functionalization with pH-responsive moieties have also been applied to other polymeric vectors like poly(L-lysine) (PLL) such as by incorporation of a charge-reversible poly(aspartamide) derivative to achieve enhanced endosomal escape and controlled gene delivery in human umbilical vein endothelial cells (HUVEC) (Sanjoh, Hiki et al. 2010). Conjugating histidine residues to the PLL polymer backbone to obtain pH-sensitive comb shaped polymer has shown improved transfection in 293T cells compared with unmodified PLL control. The improvement has been ascribed to enhanced endosomal release of DNA.

Introducing thermo-sensitive moieties to the polyplexes is another popular strategy to achieve controlled release of the nucleic acids. Pluronic block copolymers have been shown to exhibit a thermally reversible swelling/deswelling behavior, which triggers endosomal escape of polyplexes. Nanocapsules prepared from PEI and Pluronic were able to efficiently deliver siRNA, most likely due to improved endosomal escape (Lee, Choi et al. 2008). It has also been reported that thermo-responsive polymers that exhibit a lower critical solution temperature (LCST) behavior could be used to successfully

transport nucleic acids and release them in response to mild hyperthermia (Lavigne, Pennadam et al. 2007).

Photosensitive vectors utilize photosensitizers for endosomal disruption. Upon exposure to light, photosensitizers are stimulated to form reactive oxygen species leading to the damage of endosomal membranes, causing release of the RNAi vectors in the cytoplasm. Oliveira et al. has shown that by incorporating photosensitizers into siRNA delivery vectors which target epidermal growth factor receptor (EGFR), endosomal escape efficiency of siRNA vectors improved significantly, resulting in a 10-fold increase in the knockdown efficacy of EGFR (Read, Bremner et al. 2003; Oliveira, Fretz et al. 2007).

1.5 Redox-Responsive Polyplexes

One of the several stimuli, which has been often utilized for improving the efficiency of nucleic acid delivery, is the redox potential gradient existing between extracellular and intracellular environments. The existence of a high redox potential gradient between oxidizing extracellular space and the reducing environment of subcellular organelles has been exploited by incorporating disulfide bonds into the structure of polyplexes to provide them with the capability to release the therapeutic nucleic acids selectively in the subcellular reducing space. The original interest in gene delivery systems controlled by redox potential gradients was guided by the need to transiently enhance stability of the vectors during the delivery.

1.5.1 Biological rationale

A redox potential gradient exists between extracellular environment and various subcellular organelles in normal as well as pathological states. Disulfide bonds present in the structure of polyplexes are readily reduced in the reducing intracellular environment, while they are generally preserved in the oxidizing extracellular space. The intracellular reduction of disulfide bonds in polyplexes is mediated by thiol/disulfide exchange reactions with small redox molecules like glutathione (GSH) and thioredoxin; either alone or with the help of redox enzymes. GSH (L-γ-glutamyl-L-cysteinylglycine) is the most abundant thiol present in mM concentrations inside the cell but only in μM concentrations in the blood plasma (Jones, Carlson et al. 1998). GSH has multiple functions in many critical cellular processes including synthesis of proteins and DNA, amino acid transport, enzyme activity, metabolism and protection of cells (Meister and Anderson 1983). GSH also serves as a reductant by functioning to destroy free radicals, hydrogen peroxide and other peroxides. It also functions as a storage form of cysteine. The intracellular GSH concentration is an additive function of both its oxidized (GSSG) and reduced form (GSH). The glutathione redox ratio ([GSH]:[GSSG]) is maintained and determined by the activity of glutathione reductase, NADPH concentrations, and transaldolase activity. The redox state of the GSH/GSSG couple is often used as an indicator of the overall redox environment of the cell. In contrast to other redox systems in the cell, not only the [GSH]:[GSSG] ratio, but also absolute concentrations of GSH and GSSG are important for the estimation of the redox state of the cell (Schafer and Buettner

2001). This is because the Nernst equation for the reduction potential of the GSH/GSSG couple depends on $[GSH]^2/[GSSG]$. The GSH concentration and redox ratio ([GSH]:[GSSG]) are different in various subcellular compartments (Smith, Jones et al. 1996). Because of the different GSH levels in various subcellular organelles, the local GSH concentration and [GSH]:[GSSG] ratio are important for predicting the location and rate of the disulfide reduction.

The majority of GSH is usually found in the cytosol (1–11 mM), which is also the principal site of GSH biosynthesis (Kosower and Kosower 1978; Gilbert 1990; Hwang, Lodish et al. 1995). The most reducing environment in the cell is usually found within the nucleus, where it is required for DNA synthesis and repair and to maintain a number of transcription factors in reduced state (Bellomo, Vairetti et al. 1992; Wu, Bishopric et al. 1996; Arrigo 1999). The nuclear GSH levels are typically higher than those found in the cytosol and can reach up to 20 mM (Bellomo, Vairetti et al. 1992; Soboll, Grundel et al. 1995; Smith, Jones et al. 1996). Another major pool of GSH in the cell is found in mitochondria (~5 mM) (Wahllander, Soboll et al. 1979; Lash, Putt et al. 2002). Both mitochondrial and nuclear GSH pools are at least partially independent of the cytosolic pool. In contrast to the reducing environment found in the nucleus and mitochondria, the endoplasmic reticulum is more oxidizing than the cytosol (Braakman, Helenius et al. 1992; Hwang, Sinskey et al. 1992). The ratio [GSH]:[GSSG] is relatively low, typically ranging from 1:1 to 3:1. In comparison, the overall ratio in the cell is usually >30:1. One should keep in mind, however, that the redox state of the cell is not static. It depends on a variety of factors

including the stage of the cell cycle and biological status of the cell in general (Schafer and Buettner 2001).

Despite numerous studies, the redox state of endosomes and lysosomes remains a contested issue. Even though some evidence suggests the possibility of endosomal and lysosomal reduction of disulfide bonds (Shen, Ryser et al. 1985; Collins, Unanue et al. 1991; Phan, Arunachalam et al. 2000; Fivaz, Vilbois et al. 2002; Saito, Amidon et al. 2003), recent report provides evidence that both the endosomal and lysosomal environments are oxidizing (similar to ER) and disulfide reduction proceeds inefficiently (Austin, Wen et al. 2005). It was suggested that reductions previously ascribed to endosomes could have proceeded in Golgi (Feener, Shen et al. 1990). However, one cannot exclude also the possibility that a small subset of lysosomes could be reducing or that only some disulfides within certain proteins could be susceptible to endo/lysosomal cleavage. Because bioreducible polyplexes contain a large number of disulfides, it is unlikely that the limited reducing potential of endo/lysosomes plays an important role in their subcellular trafficking. The subcellular distribution of reducing capability and current understanding of subcellular trafficking of polyplexes therefore suggests that intracellular reduction of disulfide bonds in redox-sensitive polyplexes proceeds preferentially in the cytoplasm and nucleus.

1.5.2 Bioreducible polyplexes

Introducing reducible disulfide bonds into the backbone of the polycations allows polyplexes to undergo intracellular thiol-disulfide exchange reactions, leading to the cleavage of the disulfide bonds and fragmentation of the polycations. The increased disassembly rate ultimately enhances the intracellular availability of the nucleic acids that leads to enhanced transfection efficiency (Read, Bremner et al. 2003; Read, Singh et al. 2005; Soundara Manickam and Oupicky 2006; Won, Yoon et al. 2011; Beloor, Choi et al. 2012). Another major advantageous feature of the redox-responsive (bioreducible) polyplexes is that the disassembly of the polyplexes due to the breakage of disulfide bonds causes fragmentation of the vector and generates small-molecular-weight molecules, resulting in significantly decreased cytotoxicity (Jere, Arote et al. 2009; Kim and Kim 2011).

Numerous bioreducible polymers have been developed, including various novel types of polycations with unique structure and architecture as well as simple modifications of the existing non-degradable polycations like PEI. These polycations typically show improved transfection efficiency and reduced toxicity. Many of them have demonstrated successful and safe delivery of a variety of nucleic acids (pDNA, siRNA, AON) both in cell culture and in animal studies.

Bioreducible poly(amido amine)s (PAA) can be synthesized by Michael addition reaction of a variety of combinations of acrylamide and amine monomers. It is convenient to develop a panel of PAA using different types of the monomers and reaction conditions including solvent, temperature and feeding ratio. Engbersen et al. reported the synthesis of a series of novel bioreducible

PAA by Michael addition polymerization of a panel of primary amines and disulfide containing cystamine bisacrylamide (CBA). The polymers were relatively stable in physiological conditions but could be rapidly degraded in reducing environment. These PAA also showed improved transfection compared with PEI in COS-7 cells while showing lower cytotoxicity. The authors have also found that among the group of bioreducible PAA synthesized for activity screening, the ones that contained amino alcohol pendant groups exhibited the highest gene delivery efficiency (Hoon Jeong, Christensen et al. 2007; Lin, Zhong et al. 2007; Lin, Zhong et al. 2007; Lin, Blaauboer et al. 2008).

Great effort has also been made by many other groups to design the best performing bioreducible polymeric gene delivery systems for both pDNA and siRNA including the development of bioreducible poly(β-amino ester) copolymers (Christensen, Chang et al. 2007; Hoon Jeong, Christensen et al. 2007; Kim, Jeong et al. 2008; Yockman, Kastenmeier et al. 2008; Chen, Wu et al. 2009; Kim, Jeong et al. 2009; Kim, Ou et al. 2009; Nam, McGinn et al. 2010; Namgung, Brumbach et al. 2010; Kim, Lee et al. 2012; Lee, Nam et al. 2012). Lee and coworkers have demonstrated that cross-linking of low-molecular-weight PEI with reducible cross-linkers such as dithiobis(succinimidylpropionate) (DSP) and dimethyl 3,3'-dithiobispropionimidate (DTBP) could mediate significantly improved gene delivery to Chinese hamster ovary (CHO) cells (Gosselin, Guo et al. 2001). Similar approaches to crosslinking PEI with different linkers (e.g., dithiodipropionic acid) or via different chemical reactions (Michael addition reaction, ring-opening reaction) have also been extensively explored. These

cross-linked bioreducible PEI all showed improved safety profile and enhanced transgene expression compared with the standard 25 kDa PEI, indicating the important role of reducible moieties in developing efficient and safe non-viral gene delivery vectors (Yockman, Maheshwari et al. 2003; Buehler, van Zandvoort et al. 2006; Neu, Sitterberg et al. 2006; Neu, Germershaus et al. 2007; Sun, Zeng et al. 2008; Koo, Jin et al. 2010).

1.6 Conclusion

In the following chapters of this dissertation, I will present the most important findings on the development of bioreducible polyplexes and study of their physicochemical and biological properties. The effect of nucleic size on the physicochemical properties and biological activity of redox-responsive polyplexes is explored in Chapter 2. Chapter 3 focuses on incorporating hyaluronic acid into the structure of bioreducible polyplexes to improve steric stability and to achieve targeted delivery to CD44 expressing cancers. The last two chapters introduce novel design concept of multifunctional bioreducible polyplexes suitable for drug/gene combination therapies, with the additional option of PET imaging.

CHAPTER 2

EFFECT OF NUCLEIC ACID SIZE ON PHYSICAL PROPERTIES AND BIOLOGICAL ACTIVITIES OF BIOREDUCIBLE POLYPLEXES

Please note that the content of this chapter was published in the European Journal of Pharmaceutical Sciences (Li, Manickam et al. 2012). As the first author, I performed all the work in the paper except the polymer synthesis (contributed by Dr. D. Manickam, the second author) and the measurement of molecular weights of all the polymers using GPC (contributed by Dr. J. Chen, the third author). All the authors agreed with including their work in this dissertation.

2.1 Introduction

Polyplexes of nucleic acids and bioreducible polycations have demonstrated promise as delivery vectors of a variety of potential nucleic acid therapeutics (Rahbek, Howard et al. 2008; Manickam, Li et al. 2010; Namgung, Brumbach et al. 2010). The bioreducible polyplexes take advantage of the strong reducing intracellular environment in which the disulfide-containing polycations are readily broken down by thiol-disulfide exchange reactions. The intracellular degradation is then responsible for decreased toxicity of bioreducible polycations and is often credited also with increased transfection activity of due to easier DNA release. The reducing intracellular environment is primarily maintained by small redox molecules like glutathione (GSH) either with or without the help of redox enzymes (Gilbert 1997; Jiang, Fitzgerald et al. 1999; Donoghue and Hogg

2002). Recent study has indicated that intracellular protein thiols (PSH) may represent a pool of active reducing species that is even larger than that of GSH (Hansen, Roth et al. 2009).

Improved transfection activity of bioreducible polyplexes is an almost universal finding reported with various different types of bioreducible polycations, including polypeptides, polymethacrylates, and poly(amido amine)s (PAA) (Chen, Kim et al. 2006; Christensen, Chang et al. 2006; Lin, Zhong et al. 2006; Manickam and Oupicky 2006; You, Manickam et al. 2007; Piest, Lin et al. 2008). The increased transfection activity is believed to be the consequence of the decreased affinity between DNA and the bioreducible polycations after their intracellular degradation. The reduced affinity is expected to enhance transcriptional availability of DNA due to faster and easier polyplex disassembly (Read, Bremner et al. 2003; Christensen, Chang et al. 2006). This notion is supported by at least some available evidence, which suggest that artificial changes in intracellular GSH levels can change transfection activity of bioreducible polyplexes, although the effect is often small. In general, increasing intracellular GSH by incubation with a membrane-permeable derivative of GSH leads to an increase in transfection of bioreducible polyplexes (Read, Bremner et al. 2003; Christensen, Chang et al. 2006; Neu, Germershaus et al. 2007). Some reports, however, found the opposite effect as increased GSH lowered transfection (Read, Singh et al. 2005). Similar conflicting evidence is available from studies in which intracellular GSH is depleted by inhibiting its *de novo* synthesis. In most cases, a small decrease in transfection is observed after

inhibiting GSH synthesis with inhibitor of γ-glutamylcysteine synthetase, buthionine sulfoximine (Read, Bremner et al. 2003; Read, Singh et al. 2005; Christensen, Chang et al. 2006; Neu, Germershaus et al. 2007; Manickam, Li et al. 2010). The opposite effect of GSH inhibition on transfection of bioreducible polyplexes was reported in a study that showed increased transfection after inhibition of GSH biosynthesis (Hoon Jeong, Christensen et al. 2007). These results suggest that the notion of a straightforward relationship between intracellular reducing potential, enhanced disassembly, and transfection activity of bioreducible polyplexes could be an oversimplified view.

This chapter focuses on how enhanced reductive disassembly affects transfection activity of plasmid DNA and antisense oligonucleotides (AON) polyplexes based on a series of bioreducible polycations with increasing content of disulfide bonds. The hypothesis of this study is that the molecular weight of the used nucleic acid would strongly influence activity of bioreducible polyplexes because of the differences in binding affinity with polycations.

2.2 Materials and Methods

2.2.1 Materials

N,N'-hexamethylenebisacrylamide (HMBA) and N,N'-cystaminebisacrylamide (CBA) were obtained from Polysciences, Inc. (Warrington, PA). 1-(2-Aminoethyl) piperazine (AEPZ) was obtained from Acros Organics (Fisher Scientific, Pittsburgh, PA). Plasmid DNA, gWiz high-expression luciferase (gWiz-Luc) containing luciferase reporter gene was from Aldevron

(Fargo, ND). Luciferase antisense oligonucleotides (AON) (5'-AACCGCTTCCCCGACTTCC-3') and its scrambled control (5'-CCAATGTCAAGCACTT CCGTT-3') with phosphorothioate linkages were custom synthesized by Midland Certified Reagent Company (Midland, TX). 1,2-Dioleoyl-3-trimethylammonium-propane chloride (DOTAP) was purchased from Toronto Research Chemicals Inc. (North York, ON, Canada). YOYO®-1 iodide, Dulbecco's Modified Eagle Medium (DMEM), Dulbecco's Phosphate Buffered Saline (PBS), Fetal Bovine Serum (FBS) and non-essential amino acids (NEAA) were from Invitrogen (Carlsbad, CA). All other reagents and chemicals were obtained from Fisher Scientific or VWR International unless otherwise noted.

2.2.2 Synthesis and characterization of PAA

A series of five linear PAA containing different disulfide content was synthesized by Michael addition of triamine AEPZ and different molar ratio of reducible CBA and non-reducible HMBA (Scheme 1) following a published method (Lin, Zhong et al. 2006; Manickam, Li et al. 2010). Calculated amounts of HMBA, CBA and AEPZ were dissolved in methanol/water (7/3 v/v) and the polymerization was allowed to proceed in the dark at 37 °C for 72 h to form the linear polymers (Hong, You et al. 2007). The reaction mixtures were then diluted with water, acidified to pH 4 with HCl, and purified using centrifugal membrane filters (molecular weight cut-off 3 kDa). The concentrates were lyophilized and the composition of the polymers was analyzed by ^{1}H and ^{13}C NMR. The following CBA:HMBA molar ratios were used in the polymerization: 0:1, 1:3, 1:1, 3:1 and

1:0, which resulted in a series of PAA with CBA content of 0, 25, 50, 75 and 100 %. Weight- (M_w) and number- (M_n) average molecular weights of the polymers were determined by GPC using Shimadzu LC-10ADVP liquid chromatograph equipped with a multiangle light scattering detector and an interferometric refractometer (Wyatt Technology, Santa Barbara, CA). Sodium acetate (300 mM, pH 4.5) was used as an eluent at a flow rate of 1.0 mL/min and temperature of 35 °C.

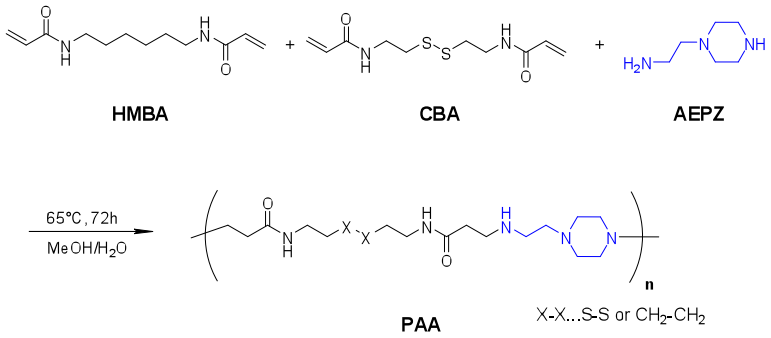

Scheme 1. Synthesis of PAA.

2.2.3 Ethidium bromide and OliGreen exclusion assay

The ability of PAA to condense DNA was determined by ethidium bromide (EtBr) exclusion assay by measuring the changes in EtBr/DNA fluorescence. DNA solution at a concentration of 20 μg/mL was mixed with EtBr (1 μg/mL), fluorescence was measured and set to 100% using an excitation wavelength of 540 nm and an emission wavelength of 590 nm. Fluorescence readings were taken following a stepwise addition of the polycation solution, and the condensation curve for each polycation was constructed. The ability of PAA to condense AON was determined in a similar way by measuring changes in OliGreen/AON fluorescence, using 490 nm excitation and 520 nm emission.

2.2.4 Preparation and characterization of DNA and AON polyplexes

gWiz-Luc DNA solution at a concentration 20 μg/mL was prepared in 30 mM sodium acetate buffer (pH 5.0). PAA/DNA polyplexes were formed by adding predetermined volume of PAA to achieve the desired N/P ratio and mixed by vigorous vortexing for 10 s. Polyplexes were further allowed to stand for 30 min prior to use. AON polyplexes were prepared by following the same protocol, except that AON was heat-denatured for 10 min at 65 °C and snap-cooled on ice prior to dilution in the buffer. The determination of hydrodynamic diameters and zeta potentials of both polyplexes was performed following previously published method (Manickam, Bisht et al. 2005). Results were expressed as mean ± standard deviation (S.D.) of 10 experimental runs each.

2.2.5 Agarose gel electrophoresis

Reduction-triggered disassembly of the polyplexes was examined by agarose gel electrophoresis using a previously described protocol (Read, Bremner et al. 2003). Briefly, DNA polyplexes were formed as described above and incubated under indicated conditions. Samples were loaded onto a 0.8% agarose gel containing 0.5 μg/mL EtBr and run for 75 min at 120 V in 0.5X Tris/Borate/EDTA (TBE) running buffer. The gel was visualized under UV. AON polyplexes were analyzed on a 2% agarose gel containing EtBr for 30 min at 80 V under conditions mentioned above.

2.2.6 Cell culture

Mouse mammary carcinoma cell line D2F2 was a kind gift from Dr. Wei-Zen Wei, Karmanos Cancer Institute (Detroit, MI). The cells were maintained in DMEM supplemented with 4 mM L-glutamine, 0.1 mM NEAA and 10% FBS at 37 °C in 5% CO_2 atmosphere.

2.2.7 Transfection of DNA and AON polyplexes

All transfection experiments were conducted in 48-well plates during logarithmic growth phase following a previously published protocol (Manickam, Li et al. 2010). Cells were seeded at a density of 40,000 cells/well 24 h prior to transfection. On a day of transfection, the cells were incubated with the polyplexes (DNA dose: 0.4 µg/well) in 150 µL of serum-free media. After 3 h incubation, polyplexes were completely removed and the cells were cultured in complete culture medium for 24 h prior to measuring luciferase expression. The medium was then discarded and the cells were lysed in 100 µL of 0.5x cell culture lysis reagent buffer (Promega, Madison, WI) for 30 min. To measure the luciferase content, 100 µL of 0.5 mM luciferin solution was automatically injected into each well containing 20 µL of cell lysate and the luminescence was integrated over 10 s using BioTek Synergy 2 Microplate Reader. Total cellular protein in the cell lysate was determined by the bicinchoninic acid (BCA) protein assay using calibration curve constructed with standard bovine serum albumin solutions (Pierce, Rockford, IL). For cell surface thiol blocking, the cells were pre-incubated with 1 mM of DTNB in DMEM for 30 min. The DTNB solution was

removed before conducting the transfection experiments as above. Transfection activity was expressed as RLU/mg cellular protein ± S.D. of quadruplicate samples. For AON transfections, the cells were transfected with 0.4 μg luciferase DNA per well using DOTAP liposomes (N/P ratio 16) 24 h before transfected with AON polyplexes (0.8 μg/well). The transfection efficiency was expressed as % knock-down compared with control scrambled AON.

2.2.8 Cell uptake by flow cytometry

The cellular association of the fluorescently-labeled polyplexes was measured using flow cytometry. Cells were plated in a 24-well plate 24 hours before transfection. Polyplexes were formed using DNA labeled with YOYO-1 by mixing at a ratio of 1 dye molecule per 100 bp of DNA. After 3 h of transfection, cells were washed with PBS, detached, and resuspended in 200 μL PBS. 10,000 events per sample were counted on FACS. Histogram plots were constructed using the CellQuest software. The mean fluorescence intensity from each sample was obtained and the cellular uptake was quantified as average mean fluorescence intensity ± SD of triplicate samples.

2.2.9 Kinetics of intracellular plasmid DNA clearance

Intracellular content of the gWiz-Luc plasmid DNA at different time points after incubation was measured using real-time PCR (RT-PCR, ABI Prism® 7300). The following probe and primers were designed in BioSearch online RealTimeDesign™ software: FAM-BHQ probe TCAGGATTACAAGATTCAAAGT

GCGCT, forward primer GAAGAGCTGTTTCTGAGG, reverse primer CGAAGAA GGAGAATAGGGT. The 18S rDNA probe and the master mix were purchased from Eurogentec (San Diego, CA). Cells were incubated with DNA polyplexes for 3 h under conditions used in the transfection studies. At predetermined times after incubation, the cells were washed twice with warm PBS and lysed with 100 µL of RT-PCR lysis buffer for 1 h at 37 °C. The lysate (25 µL) was transferred to a deep-well plate and diluted with 475 µL of sterile water. The lysate was then incubated for 15 min in 95 °C water bath to inactivate proteinase K. During the RT-PCR cycle, 5 µL of DNA template, 75 nM probe and 600 nM primer pairs were added. To determine 18S rRNA, 125 nM probe and 600 nM primer pairs were added to the template. The PCR cycle was run for 2 min at 50 °C, 10 min at 95 °C, 40 cycles for 15 s at 95 °C, and 1 min at 60 °C. The number of plasmid DNA copies was normalized to 18S rRNA and calculated as 2^n, where $n = (Ct_{18S\ rRNA} - Ct_{luc})$.

2.2.10 Statistical analysis

Significant differences between two groups were determined using Student's t-test and differences among multiple groups were determined using ANalysis Of VAriance (ANOVA). A p-value < 0.05 was considered statistically significant in all cases.

2.3 Results and Discussion

Bioreducible polycations have been widely investigated as delivery vectors of nucleic acids because of their favorable toxicity profile and the possibility to preferentially restrict release of the delivered nucleic acids to intracellular locations such as cytoplasm and nucleus. Both the decreased toxicity and controlled intracellular release are believed to be caused by degradation of disulfide-containing polycations mediated by reduced GSH abundantly present in the cytoplasm (Vercauteren, Piest et al. 2011). However, while reduced toxicity of bioreducible polycations is a nearly-universal finding, improved transfection activity of bioreducible polyplexes is not. This raises a question about the importance of the presumed increased intracellular disassembly of bioreducible polyplexes for transfection. The goal of this study was to systematically investigate how decreasing stability against disassembly affects transfection activity of plasmid DNA and AON polyplexes.

2.3.1 Synthesis and characterization of linear PAA with different disulfide content

In order to achieve the goal of this study, five polycations with similar molecular weights and with increasing disulfide content were synthesized. The disulfide content was controlled by the feeding molar ratio of reducible (CBA) and non-reducible (HMBA) bisacrylamide monomers. The weight-average molecular weight (Mw) and polydispersity index (PDI) of the five synthesized PAAs were determined by GPC and are listed in Table 1. The synthesized PAA had similar Mw ranging from 5,700 to 7,400 and polydispersity indices ranging from 1.1 to 2.0. The ratio of CBA-to-HMBA in the polymers was nearly identical to the

feeding ratio, suggesting similar reactivity of the two bisacrylamides. PAA polymer was chosen based on a piperazine triamine AEPZ because of previous reports that confirm its good transfection activity (Lin, Zhong et al. 2006; Blacklock, You et al. 2009; Manickam, Li et al. 2010). Although AEPZ may function potentially as a trifunctional monomer in the polymerization, the distinct reactivity of the AEPZ amines allows synthesis of linear polymers by a simple control of reaction stoichiometry (Wang, Liu et al. 2005; Lin, Zhong et al. 2006). The absence of a branched structure of AEPZ after its reaction with two equivalents of acrylamide was observed, indicating that the acyclic secondary amine formed after addition of a primary amine to AEPZ has a much lower reactivity than the original cyclic secondary amine and primary amine in AEPZ. Thus linear structure was preferentially formed due to the order of different reactivity of the amines: secondary amine (original) > primary amine > secondary amine (formed).

Table 1. Molecular weights of PAA.

Polymer	Reducible content (%)*	M_w	M_w /M_n
PAA-0	0	7,400	1.1
PAA-25	25	7,100	1.1
PAA-50	50	6,200	1.2
PAA-75	75	5,700	1.9
PAA-100	100	5,800	2.0

* relative content of CBA in PA: 100*[CBA]/([CBA]+[HMBA])

2.3.2 Effect of nucleic acid size on binding of PAA and nucleic acids

OliGreen is an ultra-sensitive fluorescent nucleic acid dye that binds oligonucleotides and single-stranded DNA. Its fluorescence corresponds to free unbound oligonucleotides in solution. The fluorescence intensity of OliGreen/AON decreased linearly with increasing N/P ratio (Figure 3a). Full complexation of AON was achieved with all five PAA at N/P > 0.8 as indicated by no further fluorescence decrease beyond this ratio. EtBr exclusion assay was carried out in analogous manner to test the ability of PAA to condense plasmid DNA (Figure 3b). The condensation curves for all PAA displayed typical sigmoidal shape characteristic of DNA condensation. N/P ratios above 1.8 were required to fully condense the DNA. Figure 3 documents that there were no significant differences in DNA and AON complexation ability among the five PAA, suggesting that the presence of disulfide bonds in the polycations does not affect their binding to nucleic acids.

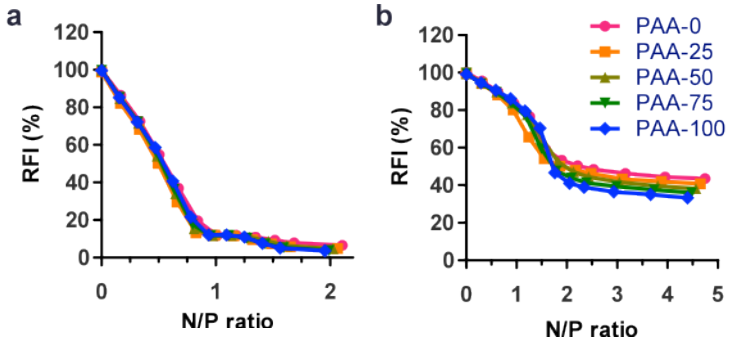

Figure 3. Nucleic acid condensation by PAA. (a) OliGreen exclusion assay to assess AON condensation and (b) EtBr exclusion assay to assess DNA condensation.

2.3.3 Effect of nucleic acid size on particle size and zeta-potential of PAA polyplexes

Size and zeta potential directly influence cellular uptake and transfection activity of polyplexes. Hydrodynamic size and zeta-potential of polyplexes were measured before every in vitro test. Polyplexes were formulated with about a 4-fold excess of polycation relative to the minimum amount needed to fully condense the corresponding nucleic acid as determined from Figure 3. Thus, DNA polyplexes were prepared at N/P = 8 and AON polyplexes at N/P = 4. As shown in Table 2, the sizes of PAA/DNA polyplexes showed no dependence on the disulfide content in PAA as they all fell into a narrow range of 96-102 nm. The sizes of all PAA/AON polyplexes (average size 64 ± 11 nm) were significantly smaller than the sizes of DNA polyplexes (average size 100 ± 5 nm), with the smallest size (53 nm) observed for polyplexes formulated with PAA with the highest disulfide content (PAA-100). All polyplexes, regardless of the type of nucleic acid, were highly positively charged with zeta potential ranging from 22 to 37 mV. The average zeta potential of DNA polyplexes (30 mV) was higher than the average zeta potential of AON polyplexes (26 mV). The independence of the physicochemical properties of polyplexes on disulfide content was important because it allowed us to minimize, although not fully eliminate, any potential confounding effects on the studied biological behavior of the polyplexes that were not directly related to the presence of disulfides.

Table 2. Hydrodynamic size and zeta potential of PAA polyplexes.

Polymer	DNA polyplexes[a]		AON polyplexes[b]	
	Size (nm)	Zeta-potential (mV)	Size (nm)	Zeta-potential (mV)
PAA-0	96 ± 2	26 ± 2	66 ± 3	27 ± 2
PAA-25	98 ± 10	30 ± 1	74 ± 2	22 ± 2
PAA-50	107 ± 1	27 ± 1	75 ± 2	26 ± 1
PAA-75	96 ± 5	28 ± 1	53 ± 2	29 ± 4
PAA-100	102 ± 1	37 ± 1	53 ± 1	25 ± 5

[a] prepared at N/P ratio 8
[b] prepared at N/P ratio 4.

2.3.4 Effect of nucleic acid size on reduction-triggered disassembly of PAA polyplexes

Reduction-triggered disassembly of the PAA polyplexes was evaluated from differences in DNA and AON release patterns in the oxidizing and reducing conditions using agarose gel electrophoresis (Figure 4). In addition to treatment with 20 mM GSH, the polyplexes were also incubated with 0.75 M NaCl to further facilitate disassembly and release of the nucleic acids. Incubation with 20 mM GSH resulted in loosening and partial dissociation of the polyplexes, documented by a partial release of both AON and DNA. Release behavior of polyplexes of both nucleic acids showed a clear dependence on the disulfide content in PAA. Partial AON release was observed at lower disulfide content in PAA (PAA-50) than DNA release (PAA-75). Addition of NaCl enhanced not only the amount of released nucleic acid but also resulted in free nucleic acids observed at lower disulfide contents in PAA. Despite the combined action of GSH and NaCl, neither

DNA nor AON were released from non-reducible PAA-0 polyplexes. Quantitative analysis of the release of AON and DNA from PAA polyplexes incubated with 20 mM GSH and 0.75 M NaCl is shown in Figure 5. Data for both AON and DNA polyplexes confirm that increasing the disulfide content leads to increased amount of released nucleic acid. PAA-100 polyplexes of DNA were more susceptible to the GSH/NaCl treatment than AON polyplexes, with almost 80% of released DNA vs. 68% of released AON. Overall, both types of nucleic acids showed similar release behavior. Interestingly, despite greatly different sizes of AON and plasmid DNA, only a small effect of the nucleic acid size on the disassembly behavior was observed.

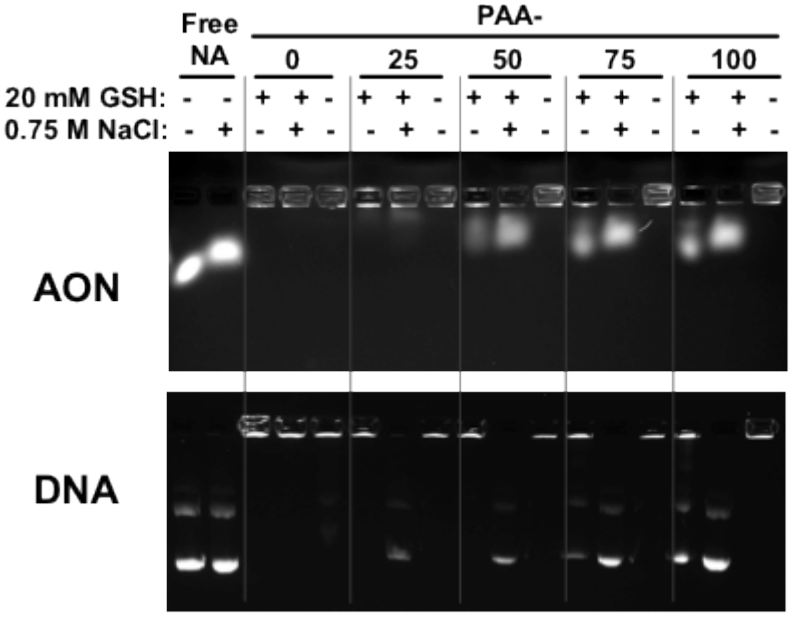

Figure 4. Reduction-triggered release of AON (top) and plasmid DNA (bottom) from PAA polyplexes. Polyplexes were prepared at N/P 4 (AON) and N/P 8 (DNA) and incubated with 20 mM GSH and 0.75 M NaCl.

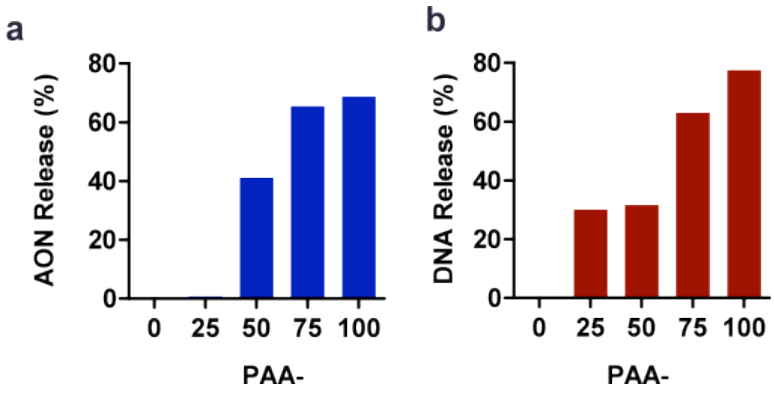

Figure 5. Quantification of the reduction-triggered release of AON (a) and plasmid DNA (b) from PAA polyplexes. Polyplexes prepared at N/P 4 (AON) and N/P 8 (DNA) were incubated with 20 mM GSH and 0.75 M NaCl and the amount of released nucleic acid quantified by analyzing the fluorescence intensity of the bands. % nucleic acid release equals the ratio of fluorescence intensity of released AON or DNA band to the fluorescence intensity of the free AON or DNA.

2.3.5 Effect of nucleic acid size on stability of PAA polyplexes against polyelectrolyte exchange

It is hypothesized that the intracellular disassembly of bioreducible polyplexes is a result of the combined effect of reduction and polyelectrolyte exchange reactions with intracellular polyelectrolytes (proteins, nucleic acids). Exchange reactions with negatively charged intracellular proteins, including actin and tubulin, have been shown to be responsible for intracellular release of plasmid DNA from PEI polyplexes (Iida, Mori et al. 2007). The effect of PAA disulfide reduction on the resistance of the polyplexes against polyelectrolyte exchange with a competing polyanion heparin was evaluated by agarose gel electrophoresis (Figure 6). In oxidizing conditions, DNA polyplexes show first signs of destabilization at a heparin concentration of 30 µg/ml while AON polyplexes start to disassemble at a heparin concentration of 20 µg/ml. Similar

behavior was observed for both AON and DNA polyplexes regardless of disulfide content. In reducing conditions of 20 mM GSH, the threshold heparin concentration required to destabilize the polyplexes and release the nucleic acids decreased with increasing disulfide content in PAA. No significant differences in susceptibility to heparin-induced DNA and AON release were observed in the absence of GSH, confirming similar DNA and AON binding affinities of all PAA. It is worth pointing out the difference in the release pattern of AON and DNA that reflects the different mechanism of condensation of the two types of nucleic acids (Figure 3) (Wan, You et al. 2009). While AON is released gradually with increasing heparin concentration, DNA is released in a more abrupt manner at a certain critical concentration of heparin. GSH treatment makes both AON and DNA polyplexes more susceptible to exchange with heparin.

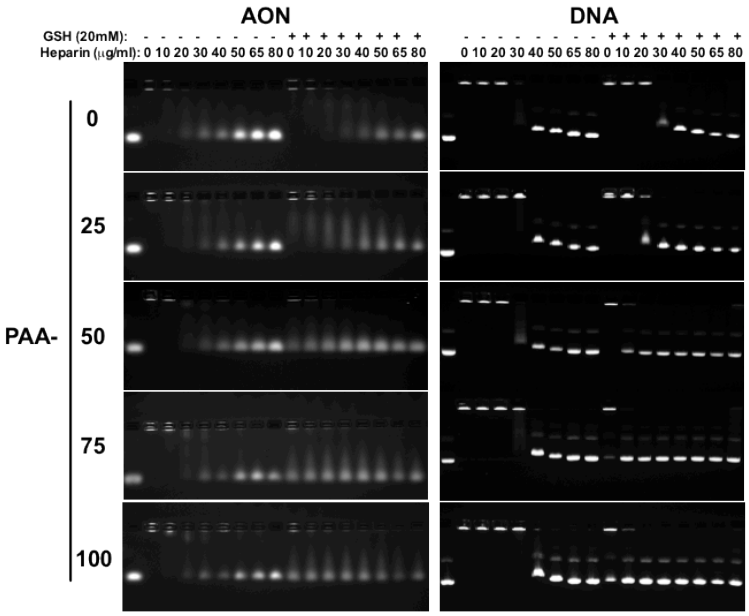

Figure 6. Effect of disulfide reduction on susceptibility of PAA polyplexes to polyelectrolyte exchange reactions. AON (left) and plasmid DNA (right) polyplexes of PAA were treated with increasing concentration of heparin and/or

20 mM GSH. AON and DNA release were analyzed by agarose gel electrophoresis.

2.3.6 Effect of nucleic acid size on stability of PAA polyplexes against serum

Systemic delivery of polyplexes through intravenous injection requires that they are stable in the presence of serum. The stability of both DNA and AON polyplexes in the presence of serum was investigated using agarose gel electrophoresis (Figure 7). No DNA or AON release was observed after incubation with serum, indicating no significant cleavage of the disulfide bonds. By contrast, free DNA and AON bind with serum components as indicated by a smear on the gel (Figure 7, lane 5). Although no free nucleic acid was observed, the increased fluorescence intensity in the wells in the presence of serum suggested that interactions with serum components result in some loosening and structural changes of the polyplexes that facilitate binding of EtBr.

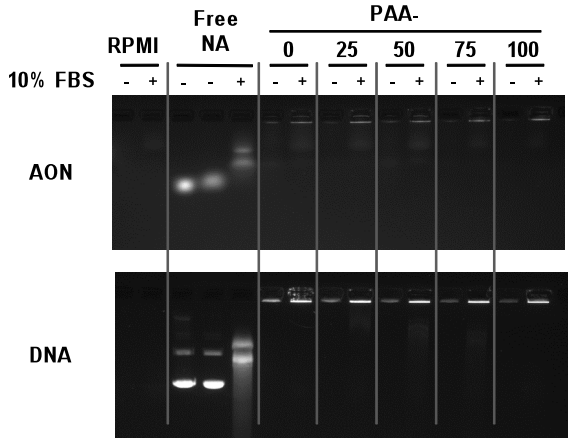

Figure 7. Effect of serum on stability of AON and DNA polyplexes. PAA polyplexes, free nucleic acids (NA) (AON, DNA), and RPMI medium were incubated with (+) or without (-) 10% FBS and the presence/content of free nucleic acids was analyzed by agarose gel electrophoresis.

2.3.7 Effect of nucleic acid size on transfection activity of PAA polyplexes

Having established that both AON and DNA polyplexes display a range of disulfide-dependent differences in their sensitivity to disassembly, we have evaluated how such differences affect transfection activity. The effect of disulfide content on transfection activity of the AON and DNA polyplexes was investigated in D2F2 murine mammary carcinoma cells (Figure 8). All PAA/AON polyplexes showed similar knock-down levels with no statistically significant (one-way ANOVA) effect of PAA disulfide content observed (Figure 8a). In contrast, transfection activity of PAA/DNA polyplexes increased with increasing disulfide content in PAA (Figure 8b), although the observed trend was not statistically significant in linear regression analysis ($P > 0.05$ for slope being non-zero). One-way ANOVA with Bonferroni multiple comparison test, however, revealed that PAA-100 polyplexes had significantly higher transfection activity than all the other polyplexes with lower disulfide content. PAA-100 polyplexes showed a 152-fold higher transfection than PAA-0/DNA and a 6-fold higher transfection compared with control PEI/DNA polyplexes. The results show that despite the similarities in the disassembly behavior, bioreducible PAA only enhanced transfection of DNA, while providing no benefits for AON. The pattern of DNA transfection dependence on disulfide content in PAA was similar to what was reported for the same PAA previously (Lin, Zhong et al. 2006). The results clearly show that intracellular degradation of PAA plays no significant role in AON delivery and indirectly suggest that disassembly is not a barrier to effective AON delivery by

polyplexes.

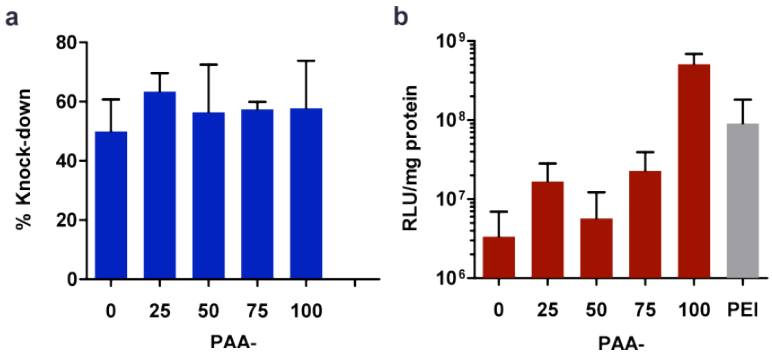

Figure 8. Effect of disulfide content on transfection activity of PAA polyplexes. D2F2 cells were transfected with (a) anti-luciferase AON polyplexes and (b) luciferase DNA polyplexes. Results are expressed as % knock-down of luciferase expression and RLU/mg protein, respectively. (mean ± S.D., n = 4)

2.3.8 Cell uptake of PAA/DNA polyplexes

Because no effect of the presence of disulfide bonds on AON transfection was observed, elucidating the reasons for increased DNA transfection was further studied. The cellular uptake of PAA/DNA polyplexes was measured (Figure 9) at the end of the 3 h incubation period by quantifying the fluorescence intensity of polyplexes formulated with DNA that was non-covalently labeled with YOYO-1. The results show about 2-fold higher DNA uptake with PAA-100/DNA polyplexes when compared with the other four PAA/DNA polyplexes.

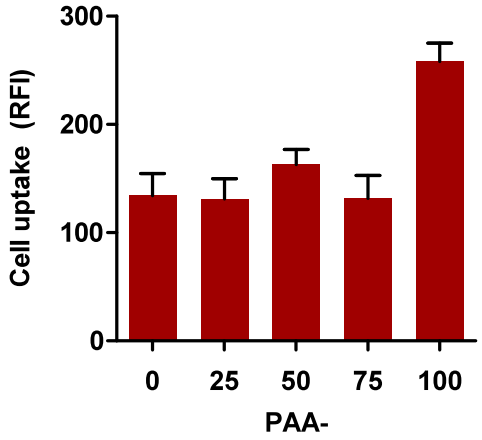

Figure 9. Effect of disulfide content on cell uptake of PAA/DNA polyplexes. D2F2 cell uptake of DNA labeled with YOYO-1 was measured after 3 h incubation with PAA polyplexes using flow cytometry. Cell uptake is shown as mean relative fluorescence intensity (RFI) ± S.D. (n = 6)

2.3.9 Intracellular clearance of pDNA after transfection with PAA polyplexes

Cell uptake shown in Figure 9 is only a snapshot at a single time point and one that is unable to distinguish between intact (viable) and degraded (nonviable) DNA. The rate of intracellular plasmid DNA clearance is also an important determinant of transfection efficiency. Intracellular clearance of plasmid DNA has been connected to disassembly rates of polyplexes and thus the kinetics of intracellular clearance of plasmid DNA delivered by PAA was further investigated (Figure 10). D2F2 cells were incubated with the polyplexes for 3 h and then harvested at 0, 6, 12, 18, 24, and 48 h after the incubation. The amount of plasmid DNA in whole cell lysate at the different time points was quantified with RT-PCR. The results from this independent experiment confirmed findings from Figure 9 that PAA-100/DNA polyplexes exhibit the highest initial cell uptake. The results show that intracellular plasmid DNA content declined rapidly in the first 18

h after incubation. Analysis of the data using first-order kinetics (ln[DNA] vs. time) revealed no statistically significant trend as the rate constants of the plasmid DNA clearance were similar regardless of the disulfide content in PAA.

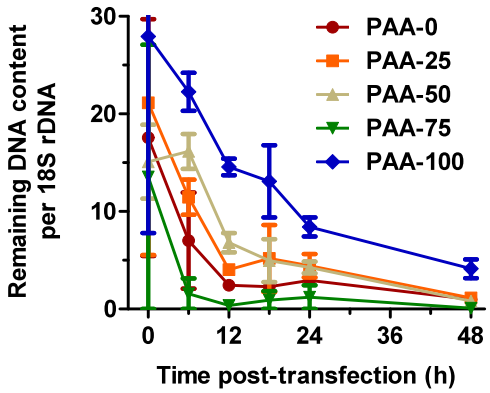

Figure 10. Intracellular clearance of plasmid DNA delivered by PAA. D2F2 cells were incubated with PAA/DNA polyplexes for 3 h. The cells were then harvested and lysed at different time points post-incubation and luciferase DNA was quantified and normalized to 18S rDNA by RT-PCR. (mean number of plasmid DNA copies per 18S rDNA ± S.D., n = 4)

2.3.10 Influence of cell surface thiols on transfection activity of PAA/DNA polyplexes

Since all the PAA/DNA polyplexes had similar physicochemical properties, we hypothesized that thiol-disulfide exchange between the disulfides in PAA/DNA polyplexes and reducing thiols in plasma membrane proteins could be responsible for the increased uptake and transfection of bioreducible DNA polyplexes. It has been reported that similar thiol-disulfide reactions on the cell surface are required for cell entry of viruses like HIV and play a role in cell entry of disulfide-containing peptides (Ryser, Levy et al. 1994; Markovic, Stantchev et al. 2004; Jain, McGinnes et al. 2007; Aubry, Burlina et al. 2009). An early study also suggested the reducing cell surface thiols are involved in cell uptake of

bioreducible lipoplexes (Kichler, Remy et al. 1995). To further investigate the role of PAA disulfide bonds in facilitating enhanced cell uptake and transfection activity, the effect of plasma membrane protein thiols on transfection activity of PAA polyplexes was studied (Figure 11). D2F2 cells were treated for 30 min before transfection with cell impermeable nonspecific thiol blocker DTNB to block external plasma membrane protein thiols. The effect of the thiol blocking on transfection activity was then studied and the results were expressed as a relative transfection, calculated as the ratio of luciferase expression in DTNB-treated vs. untreated cells. As shown in Figure 11, non-reducible polyplexes (PAA-0) showed a 27% decrease in transfection after DTNB pretreatment (i.e., relative transfection 0.73). In contrast, all bioreducible PAA polyplexes exhibited significant decrease in transfection. Polyplexes prepared with PAA-100 exhibited the largest decrease (97.6%) after blocking the plasma membrane surface thiols. As a result of the DTNB treatment, absolute levels of luciferase expression of all five PAA/DNA polyplexes was similar regardless of the disulfide content in PAA. Hence by blocking the cellular surface thiols, the transfection of disulfide-containing polyplexes is decreased to a much larger extent than transfection of non-reducible PAA polyplexes. In fact, blocking the surface thiols resulted in the bioreducible polyplexes losing their transfection advantage as all five tested PAA/DNA polyplexes exhibited similar levels of transfection in cells with the cell surface thiols blocked. This evidence suggests that the thiol-disulfide reactions at the cell membrane play a key role in enhancing transfection of the bioreducible PAA/DNA polyplexes.

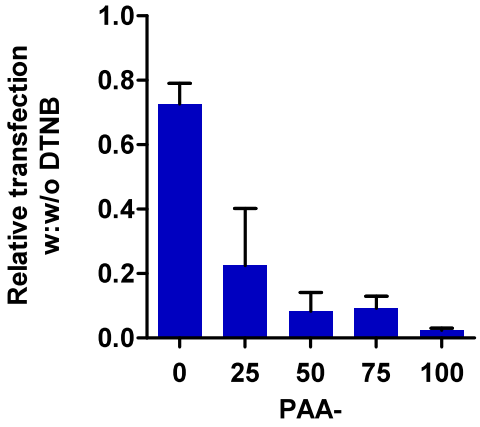

Figure 11. Effect of cell surface thiols on inhibition of transfection of PAA/DNA polyplexes. D2F2 cells were pretreated with 1 mM DTNB for 30 min before transfection. The data represent relative transfection in RLU/mg protein in cells pretreated with DTNB vs. untreated cells.

2.4 Conclusions

Bioreducible polyplexes have shown to be promising vectors for delivery of nucleic acids due to low toxicity and favorable transfection activity. The often improved transfection is usually explained by enhanced intracellular reductive disassembly of the polyplexes. This study evaluated the effect of enhanced reductive disassembly on transfection activity of plasmid DNA and AON polyplexes based on a series of bioreducible poly(amido amine)s (PAA). The presence of disulfide bonds in PAA had no effect on nucleic acid binding, hydrodynamic size and zeta potential of polyplexes. Increasing the disulfide content in PAA increased susceptibility to reduction-triggered DNA and AON release from the polyplexes. Increasing the disulfide content in PAA increased DNA transfection but had no effect on AON transfection. Plasma membrane protein thiols played a key role in the observed enhancement of DNA

transfection. The presence of disulfide bonds in PAA had no significant effect on the rate of intracellular DNA clearance, suggesting that enhanced intracellular disassembly of the bioreducible polyplexes is not a major contributing factor to the improved transfection activity.

As illustrated in this chapter, the advantages of bioreducible polyplexes are much more pronounced when delivering plasmid DNA than when delivering small nucleic acids. The following chapters will focus on improving plasmid DNA delivery by various methods including modifying the system with cancer targeting moiety (Chapter 3), developing multifunctional delivery system for gene delivery and PET imaging (Chapter 4) and combined drug/gene delivery (Chapter 5).

CHAPTER 3

CD44-TARGETED BIOREDUCIBLE POLYPLEXES FOR GENE DELIVERY

3.1 Introduction

The primary challenge for non-viral cancer gene therapy is to safely deliver an effective dose of therapeutic gene to the desired tumor tissue. Despite many advantages of non-viral vectors over viral vectors low efficiency and lack of targeting ability remain to be major problems faced by non-viral gene delivery vectors (Lo, Day et al. 2005; Yamamoto and Curiel 2005; Kaneda and Tabata 2006; Alexandrova 2009). Bioreducible polyplexes with the capability to respond to redox potential gradients across the cell membrane demonstrated promise as attractive non-viral candidates for cancer gene therapy. Incorporating disulfide bonds into the structure of polycations allows polyplexes to undergo intracellular GSH-mediated reduction which leads to rapid intracellular release of the delivered nucleic acids (Gilbert 1997; Jiang, Fitzgerald et al. 1999; Donoghue and Hogg 2002). The improved disassembly of the polyplexes ultimately enhances the transfection efficiency and decreases cytotoxicity of the polyplexes (Read, Singh et al. 2005; You, Manickam et al. 2007; Manickam, Hirata et al. 2008; Chen, Wu et al. 2009; Zhou, Wu et al. 2009). Evidence shows that many types of cancer, including melanoma exhibit significantly elevated GSH levels, which is often correlated with higher metastatic potential. The elevated GSH levels in tumor cells compared with most normal tissues might be advantageously exploited to improve activity of the redox-responsive polyplexes.

Invasive cancers have the capability to metastasize from the primary tumor site through the vasculature or lymphatic system to distant organs. The process greatly depends on the ability of cancer cells to attach to and invade through the extracellular matrix. CD44 is a cell-surface glycoprotein that functions as a signaling transmitter that controls cellular adhesion, migration, and invasion. All these processes are involved in cancer metastasis, which makes CD44 highly relevant to cancer cell invasion and metastasis (Matsumura and Tarin 1992; Dietrich, Tanczos et al. 1997; Sheridan, Kishimoto et al. 2006; Ouhtit, Elmageed et al. 2007). Overexpression of CD44 is often found in many types of metastatic cancer cells such as breast cancer, lung carcinoma and melanoma. There is increasing evidence that cancer cells that overexpress CD44 are more metastatic than cells with low CD44 levels (Naor, Nedvetzki et al. 2002; Al-Hajj, Wicha et al. 2003; Hill, McFarlane et al. 2006). In addition to the importance of CD44 as a target in metastatic cancers, growing evidence has linked CD44 with the cancer stem cell hypothesis (Al-Hajj, Wicha et al. 2003; Collins, Berry et al. 2005; Li, Heidt et al. 2007; Prince, Sivanandan et al. 2007). The validity of CD44 as a target in human cancers has been confirmed in clinical trials using anti-CD44 antibodies for the treatment of CD44-expressing tumors (Colnot, Ossenkoppele et al. 2002; Borjesson, Postema et al. 2003; Colnot, Roos et al. 2003; Koppe, Schaijk et al. 2004; Tijink, Buter et al. 2006; Rupp, Schoendorf-Holland et al. 2007; Sauter, Kloft et al. 2007).

CD44 is a receptor for hyaluronic acid (HA), which is one of several nonsulfated glycosaminoglycan components found in the extracellular matrix. HA

plays an important role, through CD44, in regulating cell adhesion and motility and mediating cell proliferation and differentiation (Entwistle, Hall et al. 1996; Collis, Hall et al. 1998). HA is a water soluble, non-immunogenic linear polysaccharide consisting of alternating D-glucoronic acid and N-acetyl-D-glucosamine units with a molecular weight ranging from 1 to 10,000 kDa (Scheme 2). HA has been utilized directly as a drug carrier that can potentially target CD44-overexpressing cancers. Since HA contains multiple functional groups available for conjugation, it has also been investigated as a targeting moiety and used to modify nanocarriers, such as liposomes and polyplexes (Pouyani and Prestwich 1994; Luo and Prestwich 1999; Luo, Ziebell et al. 2000; Eliaz and Szoka 2001; Eliaz, Nir et al. 2004; Peer and Margalit 2004; Peer and Margalit 2004; Lee, Mok et al. 2007; Hornof, de la Fuente et al. 2008; Jiang, Park et al. 2008; Lee, Lee et al. 2008; Lee, Ahn et al. 2009; Surace, Arpicco et al. 2009). Although CD44 is also found expressed in normal cells, selective targeting to tumors is still possible because HA binding is greatly affected by post-translational modifications of CD44 (Lesley, English et al. 2000; Lesley, Hascall et al. 2000; Naor, Wallach-Dayan et al. 2008). For example, B cells express CD44 but they do not bind HA until the CD44 is deglycosylated upon B cell activation (Hathcock, Hirano et al. 1993; Katoh, Zheng et al. 1995; Skelton, Zeng et al. 1998). In addition, solid tumors often exhibit a phenomenon called enhanced permeability and retention (EPR) effect, which could be used for passive targeting. This allows macromolecules and nanoparticles to preferentially accumulate within tumors due to leaky tumor vasculature and limited lymphatic

clearance (Maeda, Seymour et al. 1992; Hobbs, Monsky et al. 1998). In addition, HA can function not only as a targeting ligand but also as a hydrophilic protective shell promoting extended plasma circulation (Peer and Margalit 2004; Peer and Margalit 2004).

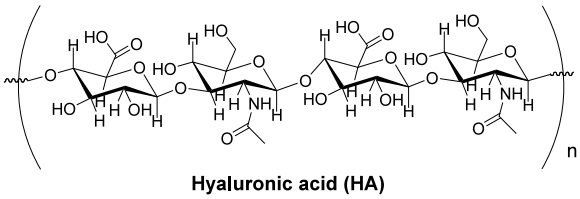

Scheme 2. Chemical structure of HA.

The molecular weight of HA has been reported to affect its targeting property and stabilization ability (Prestwich, Marecak et al. 1998; Girotto, Urbani et al. 2003; Jiang, Park et al. 2008; Surace, Arpicco et al. 2009). High-molecular-weight HA was shown to contribute to improved steric stability of nanoparticles and liposomes. However, it tends to be more easily cleared from systemic circulation by the liver membrane-bound HA receptor for endocytosis (HARE) (Zhou, McGary et al. 2003). Hence, for the purpose of our study we will use low- and medium- (6.4 kDa and 59 KDa) molecular-weight HA to achieve CD44 targeting while avoiding rapid clearance by the liver HARE.

Recent studies from our laboratory have shown improved transfection efficiency and low toxicity of a type of bioreducible hyperbranched poly(amido amine)s (RHB) in vitro due to the high intracellular GSH level of cancer cells (Chen, Wu et al. 2009). The hypothesis of this chapter is that low and medium molecular weight HA will stabilize the bioreducible polyplexes and enable targeting to the CD44-positive tumor cells. Three different approaches will be

applied to modify RHB polyplexes with HA: (i) Non-covalent stabilization of RHB/DNA polyplex by electrostatic deposition of HA layer on the surface; (ii) Post-grafting of HA to preformed RHB/DNA polyplexes by covalent conjugation using *N*-hydroxysuccinimidyl ester of HA (HA-NHS); and (iii) Preparation of graft copolymers of HA and RHB and their use for the formation of DNA polyplexes. The effect of the molecular weight and method of HA modification will be studied.

3.2 Materials and Methods

3.2.1 Materials

N,N'-cystaminebisacrylamide (CBA) was obtained from Polysciences, Inc. (Warrington, PA). HA was from Lifecore Biomedical, Inc. (Chaska, MN). Plasmid DNA, gWiz high-expression luciferase (gWiz-Luc) containing luciferase reporter gene was from Aldevron (Fargo, ND). YOYO®-1 iodide was from Invitrogen (Carlsbad, CA). All the anti-mouse CD44 and control antibodies were from Biolegend (San Diego, CA). Dulbecco's Modified Eagle Medium (DMEM), Dulbecco's Phosphate Buffered Saline (PBS), Fetal Bovine Serum (FBS) were from Fisher Scientific. All other reagents and chemicals were obtained from Fisher Scientific or VWR International unless otherwise noted.

3.2.2 Cell culture

Murine melanoma cell line B16F10 was purchased from ATCC (Manassas, VA). B16F10 cells were maintained in DMEM media supplemented with 10% FBS and cultured at 37 °C in 5% CO_2 atmosphere.

3.2.3 Flow Cytometry

The overexpression of CD44 on B16F10 cells and cellular association of the FITC-labeled HA were confirmed using flow cytometry. Cells were plated in a 24-well plate 24 hours before. Cells were detached from the plates by non-enzymatic cell dissociation solution Cellstripper^{TM} and incubated with FITC-conjugated anti-CD44 antibody or FITC-conjugated HA for 30 min on ice before complete wash with PBS and counting by flow cytometry. Histogram plots were constructed using the CellQuest software. The mean fluorescence intensity from each sample was obtained and the cellular uptake was quantified as average mean fluorescence intensity ± SD of triplicate samples.

3.2.5 Synthesis of RHB, HA-NHS, and RHB-HA

RHB polymers were synthesized Michael addition reaction of equal molar ratio of CBA and dimethyldipropylenetriamine (DMDPTA) at 50 °C in methanol/water (v/v 8/2) mixture following our previously published protocol (Chen, Wu et al. 2009) (Scheme 3). The synthesis of RHB for HA conjugation was modified by replacing 10% of DMDPTA with the same molar amount of N-Boc-ethylenediamine to introduce primary amines. After isolation of the copolymer, the Boc groups were removed by treatment with a mixture of trifluoroacetic acid: triisobutylsilane: H_2O=95: 2.5: 2.5, v/v (Brumbach, Lin et al. 2010), resulting in RHB with primary amines available for reaction with HA-NHS.

Any residual solvents were removed by extensive dialysis followed by lyophilization.

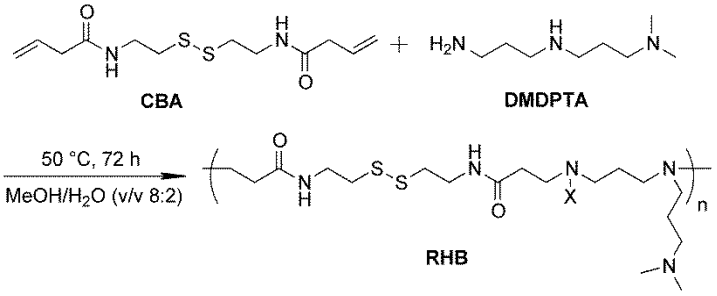

Scheme 3. Synthetic scheme of RHB, X=H or polymer chain.

The sodium salt of HA (both 6K and 60K) was converted to a tetrabutylammonium (TBA) salt by acidic ion exchange (room temperature, 8 h) with Dowex 50 W × 8–200 resin. Based on a published method (Luo and Prestwich 2001), active N-hydroxysuccinimidyl ester of HA (HA-NHS) was then synthesized by reaction with N-hydroxysuccinimidyl diphenylphosphate (SDPP) with HA.TBA. The resulting HA-NHS was isolated by precipitation in hexane, washed with excess acetone and finally dried under vacuum.

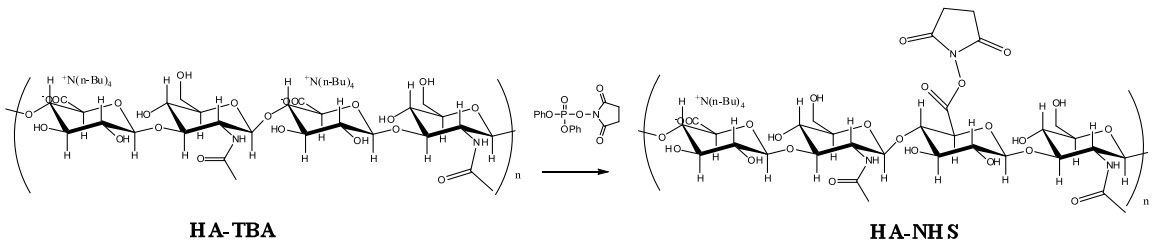

Scheme 4. Synthesis of the active NHS ester of HA.

The synthesis of RHB-HA copolymers was conducted by stirring HA-NHS (dissolved in anhydrous DMSO) and RHB (w/w 1) in 0.1 M borate buffer (pH 8.5)

with 0.15 M NaCl for 24 h. RHB-HA was then purified and isolated by dialysis and lyophilization.

3.2.6 Preparation of HA-containing RHB polyplexes

gWiz-Luc DNA solution at a concentration 20 μg/mL was prepared in 10 mM HEPES buffer (pH 7.4). RHB-6HA and RHB-60HA DNA polyplexes were formed by adding predetermined volume of HA-RHB copolymer to achieve the desired w/w ratio and mixed by vigorous vortexing for 10 s. Polyplexes were further allowed to stand for 30 min prior to use. Electrostatically stabilized RHB/DNA polyplexes (denoted as pp/6HA and pp/60HA) were prepared by adsorbing a layer of HA (6kDa or 60kDa) on the surface by adding a predetermined amount of HA to preformed RHB/DNA polyplexes and allowing the mixture to stand for 1 h. Post-grafted polyplexes (denoted as pp-6HA and pp-60HA) were prepared by adding predetermined amount of HA-NHS to preformed RHB/DNA polyplexes and letting the mixture to react for 4 h. The determination of hydrodynamic diameters and zeta potentials of polyplexes was performed by Dynamic Light Scattering (DLS). Results were expressed as mean ± standard deviation (S.D.) of 3-10 experimental runs.

3.2.7 Gel electrophoresis

The stabilization of the polyplexes against disassembly induced by serum and heparin was examined by agarose gel electrophoresis using previously published protocol (Li, Manickam et al. 2012). Briefly, gWiz-Luc DNA polyplexes

were incubated under indicated conditions with heparin or serum at 37 °C for 1 h. Samples were then loaded onto a 0.8% agarose gel containing 0.5 μg/mL EtBr and run for 75 min at 120 V in 0.5x Tris/Borate/EDTA (TBE) running buffer. The gel was then visualized under UV.

3.2.8 Cell uptake

The cellular association of the fluorescently-labeled polyplexes was measured using fluorescent microplate reader. B16F10 cells were plated in a 96-well black plate with optical bottom 24 hours before. DNA was labeled with YOYO-1 by mixing at a ratio of 1 dye molecule per 100 bp of DNA and used to prepare polyplexes as above. After 4 h of incubation with the polyplexes, the cells were washed with PBS and the fluorescence was measured by Synergy 2 Microplate Reader (BioTek, VT). The mean fluorescence intensity from each sample was obtained and the cellular uptake was quantified as average mean fluorescent units (RFU) ± SD (n=4).

3.2.9 Luciferase transfection

All transfection experiments were conducted in 48-well plates with cells at logarithmic growth phase following a previously published protocol (Read, Singh et al. 2005). Cells were seeded at a density of 40,000 cells/well 24 h prior to transfection. On the day of transfection, cells were incubated with the polyplexes (DNA conc. 2.35 μg/mL) in 170 μL of serum-free or 10% FBS-containing media. After 4 h incubation, polyplexes were completely removed and the cells were

maintained in complete culture medium for 24 h prior to measuring luciferase expression. The medium was discarded and the cells were lysed in 100 µL of 0.5x cell culture lysis reagent buffer (Promega, Madison, WI) for 30 min. To measure the luciferase content, 100 µL of 0.5 mM luciferin solution was automatically injected into each well of 20 µL of cell lysate and the luminescence was integrated over 10 s using Synergy 2 Microplate Reader (BioTek, VT). Total cellular protein in the cell lysate was determined by the Bicinchoninic acid (BCA) protein assay using calibration curve constructed with standard bovine serum albumin solutions (Pierce, Rockford, IL). Transfection activity was expressed as relative light units (RLU)/mg cellular protein ± SD of quadruplicate samples.

3.3 Results and Discussion

3.3.1 Determination of CD44 overexpression in B16F10 cells in vitro

CD44 overexpression in many metastatic cancers, including melanoma, has been utilized as a biomarker and an anti-cancer target for drug and gene delivery. The amount of CD44 in murine melanoma cells B16F10 was first confirmed by flow cytometry using FITC-conjugated anti-CD44 antibody (Figure 12a). FITC-conjugated antibody isotype was used as a negative control. The overlay image of the histograms clearly shows the elevated CD44 expression in B16F10 cells. In preparation for in vivo testing of the HA-targeted polyplexes, we have also verified CD44 expression in B16F10 cells stably expressing luciferase (B16F10.Luc) that allow easy non-invasive optical imaging of the tumor growth and metastatic spread. To confirm binding of HA to CD44 receptors in B16F10

cells, FITC-conjugated HA (6K and 60K) was incubated with the cells and uptake was determined by flow cytometry (Figure 12b and c). The results show that both low- and medium-molecular-weight HA was able to bind with CD44 receptors overexpressed in B16F10 melanoma cells. The differences in FITC-HA uptake between 4 and 37 °C support involvement of energy-dependent endocytosis in the internalization of HA in B16F10 and B16F10.Luc (Figure 12d). Specificity of the HA binding and internalization was investigated in polyplexes in studies described below.

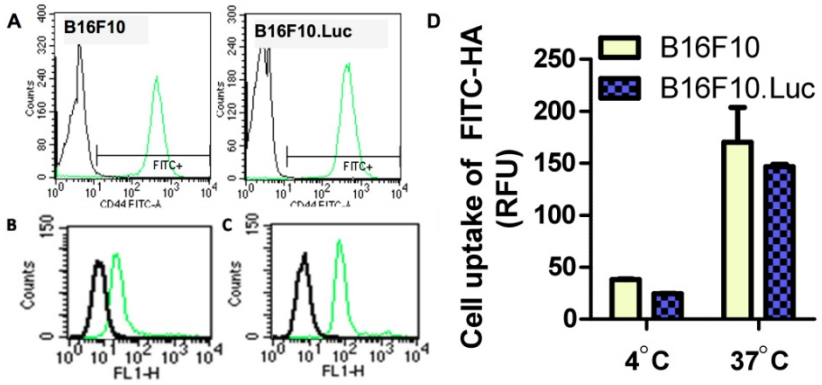

Figure 12. (A) Overexpression of CD44 in B16F10 and B16F10.Luc cells determined by FACS using FITC labeled anti-CD44 antibody. (B) Cell uptake of FITC-conjugated low-molecular-weight (6 kDa) HA and (C) medium-molecular-weight (60 kDa) HA. (D) FITC-HA (60 kDa) uptake at 4 and 37°C).

3.3.2 Physicochemical characterization of CD44-targeted RHB polyplexes

Several different strategies have been used to modify HA in the past. They include modification of the carboxyl groups, hydroxyl groups, and the reducing end of HA (Pouyani and Prestwich 1993; Bulpitt and Aeschlimann 1999; Choi, Min et al. 2009). When we first attempted direct carbodiimide-mediated coupling

of primary amines of RHB to HA, negligible coupling efficiency was observed, most likely due to the protonation of the required nucleophilic nitrogens at the reaction pH (Luo and Prestwich 2001). Modified carbodiimide chemistry has been used extensively to modify HA for coupling to other polymeric carriers and various small molecule drugs. Luo et al. have described a convenient route to achieve high degree of HA substitution using NHS ester of HA. The NHS-HA has proven to be a versatile precursor for bioconjugation of HA with a variety of molecules, including drugs and labeling dyes. In this study, we have thus used HA-NHS for direct coupling to RHB as well as post-grafting to RHB/DNA polyplexes.

In this comparative study, three approaches to HA incorporation into polyplexes were used using two different molecular weights of HA. The main goal was to determine which of the three approaches provides the best combination of CD44 targeting, steric stability, and transfection activity of polyplexes.

Size and zeta-potential of the HA-containing RHB/DNA polyplexes were measured using DLS and the results are summarized in Table 3. Unmodified RHB/DNA polyplexes show the smallest size of 87 nm with the highest zeta-potential. All the polyplexes containing HA with molecular weight 60 kDa, regardless of the method of preparation, had a relatively small size ranging from 125 to ~280 nm. In contrast, the use of low-molecular-weight HA (6 kDa), resulted in polyplexes with significantly larger sizes ranging from ~600 to ~800 nm. RHB-6HA and RHB-60HA polyplexes formed by direct complexation of DNA and HA-RHB copolymers showed the highest positive high zeta-potential,

probably due to the limited amount of HA in the polyplexes and incorporation of a portion of HA in the internal structure of the polyplexes. Post-modified polyplexes, either by the non-covalent or covalent approach, all exhibited decreased zeta-potential, which was especially pronounced for the 60K HA covalently post-modified polyplexes. These findings confirm the important role of molecular weight of HA on achieving steric stability of nanoparticles. The higher molecular weight HA provided a better stabilization, both by steric and electrostatic mechanism, than the low molecular weight HA as documented by both the smaller size of the polyplexes and their lower zeta potential. The results also suggest that approaches that incorporate HA selectively on the surface of polyplexes may provide better stabilization and presentation of HA for subsequent receptor binding. Despite the disappointing results with HA 6 kDa, there is a possibility to achieve steric stabilization of polyplexes and better surface presentation of HA by additional incorporation of stabilizing molecules like PEG.

Table 3. Hydrodynamic size and zeta-potential of optimized CD44-targeted polyplexes prepared at w/w 4 (RHB to pDNA).

	Size (nm)	*Zeta-Potential (mV)*
RHB	87 ± 2	35 ± 6
RHB-6HA	668 ± 13	34 ± 1
RHB-60HA	125 ± 1	26 ± 5
pp/6HA	630 ± 11	19 ± 2
pp/60HA	219 ± 1	-7 ± 1
pp-6HA	795 ± 30	5 ± 1
pp-60HA	279 ± 2	-7 ± 1

3.3.3 Stability of HA-containing RHB/DNA polyplexes against serum- and heparin-induced disassembly

Steric stabilization with PEG has been proven to avoid rapid clearance and limit non-specific tissue distribution of systemically administered polyplexes due to less binding with various plasma proteins (Davis 2009). It has been reported that HA can provide liposomes and polymersomes with similar steric stabilization as PEG and thus improve systemic circulation (Peer and Margalit 2004; Peer and Margalit 2004; Ito, Yoshihara et al. 2010). In order to assess the effect of HA on the stability of RHB/DNA polyplexes, all three types of HA-containing polyplexes were treated with 10% or 50% FBS and 80 μg/ml of heparin. As shown in Figure 13, RHB was able to condense DNA and protect it from serum degradation as expected but could not resist disassembly caused by heparin competition. The increased fluorescence in the starting wells of the serum-treated samples and the slight smear suggest loosening of the polyplex

structure and partial release and degradation of DNA from the RHB/DNA polyplexes. All the HA-containing polyplexes exhibited enhanced stability against serum as suggested by the decreased fluorescence in the gel compared with nonmodified polyplexes. Furthermore, polyplexes that were stabilized by covalent post-grafting also showed enhanced stability against heparin-induced disassembly. From our previous studies we know that combination of stability against serum and heparin is a good predictor of prolonged plasma circulation of polyplexes.

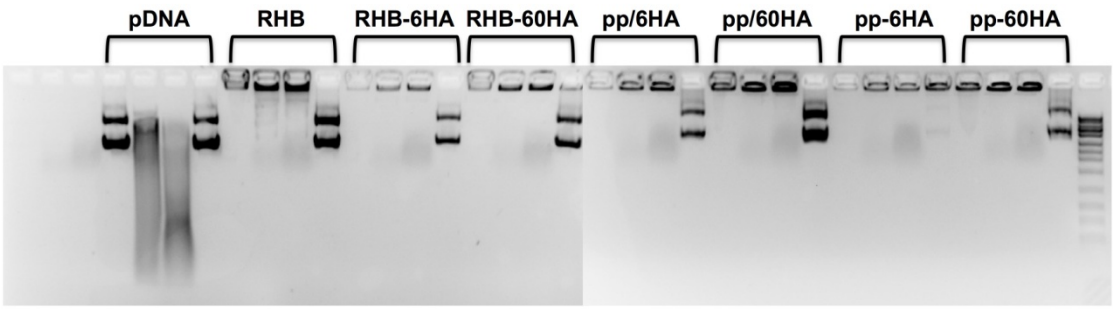

Figure 13. Agarose gel electrophoreses for the optimized polyplexes against serum and heparin. Four conditions from left to right are: 1) no treatment 2) +10% FBS 3) +50% FBS 4) +0.5mg/ml heparin, respectively.

3.3.4 Cell uptake and transfection activity of HA-containing RHB/DNA polyplexes

Unmodified RHB/DNA polyplexes have shown high *in vitro* transfection efficiency in B16F10 cells by taking advantage of the efficient non-specific cell uptake and rapid intracellular DNA release due to elevated GSH levels (Chen, Wu et al. 2009). Here, we have evaluated the targeting and transfection effect of HA in the three types of HA-containing RHB/DNA polyplexes (Figure 14). Enhanced cellular uptake in serum-free (-FBS) conditions compared with unmodified RHB/DNA was observed in the case of HA-RHB polyplexes. No

increase in the cell uptake was observed for any other HA-containing polyplexes tested. This confirms that non-specific, charge-mediated cellular uptake of non-modified polyplexes is highly efficient and that specific receptor-mediated uptake of polyplexes is a less efficient process despite its selectivity. The observation that HA-containing polyplexes with the highest positive charge had the highest cell uptake confirms this conclusion and suggests that the observed uptake is a combination of non-specific and CD44 specific uptake. In contrast, when cell uptake was tested in the presence of serum, the HA-containing polyplexes have maintained or increased their uptake when compared with the unmodified RHB/DNA polyplexes. This confirms the importance of the HA for stabilizing the polyplexes and the role serum protein binding plays in the activity of polyplexes. Surprisingly, HA 6 kDa showed an overall better performance than HA 60 kDa suggesting a complex relationship between surface shielding, steric stabilization, and receptor binding of polyplexes.

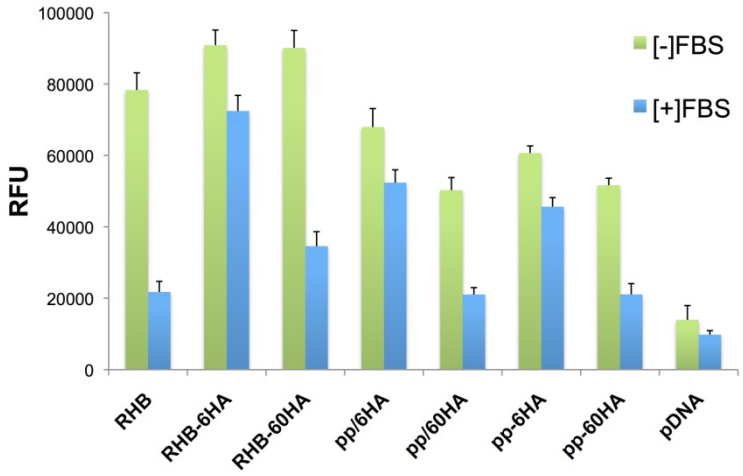

Figure 14. Cell uptake of the optimized polyplexes. pDNA was labeled with YOYO-1 before polyplexes preparation and B16F10 cells were incubated with the polyplexes for 4 h.

Figure 15 shows the effect of HA on transfection efficiency of the polyplexes. Mirroring the uptake results, it is obvious that transfection of the HA-containing polyplexes is less adversely affected by the presence of serum. Again confirming the importance and benefits of HA stabilization on the properties of polyplexes. HA-containing polyplexes are thus better suited for in vivo applications than the non-modified RHB/DNA polyplexes. Regardless of their type, polyplexes containing HA 6kDa showed better transfection activity than the corresponding polyplexes containing HA 60 kDa. While some of the effect is undoubtedly due to higher zeta potential of the polyplexes with HA 6 kDa, there is a possibility that the some of the effect is also due to the molecular weight dependence of HA binding to CD44 (Hornof, de la Fuente et al. 2008). Significantly increased avidity of binding has been observed for HA with molecular weight above 4.2 kDa due to its divalent binding to CD44 receptors for which the minimum HA chain length is 20 saccharide residues. No further increase in binding avidity was observed for HA above 6.4 kDa (Lesley, Hascall et al. 2000).

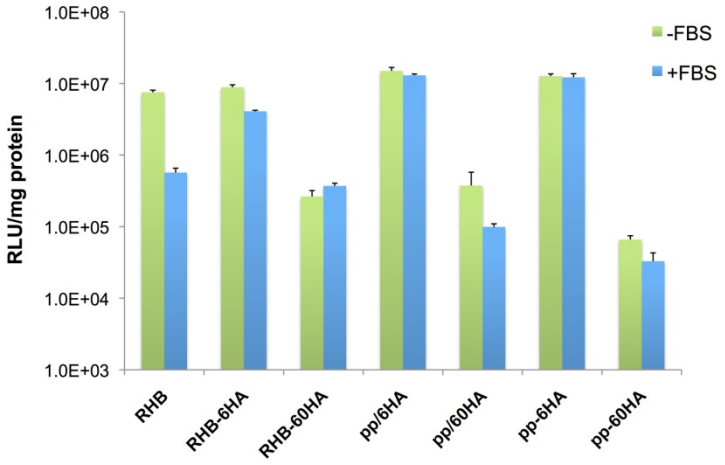

Figure 15. Luciferase transfection efficiency of the optimized CD44-targeted polyplexes in B16F10 cells.

To determine to what extent is the observed cell uptake and transfection of HA-containing polyplexes dependent on CD44-specific internalization, competitive binding experiments were conducted. Cell uptake and transfection were tested in B16F10 cells pre-treated with anti-mouse CD44 monoclonal antibody to block the CD44 cell surface receptors and to compete for binding with the HA-containing polyplexes. In these experiments, only formulations containing HA 6 kDa were used and the experiments were conducted in serum-containing conditions. Figure 16 shows significant decrease in both cell uptake and transfection efficiency of HA-containing polyplexes when cells were pretreated with anti-CD44 antibody. At the same time, the unmodified polyplexes were not affected by the antibody pretreatment. These results suggest that CD44-specific cell uptake plays an important role in the observed activity of HA-containing polyplexes and that HA can indeed provide receptor specific activity when incorporated in bioreducible polyplexes.

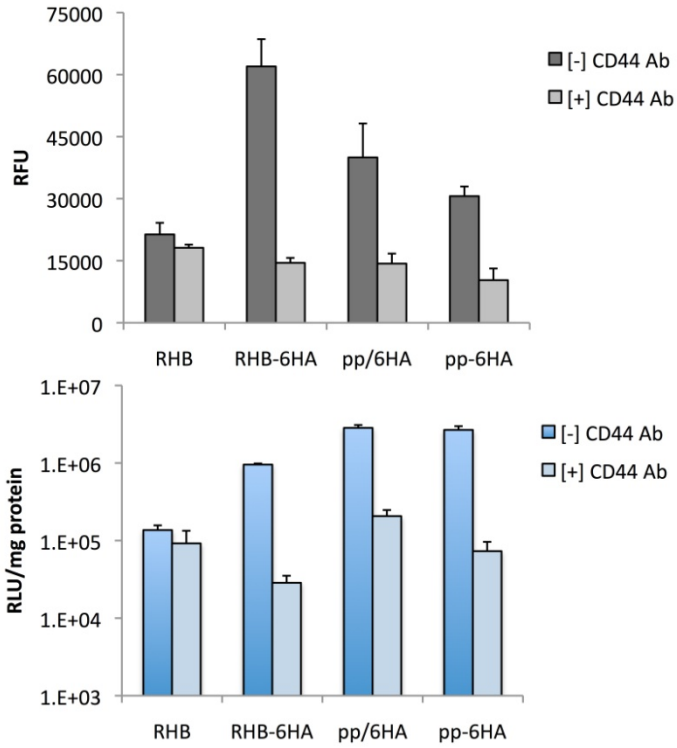

Figure 16. Effect of competitive binding on cell uptake and transfection. Cells were treated with 1 μg/ml anti-murine CD44 monoclonal antibody in DMEM containing 10% FBS for 30 min before adding polyplexes for another 4 h of incubation.

3.4 Conclusions

Three different approaches to incorporate HA into the structure of bioreducible DNA polyplexes have been explored with the goal of improving steric stability and achieving CD44-selective uptake and transfection. Our results show that higher molecular weight HA is required for steric stabilization of the polyplexes, while lower molecular weight HA was beneficial for transfection activity and CD44-specific cell uptake. Overall, none of the developed formulations was deemed suitable for advancement into *in vivo* testing. Further

studies and development are needed to combine steric stabilization with efficient CD44-selective transfection into a single formulation.

CHAPTER 4

CYCLAM-BASED BIOREDUCIBLE POLYMERIC COPPER CHELATORS FOR GENE DELIVERY AND POTENTIAL PET IMAGING

Please note that the content of this chapter was submitted for publication in Biomacromolecules. As the first author, I performed all the work described in this chapter except the determination of degree of branching of the polymers by LC-MS/MS (contributed by Yu Zhu, the second author) and NMR experiments and analysis (contributed by Dr. S. Hazeldine, the third author). All the authors agreed with including their work in this dissertation.

4.1 Introduction

The main advantages of using synthetic gene delivery vectors over viral delivery systems include enhanced safety profile, more feasible large-scale production, better control of the nucleic acids release, and providing a large platform for vector design and engineering. Of great interest in developing multifunctional carriers for gene therapy is to incorporate bio-imaging probes such as radiolabels, contrast agents, and fluorophores in the vesicles, for simultaneous visualization, characterization and quantification of many biological processes in living subjects (Zrazhevskiy, Sena et al. 2010). Such in vivo imaging probes could be applied in many imaging tools, including Positron Emission Tomography (PET), Magnetic Resonance Imaging (MRI), Computed

Tomography (CT) and Single Photon Emission Computed Tomography (SPECT).

Cyclam (1,4,8,11-tetraazacyclotetradecane) is one of the best known chemical structures used in chelating diagnostic imaging probes. It is a macrocyclic ligand with four secondary amimes that forms highly stable complexes with virtually all transition metal ions. Macrocyclic chelators and their metal complexes have numerous biomedical applications, including PET and MRI (Murugesa, Shetty et al. 2001; Sun, Wuest et al. 2002; Boswell, Regino et al. 2009). The *in vivo* stability of the macrocyclic metal chelates is significantly higher than stability of acyclic chelators such as ethylenediaminetetraacetic acid (EDTA) (Sun, Wuest et al. 2002). Derivatives of cyclam and its relative cyclen (1,4,7,10-tetraazacyclododecane) have been subject of intensive research in the development of PET imaging probes using ^{64}Cu (Leung 2004; Sun, Kim et al. 2004; Boswell, Regino et al. 2009; Jin, Furukawa et al. 2011). Benefits of cyclams in PET imaging include high complexation affinity and high stability (the stability constant of complex of cyclam with Cu^{2+}, log K, is 27.2), which substantially benefit the systemic delivery of these imaging probes (Sun, Wuest et al. 2002). At the same time, ^{64}Cu shows great promise in PET imaging and targeted radiotherapy due to its half-life ($t_{1/2}$ = 12.7 h), decay characteristics (β+ (19%); β- (40%)), and easy large-scale production (Philpott, Schwarz et al. 1995; Sun, Wuest et al. 2002). The ^{64}Cu-complexes of the bicyclam compound AMD3100 have been shown to be an effective and stable PET imaging agent to image CXCR4 positive tumors in vivo (Jacobson, Weiss et al. 2009;

Nimmagadda, Pullambhatla et al. 2010). The ability to form metal complexes combined with the cationic nature at physiological pH make cyclam a suitable building block for designing nucleic acid delivery vectors with the possibility of easy labeling for simultaneous in vivo PET imaging. There are no previous reports of cyclam-based polycations used in gene delivery, although several reports describe incorporation of cyclen into gene delivery systems but their metal chelates were not described (Xiang, Feng et al. 2010; Huang, Ou et al. 2011; Huang, Zhong et al. 2011; Liu, Ma et al. 2011; Huang, Ren et al. 2012).

This chapter describes the studies on using cyclam as the building block of reducible polycationic chelators (RPC) that could be used as a novel type of theranostic vector for combined gene delivery and PET imaging. In this initial study, the synthesis and effect of Cu(II) complexation with RPC on physicochemical properties of RPC/DNA polyplexes and their gene delivery performance in vitro were explored.

4.2 Materials and Methods

4.2.1 Materials

Cyclam was purchased from Alfa Aesar (Ward Hill, MA). Heparin (sodium salt) was purchased from Sigma-Aldrich (St. Louis, MO). Dulbecco's Modified Eagle Medium (DMEM), Dulbecco's Phosphate Buffered Saline (PBS), Fetal Bovine Serum (FBS), L-Glutamine, and Penicillin-Streptomycin (Pen-Strep) solution were from Thermo Scientific (Waltham, MA). All other reagents and

chemicals were obtained from Fisher Scientific or VWR International unless otherwise noted.

4.2.2 Synthesis and characterization of RPC

RPC were synthesized by direct Michael addition polymerization of different molar ratios of cyclam and CBA. Calculated amounts of cyclam and CBA were weighted and dissolved in methanol/water mixture (v/v 7:3). Polymerization was allowed to proceed in the dark at 37 °C for 24-48 h and the reaction was stopped before gelation occurred and access of cylam was added to complete the reaction. The reaction mixture was then added dropwise to excess of 1.25 M HCl in ethanol so that pH of the mixture was kept around 3. The resulting precipitated RPC.HCl was isolated by centrifugation, washed twice with ethanol to remove excess HCl, and the product was dried in vacuum. The polymers were then dissolved in water and further purified by dialysis against water for 2 days (MWCO 1,000 for RPC/3 and MWCO 3,500 for RPC/2 and 1.8). The polymers were then lyophilized after dialysis.

The polymers were analyzed by ^{1}H NMR to confirm the completion of the reaction and polymer composition. Weight- and number-average molecular weights as well as polydispersity index (PDI) were determined by Size Exclusion Chromatography (SEC) using Viscotek GPCmax chromatography system consisting of an autosampler, a pump, a CTO-10ASVP Shimadzu column oven, a refractive index detector, a low- and right-angle light scattering detector, and OmniSEC software for chromatographic data analysis/storage (Malvern

Instruments, UK). The columns used in series were single pore AquaGel^{TM} columns (cat# PAA-202 and PAA-203) by PolyAnalytik (London, ON, Canada). Sodium acetate buffer (0.3 M, pH 5) was used as an eluent at flow rate of 0.3 mL/min.

4.2.3 Determination of degree of branching

The degree of branching was determined using a degradative method with LC-MS/MS detection following a published procedure (Christensen, Chang et al. 2006). Two mg of each RPC were dissolved in 1 mL sodium phosphate buffer (20 mM, pH 7.2) before adding 3.75 mg tris(2-carboxyethyl) phosphine (TCEP) as a reducing agent to cleave all the disulfide bonds. The mixture was then stirred at room temperature for 1 h, followed by addition of 2.5 mg of N-ethylmaleimide (NEM) to cap the free thiols. The reaction was then kept at room temperature for additional 2 h. The resulting NEM-derivatized fragments were analyzed by AQUITY UPLC® TQD system (Waters, MA). Chromatographic analysis was performed using ACQUITY UPLC® BEH ShieldRP18 column (2.1 x 100 mm, 1.7 µm). A gradient solvent system consisted of 0.1% formic acid (FA) in acetonitrile (solvent B) and 0.1% FA in water (solvent A). The gradient was increased from 5% to 95% solvent B over 3 min at a flow rate of 0.2 mL/min. Spectra were acquired using single ion recording (SIR) mode for m/z=457.46, 713.60, 969.79, 1225.79. The ratio of degraded fragments of terminal (T), linear (L), single-branched (S) and double-branched (D) cyclam units was determined by peak integrations in LC-MS/MS chromatograms. The relative degree of

branching (DB) was calculated using the following equation for AB_3 type polymers (Holter, Burgath et al. 1997):

$$DB = \frac{2D + S}{\frac{2}{3}(3D + 2S + L)}$$

4.2.3 Formation of RPC complexes with Cu(II)

Cu(II) complexes of RPC were formed by incubating polymer solutions with $CuCl_2$ in sodium acetate buffer (0.1 M, pH 6.0) for 1 h at room temperature. Complex formation was evaluated from the changes in absorption spectra (400 - 800 nm) measured by Synergy 2 Microplate Reader (BioTek, VT).

4.2.4 EtBr exclusion assay

The ability of RPC polycations to condense gWiz-Luc DNA was determined by EtBr exclusion assay by measuring the changes in EtBr/DNA fluorescence. DNA solution at a concentration of 20 μg/mL in 10 mM HEPES buffer (pH 7.4) was mixed with EtBr (1 μg/mL) and fluorescence was measured and set to 100% using an excitation wavelength of 540 nm and an emission wavelength of 590 nm. Fluorescence readings were then taken following a stepwise addition of a polycation solution, and the condensation curve for each polycation was constructed.

4.2.5 Preparation and characterization of RPC polyplexes

gWiz-Luc DNA solution in 10 mM HEPES (pH 7.4) was prepared to give a DNA concentration of 20 μg/mL in the polyplexes. Polyplexes were formed by

adding predetermined volume of polymer to achieve the desired polycation/DNA weight/weight (w/w) ratio and mixed by vigorous vortexing for 10 s. Polyplexes were further allowed to stand for 30 min prior to use. The determination of hydrodynamic diameters and zeta potentials of polyplexes was performed by Dynamic Light Scattering (DLS). Results were expressed as mean ± standard deviation (S.D.) of 3-10 experimental runs.

4.2.6 Agarose gel electrophoresis

The disassembly of the polyplexes was examined by agarose gel electrophoresis using previously published protocol (Manickam, Li et al. 2010). Briefly, gWiz-Luc DNA polyplexes were incubated under indicated conditions of different concentrations of heparin with or without a reducing agent (either GSH or DTT) at 37 °C for 1 h. Samples were then loaded onto a 0.8% agarose gel containing 0.5 μg/mL EtBr and run for 75 min at 120 V in 0.5x Tris/Borate/EDTA (TBE) running buffer. The gel was then visualized under UV.

4.2.7 Cell culture

Human breast cancer cell line MDA-MB-231 was a kind gift from Dr. Jing Li, Karmanos Cancer Institute (Detroit, MI). The cells were maintained in RPMI 1640 medium supplemented with 10% FBS. Murine melanoma cell line B16F10 and human hepatocellular carcinoma cell line Hep G2 were purchased from ATCC (Manassas, VA). B16F10 cells were maintained in DMEM media supplemented with 10% FBS and Hep G2 cells were maintained in MEM media

supplemented with 10% FBS. All the cells were cultured at 37 °C in 5% CO_2 atmosphere.

4.2.8 Transfection of DNA polyplexes

All transfection experiments were conducted in 48-well plates with cells at logarithmic growth phase following a previously published protocol (Read, Singh et al. 2005). Cells were seeded at a density of 40,000 cells/well 24 h prior to transfection. On the day of transfection, cells were incubated with the polyplexes (DNA conc. 2.35 µg/mL) in 170 µL of serum-free or 10% FBS-containing media. After 4 h incubation, polyplexes were completely removed and the cells were cultured in complete culture medium for 24 h prior to measuring luciferase expression. The medium was discarded and the cells were lysed in 100 µL of 0.5x cell culture lysis reagent buffer (Promega, Madison, WI) for 30 min. To measure the luciferase content, 100 µL of 0.5 mM luciferin solution was automatically injected into each well of 20 µL of cell lysate and the luminescence was integrated over 10 s using Synergy 2 Microplate Reader (BioTek, VT). Total cellular protein in the cell lysate was determined by the Bicinchoninic acid protein assay using calibration curve constructed with standard bovine serum albumin solutions (Pierce, Rockford, IL). Transfection activity was expressed as relative light units (RLU)/mg cellular protein ± SD of quadruplicate samples.

4.2.9 Cytotoxicity of polycations

Toxicity of polycations was evaluated by MTS assay in MDA-MB-231 and Hep G2 cells. The cells were plated into 96-well microplates at a density 20,000 cells/well. After 24 h, culture medium was replaced by 150 μL of serial dilutions of a polymer in serum-supplemented medium and the cells were incubated for 24 h. Polymer solutions were aspirated and replaced by a mixture of 100 μL serum-free media and 20 μL of MTS reagent (CellTiter 96® AQueous Non-Radioactive Cell Proliferation Assay, Promega). After 2 h incubation, the absorbance was measured spectrophotometrically in Synergy 2 Microplate Reader (BioTek, VT) at a wavelength of 490 nm. The relative cell viability (%) was calculated as [A]sample/[A]untreated × 100%. The IC50 were calculated as polymer concentration, which inhibits growth of 50% of cells relative to untreated cells. The IC50 values were calculated based on “log(inhibitor) vs. response - absolute IC50” curve fitting procedure in GraphPad Prism, with constrains of Fifty=50, Top=100 and a formula Y=Bottom+(Top-Bottom)/ (1+10^((LogIC50-X)*HillSlope + log((Top-Bottom)/(Fifty-Bottom)-1))).

4.2.10 Statistical analysis

Significant differences between two groups were determined using Student’s t-test and differences among multiple groups were determined using ANalysis Of VAriance (ANOVA). A p-value < 0.05 was considered statistically significant in all cases.

4.3 Results and Discussion

4.3.1 Synthesis and characterization of RPC

A series of three RPC was synthesized by direct copolymerization of cyclam and CBA. The polymerization was achieved by Michael addition of different molar ratios of a disulfide containing bisacrylamide and cyclam (Scheme 5). Since cyclam contains four secondary amines available for the polymerization, it was important to identify reaction conditions to avoid excessive crosslinking and formation of a gel. The polymerization conditions were first optimized by testing different temperatures, solvents and feeding ratios of the two monomers. The polymerization was found to be easily controlled without rapid gel formation when conducted in methanol:water (v/v 7:3) at 37 °C. Changing the cyclam:CBA stoichiometry allowed controlling degree of branching of the synthesized polymers. Cyclam:CBA molar ratio > 0.9 was needed to avoid gel formation within 24 h. In this study, three RPC polymers were obtained using molar feeding ratio of cyclam:CBA molar ratios of 1.5, 1, and 0.9; corresponding to amine:acrylamide functional group ratios of 3, 2, and 1.8, respectively. The reaction conditions for each RPC polymer are summarized in Table 4.

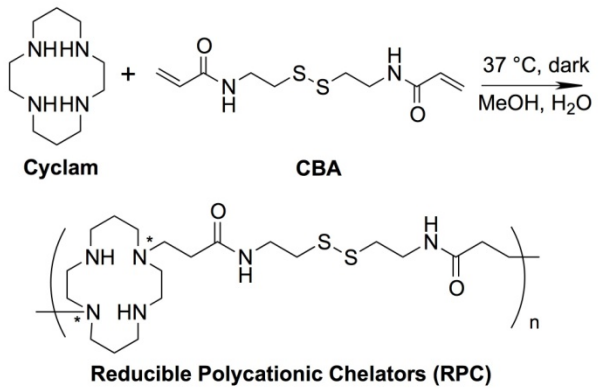

Scheme 5. Synthesis of RPC. *Exact location of the CBA attachment could not be determined. Any of the secondary amines are susceptible to modification.

The RPC polymers were analyzed by ^{1}H NMR to confirm completion of the reaction by disappearance of the characteristic CBA acrylamide peaks (5.5 – 6.5 ppm). ^{1}H NMR was also used to determine the composition of RPC. Based on the integration of the signature peaks (4H) from cyclam (1.8 – 2.0 ppm) and the signature peaks (4H) from CBA (3.4 – 3.6 ppm) (Figure 17a), the final molar content of cyclam in each RPC polymer product was determined and the results are summarized in Table 4. The molecular weights and PDI determined by SEC are also listed in Table 4. RPC/3 had the lowest Mw of 4,400 while the RPC/2 and 1.8 showed similar Mw of 13,700 and 13,800, respectively. The SEC data also showed a decrease in PDI with decreasing cyclam content. However, the low PDI values for RPC/2 and 1.8 might be underestimated considering the nature of the reaction. This might be due to the limitation of the SEC column to fully separate branched polycations at low-molecular-weight regions.

Since there are four secondary amines on the cyclam ring available for reaction, and quick gel formation at feeding ratio (amine to acrylamide) below 1.8 was observed, it was expected that branching occurs and varies depending on the feeding ratio of the two monomers. To test the degree of branching for each RPC polymer, each disulfide bond was broken down by a thiol-free reducing agent TCEP, followed by capping the thiol group using NEM to form a stable thioether bond. The degradation fragments were then analyzed by LC-MS/MS. The chemical structure of all the possible fragments and their mass after ionization (m/z) are listed in Figure 17b. All the four possible degradation

products could be found in all three RPC polymers. Figure 17c shows an example of the LC-MS/MS spectrum for RPC/2. Calculated degrees of branching of RPC polycations are listed in Table 4. The results show that RPC/3 exhibited the most linear structure when compared with the other two polycations. No significant difference in the degree of branching was found between RPC/2 and RPC/1.8.

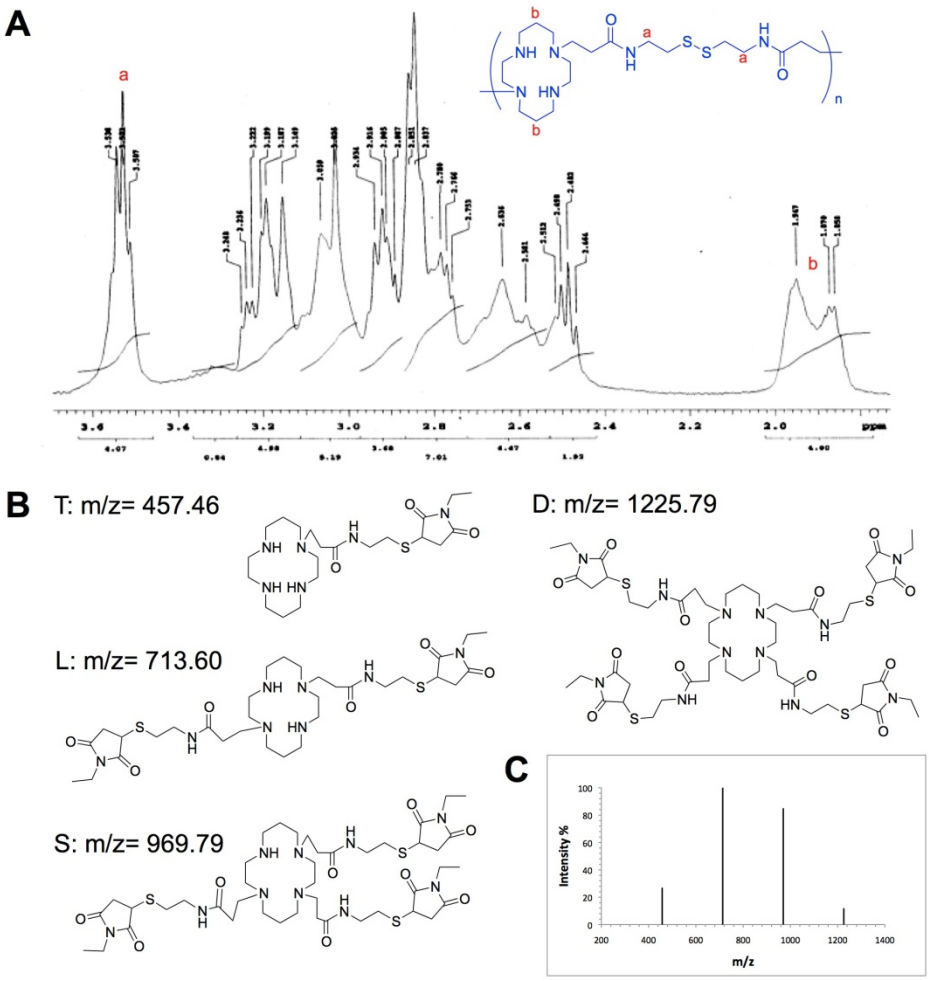

Figure 17. Characterization of RPC polycations. (A) Typical ^{1}H NMR (D_2O) spectrum (RPC/2); (B) Chemical structures and (C) typical LC-MS/MS spectrum of reduced RPC/2 fragments.

Table 4. Synthesis and characterization of RPC polycations.

	Feeding Ratio (amine to acrylamide)	Feeding Ratio (cyclam to CBA)	Reaction time (h)	Final Cyclam %	Mn	Mw	PDI	Degree of Branching
RPC/3	3	1.5	48	56.6	3,100	4,400	1.41	0.07
RPC/2	2	1	48	49.6	12,000	13,700	1.14	0.24
RPC/1.8	1.8	0.9	24	47.8	12,900	13,800	1.07	0.26

4.3.2 Copper(II) complexation of RPC polymers

To explore the potential for PET imaging of RPC polymers, nonradioactive $CuCl_2$ was used in this preliminary study to evaluate if the cyclam moiety in the RPC polymers retained its ability to form complexes with Cu(II) (Scheme 6). Cu(II) complexes with RPC were easily prepared in acetate buffer and characterized by UV-vis spectroscopy (Figure 18). Cyclam was used as a positive control and $CuCl_2$ was used as a negative control for monitoring free uncomplexed Cu(II). The results show that for cyclam (Figure 18b), titration with $CuCl_2$ led to appearance of a peak in the UV-visible spectrum (λ_{max} = 510 nm) that reached a maximum absorbance when 1 molar equivalent of $CuCl_2$ was added. The sharp peak at the equivalent point indicates the formation of a well-defined uniform metal complex (Lo, Salam et al. 2011). Addition of excess Cu(II) gives absorbance above 600 nm, which corresponds to the unbound $CuCl_2$. All three RPC polymers (Figure 18c-e) showed absorption maximum at λ_{max} = 570 nm that reached maximum absorbance at a near equimolar cyclam:Cu ratio indicating that cyclam units in the RPC are sterically accessible to Cu(II) complexation. However, Cu(II) complexes of RPC exhibited broader peaks with

λ_{max} shifted to higher wavelength, suggesting different Cu(II) complexation ability caused by the heterogeneity in cyclam structures in the polymers. RPC/1.8 exhibited the broadest absorption peak among the three polymers, a likely consequence of its highest degree of branching. Overall, all RPC polymers have retained their ability to form Cu(II) complexes, which makes them promising theranostic agents for future use in gene delivery combined with PET imaging.

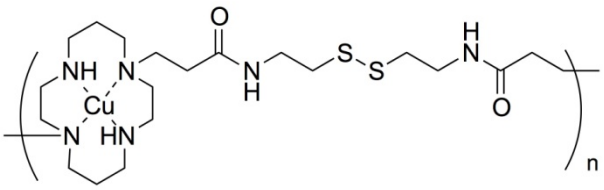

Scheme 6. Structure of the complex of RPC with copper(II).

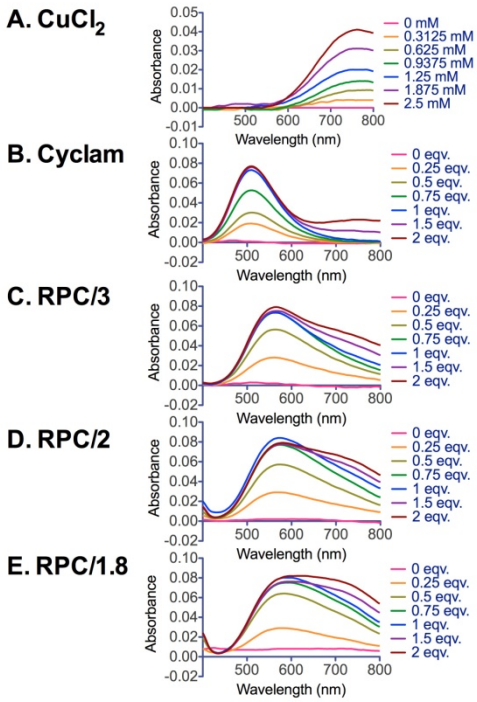

Figure 18. Cu(II) complexation of RPC polymers (C-E). Cyclam (B) was used as positive control and $CuCl_2$ (A) was used to monitor free Cu(II). The absorption spectra were obtained by UV-vis spectroscopy after 1 h incubation with $CuCl_2$.

The transfection activity of the RPC polycations and their Cu(II) complexes was tested next. Conformational changes caused by binding with transition metal ions like Cu(II) (Paisey and Sadler 2004) increase rigidity of the cyclam ring due to locked positions of the secondary amines. The hypothesis was that the likely increased rigidity will affect DNA binding ability and polyplex formation of RPC. The presence of Cu(II) in the RPC structure also increases the overall positive charge and charge density of the polycations, which may further affect the electrostatic interactions during the formation of DNA polyplexes, cytotoxicity of RPC, stability of the polyplexes against disassembly, and ultimately transfection activity of the polyplexes. Finally, there is a potential for increased toxicity of the Cu(II) complexes of RPC due to adverse effects of the heavy metal ion itself. Hence, a comprehensive evaluation of the physical properties and biological activity of the RPC polycations as well as their Cu(II) complexes was conducted. RPC with 50% and 100% of the cyclam moieties complexed with Cu(II) were selected and compared the results with the copper-free RPC.

4.3.3 DNA condensation

To test the DNA condensation capability of RPC and their Cu(II) complexes, EtBr exclusion assay was conducted (Figure 19). All the RPC were able to fully condense DNA at w/w > 2 as indicated by no further fluorescence decrease beyond this ratio, while the cyclam monomer failed to condense DNA into polyplexes. All three PRC displayed similar condensation curves of typical

sigmoidal shape. Condensation curves for the Cu(II) complexed RPC polymers could not be reliably obtained because of the observed fluorescence quenching by the copper present. Thus, the effect of Cu(II) complexation on improved binding of RPC could not be determined by this method.

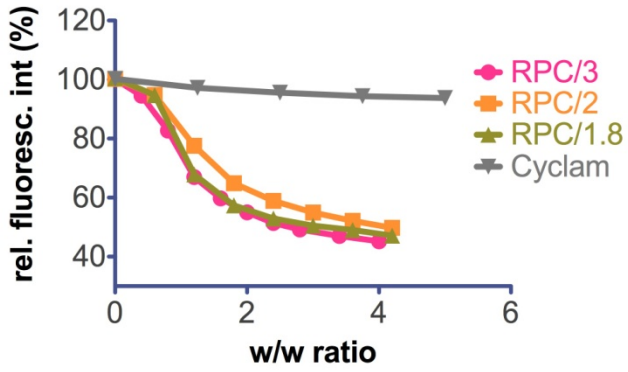

Figure 19. DNA condensation of RPC polymers and cyclam monomer by EtBr exclusion assay.

4.3.4 Particle size and zeta-potential of DNA polyplexes

The physical properties of DNA/polycation complexes have crucial effect on both in vitro and in vivo biological performance. Polyplexes with appropriate size and surface charge greatly benefit the cellular uptake and gene transfer ability. Hydrodynamic size and zeta-potential of polyplexes were measured by DLS before every in vitro test. Representative particle size and zeta-potential data of three RPC polyplexes prepared at different w/w ratios are summarized in Table 5. The sizes of RPC/DNA polyplexes fell into a broad range of 80-205 nm. All polyplexes were positively charged with zeta potential ranging from 13 to 29 mV. No significant increase in the surface charge of the polyplexes was observed above the equivalent w/w ratio 2. Low zeta-potential that was found in RPC/3

polyplexes prepared at lower w/w ratio is probably due to the low molecular weight of the polycation.

After complexation with 50% and 100% Cu(II), no significant difference in surface charge of the polyplexes was observed. However, Cu(II) complexed RPC/2 and RPC/1.8 polyplexes showed a decreasing trend in the hydrodynamic sizes with increasing metal complexation. This trend was not found in the Cu(II) complexed RPC/3 polyplexes. The effect of copper complexation seems to be more pronounced in the polycations with higher degree of branching.

Table 5. Size and zeta-potential of RPC/DNA polyplexes at different w/w ratios.

Polymer	w/w	[-] Cu(II)		[+] 50% Cu(II)		[+] 100% Cu(II)	
		Size (nm)	Zeta-potential (mV)	Size (nm)	Zeta-potential (mV)	Size (nm)	Zeta-potential (mV)
RPC/3	5	102±2	13±1	92±1	18±1	114±1	16±3
	10	124±7	14±2				
	15	111±3	17±5				
	20	114±3	15±3				
	25	125±2	17±3				
RPC/2	5	119±2	21±4	136±6	26±6	75±0	17±2
	10	125±2	26±2				
	15	205±9	16±2				
	20	167±3	17±2				
	25	163±3	16±3				
RPC/1.8	5	87±2	16±2	82±10	20±3	69±2	19±2
	10	90±3	23±4				
	15	121±3	29±3				
	20	81±3	20±2				
	25	80±1	17±2				

4.3.5 Effect of reduction on stability of polyplexes against polyelectrolyte exchange

The effect of RPC disulfide reduction on the resistance of the polyplexes against polyelectrolyte exchange with a competing polyanion heparin was evaluated by agarose gel electrophoresis (Figure 20). In the absence of a reducing agent, the polyplexes show first signs of destabilization at a heparin concentration of 80 μg/mL. In reducing conditions of 20 mM GSH that mimic the redox status in the cell nuclei (Soundara Manickam and Oupicky 2006), PRC/3 polyplexes disassembled and DNA was released without involvement of heparin. Polyplexes formed with PRC of more branched structure did not release DNA as readily as suggested by the fact that 20 mM GSH alone was not sufficient to destabilize the polyplexes. However, addition of a low concentration of heparin (40 μg/mL) caused complete DNA release (disappearance of fluorescent signal in the well) from RPC/2 polyplexes and a higher concentration of heparin was required to fully release DNA from RPC/1.8 polyplexes. Replacing GSH with a stronger reducing agent DTT resulted in complete DNA release from all three polyplexes without the presence of heparin. This result suggests that the differences in degree of the polycations branching affect sensitivity to reduction-triggered disassembly of polyplexes, with the least branched polycations exhibiting the highest sensitivity to reduction. This finding is most likely the result of hindered accessibility of the disulfide bonds to the reductant in the more branched polycations compared with the less branched polycations.

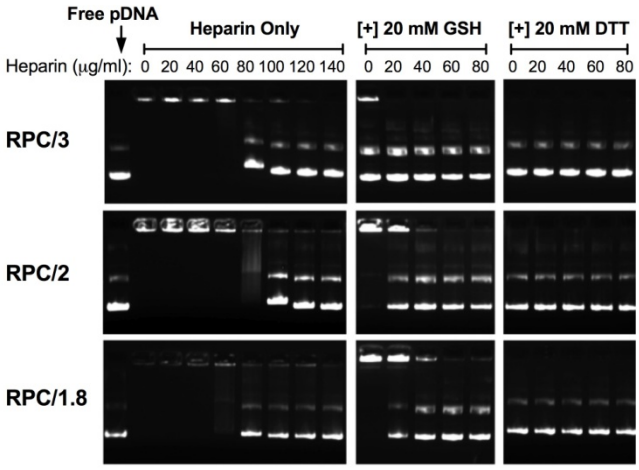

Figure 20. DNA release from polyplexes by agarose gel electrophoresis with heparin -/+ 20 mM GSH or DTT. All the RPC/DNA polyplexes were prepared at w/w 5.

The polyplex stability of Cu(II) complexed RPC against heparin was tested using the same gel electrophoresis method as above. Figure 21 shows the results for RPC/1.8 polyplexes as an example. Cu(II)-free RPC/1.8 polyplexes started to show signs of disassembly and traces of DNA release at heparin concentration 70 μg/ml and complete DNA release above 80 μg/ml. For Cu(II) complexed RPC/1.8 polyplexes, at heparin concentration of 80 μg/ml, only partial DNA was released. This result shows that the presence of Cu(II) in the polycation, which is expected to increase charge density of the polycations, increases the stability of polyplexes against polyanion exchanges. However, this might not benefit gene delivery efficiency of these RPC polyplexes due to increased difficulty of polyplex disassembly and DNA release.

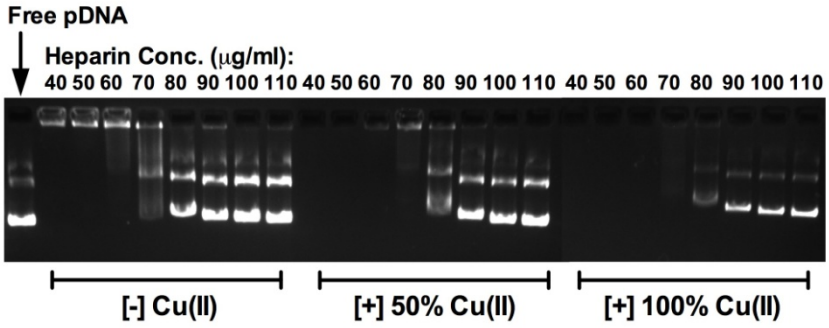

Figure 21. Stability of Cu(II) complexes of RPC/1.8 against heparin disassembly.

4.3.6 Transfection efficiency

In vitro transfection efficiency of RPC polyplexes at different w/w ratios was evaluated in murine melanoma cell line B16F10 and human breast cancer cell line MDA-MB-231 (Figure 22). PEI polyplexes at w/w 1.2 (N/P 10) were used as a positive control. The results showed that in B16F10 cells, all the RPC polyplexes exhibited high transfection efficiency comparable with PEI above certain w/w ratio, while the cyclam monomer failed to mediate any significant transfection. The effect of w/w ratio on transfection activity was especially pronounced in PRC/3 polyplexes, which might be attributed to the low molecular weight of the polymer and high sensitivity to disulfide reduction. Serum usually has negative effect on in vitro transfection activity due to the interaction of positively charged polyplexes with serum proteins like albumin (Dong, Li et al. 2010; Li, Wang et al. 2012; Zheng, Zhong et al. 2012). Here, the influence of serum on transfection of RPC/1.8 polyplexes was not as significant as the negative effect observed for RPC/3 and RPC/2 polyplexes, especially when prepared at high w/w ratio. In MDA-MB-231 cells, the transfection activity of the RPC polymers was not as high as in B16F10 cells. Nevertheless, RPC/2 and

RPC/1.8 still showed transfection activity comparable with PEI in serum-free condition. Cytotoxicity of RPC polyplexes was significantly higher in MDA-MB-231 cells compared with B16F10, thus the results for transfection efficiency of RPC/2 polyplexes prepared above w/w 20 and RPC/1.8 polyplexes prepared above w/w 10 are not included in Figure 22b.

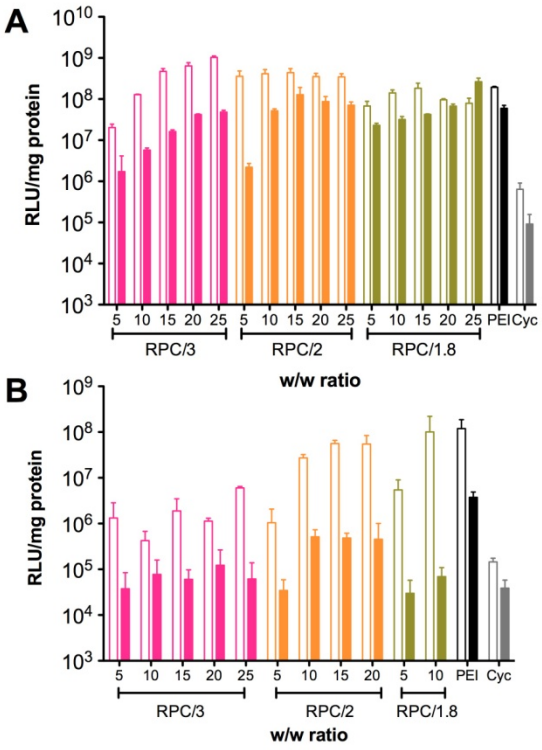

Figure 22. Transfection efficiency of RPC polyplexes prepared using different w/w ratio in (A) B16F10 cells and (B) MDA-MB-231 cells. All transfection experiments were conducted in serum-free (empty bars) and 10% FBS-containing medium (solid bars) during polyplex incubation.

The in vitro luciferase transfection efficiency of 50% and 100% Cu(II) complexed RPC polymers were conducted as above using B16F10 cells in the presence of 10% serum. As shown in Figure 23, for RPC/3 and RPC/2 polyplexes, the transfection efficiency of both 50% Cu(II) and 100% Cu(II)

polyplexes showed a slight decrease (2- to 5- fold), which might be attributed to the increased difficulty in intracellular polyplex disassembly due to increased charge density of the Cu(II) complexes as discussed above. However, RPC/1.8 with 100% Cu(II) complexation showed a 20-fold increase in the transfection efficiency compared with Cu(II)-free polyplexes. Since the properties of RPC/2 and RPC/1.8 are similar, the most likely explanation for the observed transfection increase is the higher toxicity (as judged by decreased protein content in the cell lysate) of the copper complexes of RPC/1.8 as described below.

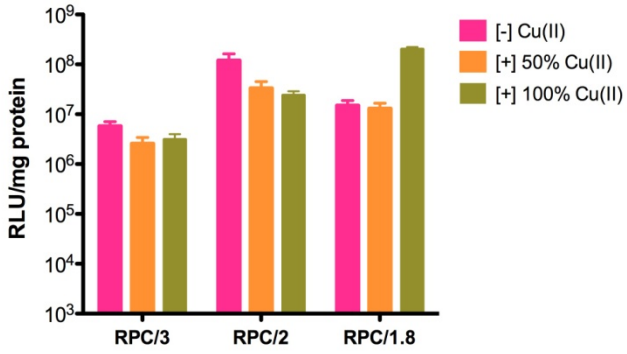

Figure 23. Transfection efficiency of Cu(II) complexes of RPC polymers in B16F10 cells in the presence of serum. The RPC and Cu(II) complexed RPC polyplexes were prepared at w/w 15.

4.3.7 Cytotoxicity

It has been well recognized that bioreducible polycations exhibit significantly decreased cytotoxicity compared with non-reducible counterparts (Chen, Wu et al. 2009). Here, the in vitro cytotoxicity of RPC polymers was evaluated by MTS assay in human breast cancer MDA-MB-231 cells because we found in the previous transfection experiments that these cells are more sensitive to the polycation toxicity. The cytotoxicity of RPC was also tested in human liver

hepatocellular Hep G2 cells, which is a well-recognized cell line model used for in vitro predictive toxicity screening (Mersch-Sundermann, Knasmuller et al. 2004; Bokhari, Carnachan et al. 2007) (Figure 24). IC50 values for each polymer in these two cell lines are summarized in Figure 24b. The cytotoxicity of RPC polymers is significantly decreased compared with 25 kDa PEI in MDA-MB-231 cells (IC50 14 μg/ml (Wang, Wang et al. 2007)). The cytotoxicity of RPC was even lower in Hep G2 cells compared with PEI (IC50 18 μg/ml (Wang, Gao et al. 2006)), suggesting decreased toxicity in the liver, which might benefit future in vivo applications. In both cell lines, RPC with higher molecular weight and higher degree of branching showed increased toxicity. Interestingly, in MDA-MB-231 cells, RPC/2 showed 2-fold higher IC50 than RPC/1.8, while little difference was observed in Hep G2 cells, suggesting the cytotoxicity of these polycations is cell type dependent.

A

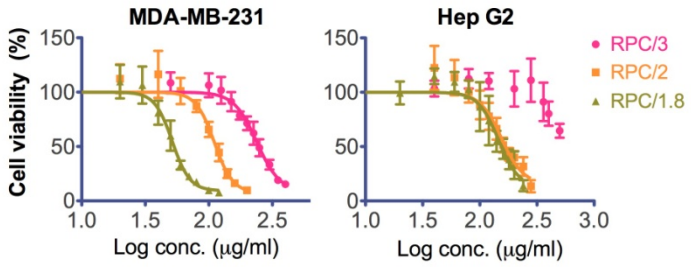

B

IC50 (μg/ml)	MDA-MB-231	Hep G2
RPC/3	247.6±15.9	~369.5
RPC/2	113.6±12.0	167.5±16.2
RPC/1.8	53.3±3.9	154.3±13.4

Figure 24. Cytotoxicity of RPC polycations in (A) MDA-MB-231 cells and Hep G2 cells by MTS assay. Calculated IC50 values of RPC are listed in the table (B).

The cytotoxicity of the Cu(II) complexed RPC polycations was evaluated by conducting MTS assay in MDA-MB-231 cells as before (Figure 25). For all the three polycations, 100% Cu(II) complexed RPC polymers had significantly increased cytotoxicity compared with copper-free RPC. This is most likely due to increased damage to the cell membrane due to higher charge density and rigidity of the copper-complexed RPC. No toxicity was observed with equivalent concentrations of free copper in the form of $CuCl_2$. Interestingly, 50% Cu(II) complexed RPC had significantly lower cytotoxicity compared with Cu(II)-free RPC in the case of all three polycations. The reason for this observation remains unclear but the fact that toxicity of the Cu(II) complexes is highly dependent on the degree of metal complexation needs to be taken into account when selecting appropriate doses of ^{64}Cu(II) for future PET imaging.

A

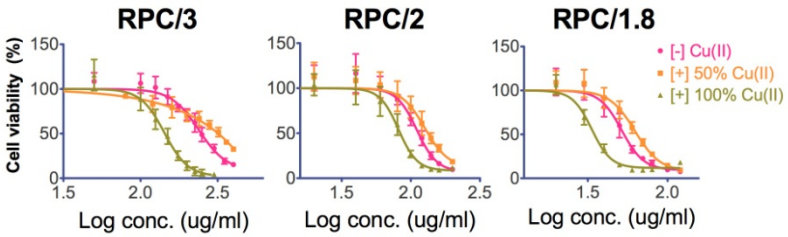

B

IC50 (μg/ml)	RPC/3	RPC/2	RPC/1.8
[-] Cu(II)	247.6±15.9	113.6±12.0	53.3±3.9
[+] 50% Cu(II)	319.2±15.1	132.9±13.2	64.4±4.4
[+] 100% Cu(II)	143.8±10.9	83.9±3.2	34.7±2.6

Figure 25. (A) Cell viability curves of Cu(II) complexes of RPC polycations in MDA-MB-231 cells by MTS assay. (B) IC50 values calculated from data in (A).

4.4 Conclusions

A new type of bioreducible cyclam-based polymeric chelators for combined gene delivery and potential PET imaging was developed. These RPC

polycations could be easily synthesized by one-step Michael addition reaction and they showed low cytotoxicity, high transfection efficiency in vitro. The capability of RPC to form Cu(II) complexes makes it promising for future *in vivo* simultaneous PET imaging. The Cu(II) complexation of RPC affects polyplex disassembly process as well as transfection efficiency and cytotoxicity in vitro depending on the degree of Cu(II) complexation.

CHAPTER 5

DUAL-FUNCTION CXCR4 ANTAGONIST POLYPLEXES TO DELIVER GENE THERAPY AND INHIBIT CANCER CELL INVASION

Please note that part of the content of this chapter was published in Angewandte Chemie Int. Ed. (Li, Zhu et al. 2012). As the first author, I performed all the work in the paper except for preparing Scheme 7 and determining the purity of polymer by LC-MS/MS (contributed by Yu Zhu, the second author). NMR analysis was done by Dr. S. Hazeldine. All the authors agreed with including their work in this dissertation.

5.1 Introduction

Synthetic polycations have been investigated widely as delivery vectors of nucleic acid therapeutic. Polycations form polyplexes with the nucleic acids, thereby protecting them from degradation and facilitating transport across cellular membranes. Significant effort has been devoted to synthesizing polycations that have improved transfection activity and reduced toxicity (Schaffert, Troiber et al. 2011). Traditionally, polycations have been viewed as pharmacologically inert components of delivery systems. This chapter describes a conceptually new approach that polycations can have both a delivery function as well as pharmacologic activity, to enhance the therapeutic outcome of gene and RNA interference therapies. It is a novel class of polycations that not only deliver

plasmid DNA but also function as CXCR4 antagonists that inhibit cancer cell invasion and thus could limit metastasis in various approaches to gene therapy for cancer (Scheme 7).

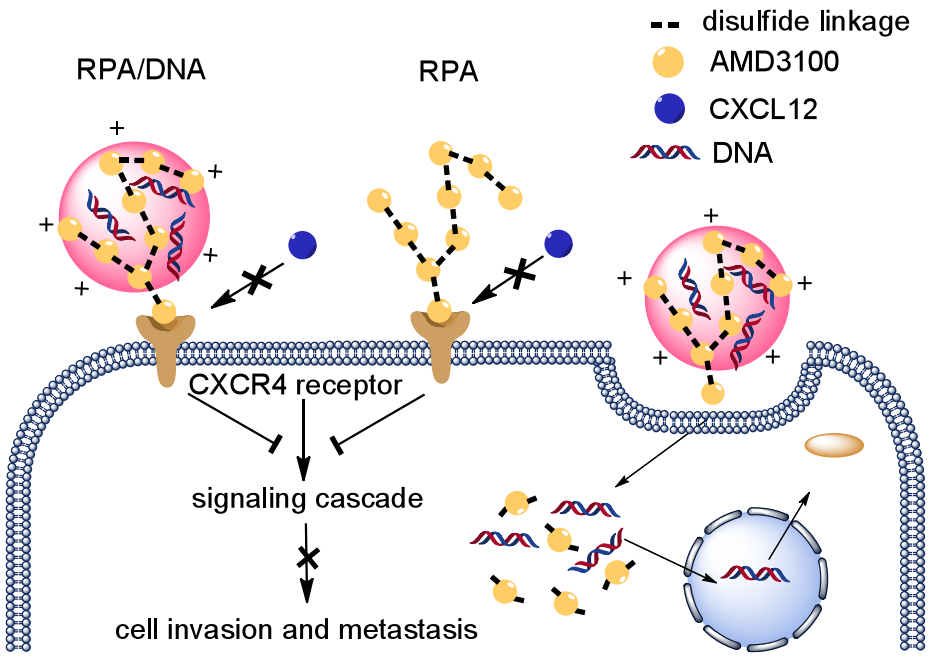

Scheme 7. Mechanism of action of dual-function polycations as CXCR4 antagonists and gene delivery vectors.

CXCR4 is a highly conserved transmembrane G-protein-coupled chemokine receptor that exclusively binds its ligand CXCL12. Consistent with the seed-and-soil hypothesis of metastatic dissemination (Burger and Kipps 2006; Hanahan and Weinberg 2011), the sites of metastasis are determined not only by the characteristics of the cancer cells but also by the microenvironment of the specific organ for tumor cell adhesion and support subsequent tumor proliferation and progression (Harvey, Mellor et al. 2007). This process is often mediated by chemokine-receptor interactions and several studies showed that cancer cells utilize chemokine receptor CXCR4 and its sole ligand stromal CXCL12 to

metastasize to distant sites (Luker and Luker 2006). Upregulation of CXCL12 is often found in sites commonly affected by metastases in cancer types known to overexpress CXCR4 (Muller, Homey et al. 2001; Taichman, Cooper et al. 2002; Liang, Yoon et al. 2005; Chinni, Sivalogan et al. 2006; Rhodes, Short et al. 2011). For example, breast cancer cells often overexpress CXCR4 and their metastases are commonly found in sites with high levels of CXCL12, including lung, lymph nodes, liver, and bone marrow (Paget 1989; Muller, Homey et al. 2001; Taichman, Cooper et al. 2002). CXCR4 expression is often associated with poor survival and aggressive types of cancer (Akashi, Koizumi et al. 2008; Wallace, Prueitt et al. 2008).

CXCR4/CXCL12 axis regulates survival, proliferation, migration and invasion of various cancer cells by activating various intracellular signaling transduction pathways that affect cell survival and migration, including phosphatidylinositol-3-kinase (PI3K) and the mitogen-activated protein kinase pathways (Vlahakis, Villasis-Keever et al. 2002; Curnock, Sotsios et al. 2003; Kayali, Van Gunst et al. 2003; Luo, Manning et al. 2003; Peng, Peek et al. 2005). CXCR4 also activates Erk1/2, which phosphorylates transcription factors including Elk-1 to promote cancer cell proliferation and survival (Chang and Karin 2001). CXCR4/CXCL12 is involved in activating focal adhesion complexes and promoting adhesion through integrins. This combined with increasing secretion of matrix metalloproteinases that mediate degradation of extracellular matrix contributes to invasion of cancer cells (Fernandis, Prasad et al. 2004; Hartmann, Burger et al. 2005; Luker and Luker 2006).

Among the most widely investigated CXCR4 inhibitors are cyclam derivatives, including AMD3100 (Dessolin, Galea et al. 1999; Khan, Greenman et al. 2007; Rosenkilde, Gerlach et al. 2007; Khan, Nicholson et al. 2009; Bridger, Skerlj et al. 2010; Lam, Bhattacharya et al. 2010). AMD3100 is a highly specific CXCR4 antagonist, as it inhibits binding to its chemokine ligand CXCL12 and downstream signaling (De Clercq 2003). The AMD3100 binding site on CXCR4 and its antimetastasis activity have been well studied and characterized (Hatse, Princen et al. 2002). Receptor mutagenesis studies identified the essential interaction sites for AMD3100 as being $Asp^{171, 262}$ in the highly conserved motif located in the CXCR4 transmembrane domains IV and VI. One cyclam moiety interacts directly with the carboxyl Asp^{171} and the other with Asp^{262}. Not all eight amino groups of AMD3100 are required for that activity (Bridger, Skerlj et al. 2010), making it a suitable building block of potential CXCR4 antagonizing polycations.

Here, this study describes the design and development of an AMD3100-based biodegradable polycations with CXCR4 antagonistic activity with potential for combined drug/gene cancer therapies. The dual-function polycations prevent cancer cell invasion by inhibiting CXCL12-stimulated CXCR4 activation, while at the same time efficiently and safely deliver plasmid DNA into cancer cells.

5.2 Materials and Methods

5.2.1 Materials

AMD3100 octahydrochloride hydrate was purchased from Sigma-Aldrich (St. Louis, MO). The base form of AMD3100 used in synthesis was obtained from Ontario Chemicals, Inc. (Guelph, ON, Canada). Cell culture inserts (for 24-well plates, 8.0 μm pores, Translucent PET Membrane, cat# 353097) and BD Matrigel^{TM} Basement Membrane Matrix (cat# 356237) were purchased from BD Biosciences (Franklin Lakes, NJ). Human CXCL-12 (SDF-1α) was from Shenandoah Biotechnology, Inc. (Warwick, PA). L-Glutamine, and Penicillin-Streptomycin (Pen-Strep) solution were from Thermo Scientific (Waltham, MA). G418 sulfate and Minimum Essential Medium (MEM) were from Mediatech, Inc. (Manassas, VA). Diff-Quick staining kit was from IMEB Inc. (San Marcos, CA). All other reagents and chemicals were obtained from Fisher Scientific or VWR International unless otherwise noted.

5.2.2 Synthesis and characterization of RPA

RPA was synthesized by Michael addition of equal molar ratio of AMD3100 and CBA. Typically, CBA (104 mg, 0.4 mmol) and AMD3100 (200.8 mg, 0.4 mmol) were added into a glass vial containing methanol/water mixture (4 mL, 7/3 v/v). Polymerization was carried out under nitrogen protection in dark at 37 °C for 72 h. Then, additional 20 mg of AMD3100 was added to the reaction mixture to consume any residual acrylamide groups, and stirred was continued for another 6 h. The reaction mixture was then added dropwise to excess of 1.25 M HCl in ethanol so that pH of the mixture was kept around 3. The resulting precipitated RPA.HCl was isolated by centrifugation, washed twice with ethanol

and dried in vacuum. The polymer was dissolved in water and dialyzed against water for 2 days (MWCO 3.5kDa) before final freeze-drying.

The polymer was analyzed by 1H NMR to confirm completion of the reaction from disappearance of the acrylamide signal of CBA. The composition of the polymer was determined by elemental analysis from N, S, and Cl content (Atlantic Microlab, Inc., Norcross, GA). Removal of any potentially unreacted AMD3100 was confirmed by analyzing its content in RPA using LC-MS/MS (AQUITY UPLC® TQD system, Waters, MA) equipped with AQUITY UPLC® BEH Shield RP18 column (2.1mm×100mm, 1.7 μm). A gradient of aqueous solution of (2 mM ammonium formate + 0.1% formic acid) and acetonitrile was used. AMD3100 was monitored at the parent/daughter ions of (m/z) 503.61 → (m/z) 105.00.

Weight- and number-average molecular weights and PDI were determined by SEC using Viscotek GPCmax chromatography system consisting of an autosampler, a pump, a CTO-10ASVP Shimadzu column oven, a refractive index detector, a low- and right-angle light scattering detector, and OmniSEC software for chromatographic data analysis and storage (Malvern Instruments, UK). The columns used were single pore AquaGel^{TM} columns (cat# PAA-202 and PAA-203) by PolyAnalytik (London, ON, Canada). Sodium acetate buffer (0.3 M, pH 5) was used as an eluent at flow rate of 0.3 mL/min.

5.2.3 Cell culture

Murine melanoma cell line B16F10 and human hepatocellular carcinoma

cell line HepG2 were purchased from ATCC (Manassas, VA). B16F10 cells were maintained in DMEM supplemented with 10% FBS. Hep G2 cells were maintained in MEM supplemented with 10% FBS. Human epithelial osteosarcoma U2OS cells stably expressing human CXCR4 receptor fused to the N-terminus of enhanced green fluorescent protein were purchased form Fisher Scientific. The cells were cultured in DMEM supplemented with 2 mM L-Glutamine, 10% FBS, 1% Pen-Strep and 0.5 mg/ml G418.

5.2.4 Polycation toxicity

Toxicity of polycations was evaluated by MTS assay in Hep G2 cells and CXCR4+ U2OS cells. The cells were plated into 96-well microtiter plates at a density of 20,000 cells/well. After 24 h, culture medium was replaced by 150 µl of serial dilutions of a polymer in serum-supplemented medium and the cells were incubated for 24 h. Polymer solutions were aspirated and replaced by a mixture of 100 µl serum-free media and 20 µl of MTS reagent (CellTiter 96® AQueous Non-Radioactive Cell Proliferation Assay, Promega). After 2 h incubation, the absorbance was measured spectrophotometrically in Synergy 2 Microplate Reader (BioTek, VT) at a wavelength of 490 nm. The relative cell viability (%) was calculated as [A]sample/[A]untreated × 100%. The IC50 were calculated as polymer concentration, which inhibits growth of 50% of cells relative to untreated cells. The IC50 values were calculated based on “log(inhibitor) vs. response - absolute IC50” curve fitting procedure in GraphPad Prism, with constrains of

Fifty=50, Top=100 and a formula Y = Bottom + (Top-Bottom)/(1+10^((Log IC50-X)*HillSlope + Log((Top-Bottom)/(Fifty-Bottom)-1))).

5.2.5 EtBr exclusion assay

The ability of the studied polycations to condense gWiz-Luc DNA was determined by EtBr exclusion assay by measuring the changes in EtBr/DNA fluorescence. DNA solution at a concentration of 20 μg/mL in 10 mM HEPES buffer (pH 7.4) was mixed with EtBr (1 μg/mL) and fluorescence was measured and set to 100% using an excitation wavelength of 540 nm and an emission wavelength of 590 nm. Fluorescence readings were taken following a stepwise addition of a polycation solution, and the condensation curve for each polycation was constructed.

5.2.6 Reduction-triggered release of DNA from polyplexes

Redox-triggered disassembly of the polyplexes was examined by agarose gel electrophoresis. Briefly, gWiz-Luc DNA polyplexes were incubated with or without 20 mM GSH either in the presence or absence of 0.15 M NaCl at 37 °C for 1 h. Samples were then loaded onto a 0.8% agarose gel containing 0.5 μg/mL EtBr and run for 75 min at 120 V in 0.5x Tris/Borate/EDTA (TBE) running buffer. The gel was visualized under UV.

5.2.7 Formation and characterization of RPA polyplexes

gWiz-Luc DNA solution in 10 mM HEPES (pH 7.4) was prepared to give a DNA concentration in the final polyplexes = 20 μg/mL. Polyplexes were formed by adding predetermined volume of polymer to achieve the desired polycation/DNA weight/weight (w/w) ratio and mixed by vigorous vortexing for 10 s. Polyplexes were further allowed to stand for 30 min prior to use. The determination of hydrodynamic diameters and zeta potentials of polyplexes was performed by Dynamic Light Scattering following previously published method. Results were expressed as mean ± standard deviation (S.D.) of 3-10 experimental runs.

5.2.8 CXCR4 redistribution assay

CXCR4+ U2OS cells were plated in 96-well plate 18-24 h before the experiment at a seeding density of 8,000 cells per well. The cells were first washed with 100 μL assay buffer (DMEM supplemented with 2 mM L-Glutamine, 1% FBS, 1% Pen-Strep and 10 mM HEPES) twice and then incubated with different concentrations of the polycations or AMD3100 in assay buffer containing 0.25% DMSO at 37 °C for 30 min. In experiments with RPA/DNA and RHB/DNA polyplexes, DNA concentration was 0.5 μg/mL. Human SDF-1α (CXCL-12) was then added to each well to make final concentration 10 nM. DMSO alone was used as the negative control, and hSDF-1α alone was used as the positive control. After 1 h incubation at 37 °C, the cells were fixed with 4% formaldehyde at room temperature for 20 min followed by 4-time washing with PBS. All the images were taken by EVOS fl microscope at 20X.

The quantification of the receptor redistribution was conducted by ImageXpress® Micro high throughput imaging system by Molecular Devices (Sunnyvale, CA). The system enables high-quality imaging of 96-well plates based on automatic focusing of fluorescently labeled cell nuclei (by DAPI or Hoechst dye) followed by image analysis by MetaXpress software (High Throughput Mode) based on the average green fluorescent granule intensity (internalized GFP-CXCR4). Untreated cells U2OS cells stimulated with 10 nM CXCL12 were used as negative control (100% CXCR4 translocation) and 300 nM AMD3100 treated cells were used as positive controls (0% CXCR4 translocation). The method was verified by establishing a dose response curve of AMD3100 and its calculated EC50 was comparable with cell line data sheet from Fisher Scientific. The operation of the instrument and analysis of the data were conducted with the help of Steve Swaney at the Center for Chemical Genomics of Life Sciences Institute, University of Michgan (Ann Arbor, MI).

5.2.9 Cell invasion assay

The upper sides of the transwell inserts were coated with 40 μl Matrigel diluted in serum-free medium (v/v 1:3) per insert. The 24-well plates with coated inserts were then placed in 37 °C incubator for 2 h. CXCR4+ U2OS cells were trypsinized and resuspended in different concentrations of drugs in serum-free medium for 30 min before adding to the inserts at a final concentration of 10,000 cells in 300 μl medium per insert. 20 nM CXCL12 in serum-free medium as the chemo-attractant was then added to corresponding wells in the companion plate.

After 16 h, the non-invaded cells on the upper surface of the inserts were removed with a cotton swab. The invaded cells were then fixed and stained by dipping the inserts into Diff-Quick solution. The images were taken by EVOS xl microscope. Five 20X imaging areas were randomly selected for each insert and each sample was conducted in triplicate.

Statistical significance of the observed differences in cell invasion was analyzed using non-parametric ANOVA with Dunn's multiple comparison test using GraphPad InStat (v. 3.10). $P<0.05$ was considered significant.

5.2.10 DNA transfection by RPA/DNA polyplexes

All transfection experiments were conducted in 48-well plates with cells at logarithmic growth phase. Cells were seeded at a density of 40,000 cells/well 24 h prior to transfection. On a day of transfection, the cells were incubated with the polyplexes (DNA conc. 2.35 μg/ml) in 170 μL of serum-free or 10% FBS-containing media. After 4 h incubation, polyplexes were completely removed and the cells were cultured in complete culture medium for 24 h prior to measuring luciferase expression. The medium was discarded and the cells were lysed in 100 μL of 0.5x cell culture lysis reagent buffer (Promega, Madison, WI) for 30 min. To measure the luciferase content, 100 μL of 0.5 mM luciferin solution was automatically injected into each well of 20 μL of cell lysate and the luminescence was integrated over 10 s using Synergy 2 Microplate Reader (BioTek, VT). Total cellular protein in the cell lysate was determined by the Bicinchoninic acid protein assay using calibration curve constructed with standard bovine serum albumin

solutions (Pierce, Rockford, IL). Transfection activity was expressed as RLU/mg cellular protein ± SD of quadruplicate samples.

5.2.11 Intracellular distribution of RPA/DNA polyplexes

Luciferase DNA was labeled with Label IT®-Tracker™ CX-Rhodamine Kit (Mirus, Madison, WI) according to manufacturer's protocol. 120,000 CXCR4+ U2OS cells were plated in glass-bottom dish (MatTek P35GC-0-14-C) 24 h before the experiment. The cells were incubated with RPA/DNA polyplexes prepared at w/w 5 (2.35 μg/mL DNA) for 3 h before adding 10 nM hCXCL12. The cells were incubated for another 1 h before a PBS wash, fixation and imaging by Perkin Elmer Spinning Disk confocal microscope.

5.3 Results and Discussion

5.3.1 Synthesis and characterization of RPA

Although several reports have described lipid-based delivery vectors that incorporated peptide-targeting ligands to increase delivery to CXCR4-overexpressing cells (Driessen, Fujii et al. 2008; Egorova, Kiselev et al. 2009), no attempts have been made to synthesize polymeric CXCR4 antagonists that take advantage of their antagonistic properties to enhance the outcomes of gene therapies. Here, such polycations, named RPA, were synthesized by direct Michael addition polymerization of AMD3100 with a disulfide-containing bisacrylamide CBA (Figure 26a). Excessive crosslinking or gel formation during the reaction were avoided by optimizing AMD3100:CBA stoichiometry, reaction

temperature, and the solvent used. Soluble RPA was synthesized using a molar ratio of AMD3100 to CBA 1:1 in MeOH/water (v/v 7:3) at 37°C. The reaction was terminated by addition of excess AMD3100 to assure consumption of all residual acrylamides and presence of the terminal cyclam residues in the prepared RPA. RPA was purified by precipitation and extensive dialysis using 3.5-kDa molecular weight cut-off membranes.

The completion of the reaction was confirmed by 1H NMR (Figure 26b). From the NMR spectrum, there are no unreacted acrylamide residues. Furthermore, the peaks for the center methylenes of the $(CH_2)_3$ sections of the cyclam rings (~2 ppm) show a double peak with integral intensity ratios of 2:1, from which we can infer no selectivity in the reaction of CBA with the three available amines in each cyclam ring. The weight-average molecular weight, M_w, of the RPA used in this study was 13.9 kDa, and the polydispersity index, M_w/M_n, was 1.26 (Figure 26c). The purity of RPA was > 99.8% as confirmed by LC-MS/MS.

A control bioreducible polycation that lacks CXCR4 activity, RHB, was synthesized by copolymerization of CBA with N,N-dimethylaminodipropylenetriamine as described previously in Chapter 3 by following a published method (Chen, Wu et al. 2009). The RHB had M_w = 11.3 kDa and M_w/M_n = 1.95.

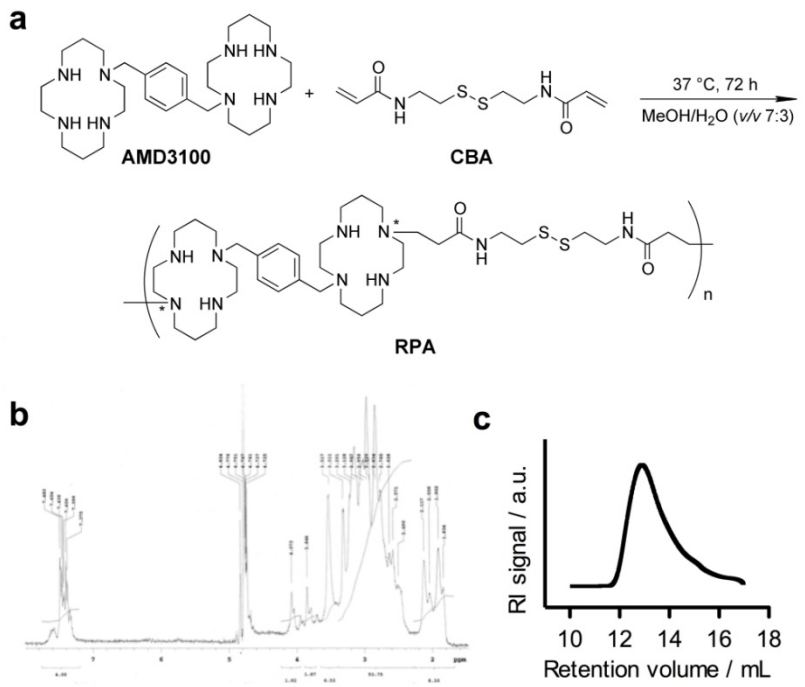

Figure 26. Synthesis and characterization of RPA. (a) RPA synthesis by Michael addition polymerization (*any secondary amine of the ring could be substituted and there could be multiple substitutions per ring); (b) 1H NMR of RPA in D_2O; (c) Size exclusion chromatogram of RPA.

5.3.2 Cytotoxicity of RPA

Bioreducible polycations typically exhibit low cytotoxicity due to rapid intracellular degradation mediated by GSH. Cytotoxicity of RPA was measured by MTS assay in HepG2 liver cells and in U2OS osteosarcoma cells overexpressing CXCR4 (Figure 27). In both cell lines RPA had remarkably low toxicity compared with 25-kDa poly(ethyleneimine) (PEI) control. The IC50 of RPA was almost 50 times higher than that of PEI in Hep G2 cells (599 vs. 12 μg/mL) and 116 times higher in U2OS cells (464 vs. 4 μg/mL). The IC50 of control polymer RHB was 57 μg/mL in Hep G2 cells.

It is expected that bioreducible polycations have decreased cytotoxicity in vitro compared with non-reducible polycations such as PEI. However, it is very unlikely that the bioreducible nature is the only contributor to the remarkably high IC50 of RPA. It has been reported that the cytotoxicity of polycations is caused by loss of cell membrane integrity followed by mitochondria-mediated apoptosis (Moghimi, Symonds et al. 2005). One possible explanation for the results observed here is that the AMD3100 component in RPA associated with CXCR4 binding ability might decrease cell membrane damage, therefore decreasing the overall cytotoxicity in vitro.

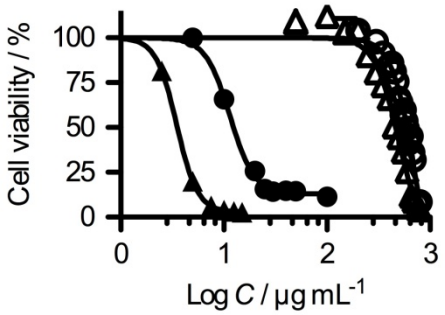

Figure 27. Comparison of cytotoxicity of RPA and PEI 25 kDa in HepG2 cells (RPA: ○, PEI: ●) and $CXCR4^+$ U2OS cells (RPA: △, PEI: ▲) determined by MTS.

5.3.3 Physicochemical characterization of RPA/DNA polyplexes

DNA condensation ability of RPA was first compared with PEI, RHB, and AMD3100 by EtBr exclusion assay (Figure 28a). The condensation curves for all three polycations displayed typical sigmoidal shape, characteristic of DNA condensation by polycations. At pH 7.4, a w/w ratio above 2 was required for RPA to fully condense the DNA, which was higher than that required in case of

RHB (w/w 1) and PEI (w/w 0.5). AMD3100 has six secondary amines and two tertiary amines and is thus, to a very limited extent, also able to condense DNA as demonstrated by a decrease in EtBr fluorescence by about 30%.

The redox stability of RPA/DNA polyplexes was tested by agarose gel electrophoresis after GSH treatment. As shown in Figure 28b, 20 mM GSH triggered DNA release form RPA/DNA polyplexes due to the depolymerization of RPA, which decreased its affinity to DNA.

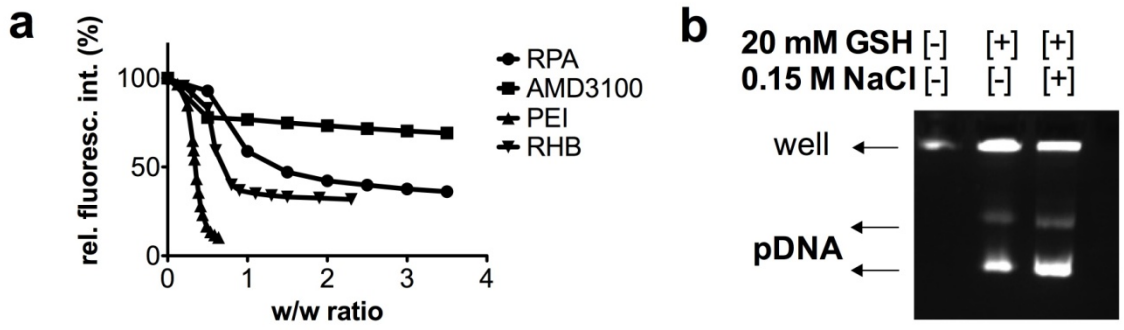

Figure 28. (a) DNA dondensation by EtBr Exclusion assay; (b) Reduction-triggered DNA release from RPA/DNA polyplexes (polyplexes were prepared at w/w 5).

The sizes and zeta-potentials of RPA/DNA polyplexes prepared at different w/w ratios were measured by dynamic light scattering and the results are summarized in Table 6. RPA and plasmid DNA formed polyplexes that were positively charged and had a relatively small size compared with PEI and RHB polyplexes. The small sizes of RPA polyplexes were further confirmed by Atomic Force Microscopy (AFM) conducted by Yi Zou from Prof. Guangzhao Mao's lab in Department of Chemical Engineering and Material Sciences, Wayne State University (data not shown).

Table 6. Sizes and zeta-potentials for different w/w ratios of RPA, RHB and PEI.

	w/w	Size (nm)	Zeta-potential (mV)
RPA	5	56 ± 0	25 ± 4
	10	70 ± 6	28 ± 4
	15	57 ± 1	31± 4
	20	62 ± 4	33 ± 4
	25	57 ± 0	26 ± 4
RHB	5	157 ± 2	31 ± 5
PEI	1.2 (N/P 10)	84 ± 1	33 ± 4

5.3.4 CXCR4 antagonism of RPA

When CXCL12 binds to CXCR4 it induces downstream signaling through multiple pathways, including Ras and PI3 kinase. Treatment with CXCR4 antagonists not only prevents the CXCL12-induced downstream signaling but it also inhibits endocytosis of the receptor (Forster, Kremmer et al. 1998; Orsini, Parent et al. 1999; Hatse, Princen et al. 2002; Dar, Goichberg et al. 2005). To evaluate CXCR4 antagonism by RPA and RPA/DNA, CXCR4 receptor redistribution assay was conducted (Figure 29). The assay uses U2OS cells stably expressing human CXCR4 receptor fused to the N-terminus of enhanced green fluorescent protein (EGFP). The assay monitors cellular translocation of the GFP-CXCR4 receptors in response to stimulation with human CXCL12. Here, the internalization of the CXCR4 receptors into endosomes in CXCL12-stimulated cells was oberved, as suggested by the punctate distribution of the GFP fluorescence (Figure 29b) away from the original diffuse pattern in non-

stimulated cells (Figure 29a). To exclude the possibility that the observed effect was caused by nonspecific electrostatic binding of RPA to the negatively charged binding site of the CXCR4 receptor, control polycation RHB without AMD3100 moiety was also tested, but no CXCR4 antagonistic properties was observed (Figure 29f).

Next, we explored whether polyplexes themselves exhibit CXCR4 antagonism. CXCR4 internalization was inhibited more efficiently by RPA/DNA prepared at w/w 5 (2.5 μg/mL total RPA) than at w/w 1 (Figure 29g and h). DNA is not fully condensed in polyplexes at w/w 1 (Figure 28a); thus, the formulation contains only a minimum amount of free RPA. The findings at w/w 1 thus suggest that the polyplexes themselves may inhibit CXCR4 to some extent. Similar to RHB polymer, no CXCR4 antagonism was observed with RHB/DNA polyplexes (Figure 29i), confirming that the specific CXCR4 antagonism of RPA and RPA/DNA is due to the AMD3100 moiety in RPA.

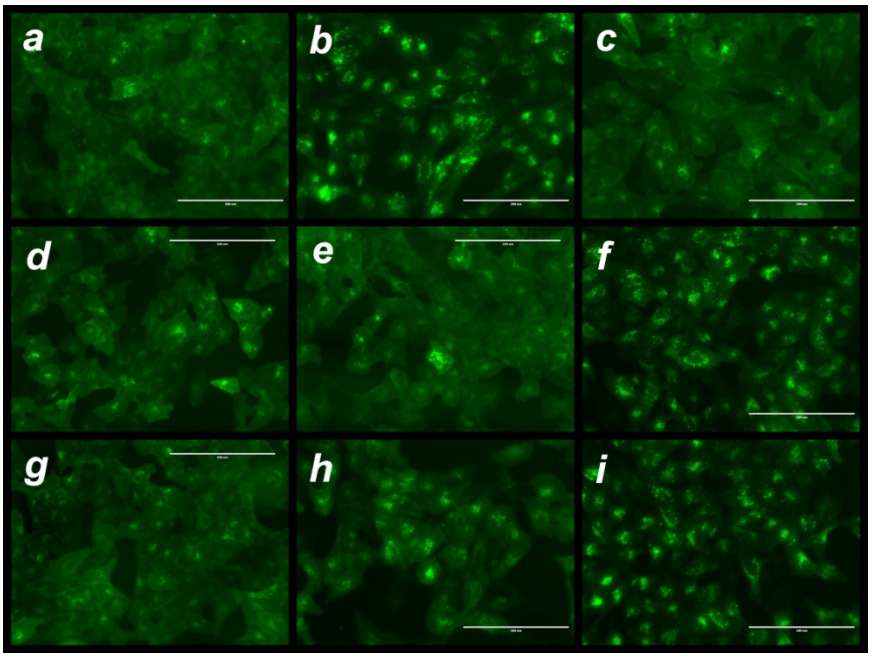

Figure 29. CXCR4 antagonism of RPA and RPA/DNA polyplexes. CXCR4 receptor redistribution assay was conducted in U2OS cells expressing GFP-tagged CXCR4 (a). Before stimulation with 10 nM CXCL12, the cells were treated for 30 min with (b) no drug; (c) 0.24 μg/mL AMD3100.8HCl; (d) 1.5 μg/ml RPA.HCl; (e) 2.5 μg/ml RPA.HCl; (f) 1.5 μg/ml RHB.HCl; (g) RPA/DNA polyplexes (w/w 5, total RPA conc. 2.5 μg/ml); (h) RPA/DNA polyplexes (w/w 1, total RPA conc. 0.5 μg/ml); and (i) RHB/DNA polyplexes (w/w 5, total RHB conc. 2.5 μg/ml). The scale bars for all the images are 200 μm.

To determine the half-inhibitory (EC50) concentrations of RPA, the CXCR4+ U2OS cells were treated with increasing concentrations of RPA.HCl before stimulating them with human CXCL12. AMD3100 was used as positive control. The level of CXCR4 antagonism was evaluated by quantifying the fluorescent intensity of granules (endocytosed GFP-CXCR4) in the individual images. The dose-response curves for AMD3100 and RPA.HCl were established based on % CXCR4 translocation and EC50 values were calculated accordingly (Figure 30). Based on the results of elemental analysis (data not shown), the equivalent AMD3100 content in RPA could be obtained (60% weight of

RPA.HCl). Thus the efficacy of AMD3100 moieties in RPA.HCl decreased about 50 fold compared with the free drug. The compromised CXCR4 antagonism of polymerized drug is acceptable considering its secondary function as gene delivery vector. Excess of polycations is usually required in the polyplex formulations in order to achieve efficient transfection and the required RPA concentrations fall in the range needed for safe and efficient gene delivery. However, the efficacy of RPA could be further improved by better polymer design since it is most likely that only the terminal AMD3100 moieties in the RPA polymer chains have retained their antagonistic ability.

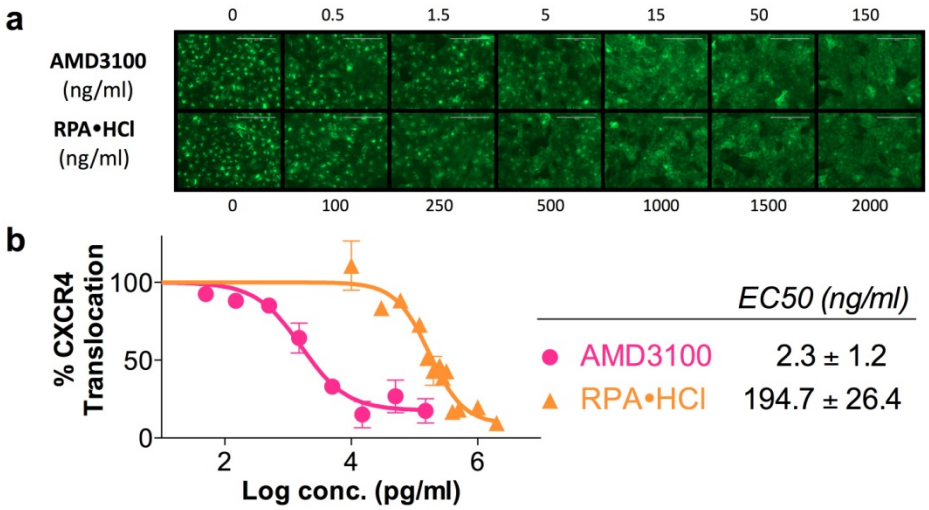

Figure 30. Dose-dependent CXCR4 antagonistic ability of AMD3100 and RPA.HCl. (a) Representative images of redistribution of CXCR4 receptors on U2OS cells treated with increasing concentrations of AMD3100 and RPA; (b) Dose-response curve of CXCR4 inhibition (% receptor translocation) and calculated EC50 value based on images obtained from (a).

5.3.5 Antimetastatic ability of RPA by cell invasion assay

The CXCR4/CXCL12 axis plays a critical role in cancer metastasis due to its function in trafficking and homing of cancer cells to organs that express high

levels of CXCL12. Blocking the CXCR4/CXCL12 interactions with small-molecule antagonists suppresses metastasis in a variety of cancers (Yoon, Liang et al. 2007; Liang, Zhan et al. 2012). To further confirm the CXCR4 antagonism of RPA and RPA/DNA polyplexes, the anti-metastatic ability was evaluated by a Matrigel cell invasion assay. As shown in Figure 31, RPA and RPA/DNA polyplexes effectively block CXCL12-mediated invasion of CXCR4+ U2OS cells. Both free RPA and RPA/DNA blocked invasion of 71-77% of cells, similar to that of AMD3100 (75%). The DNA dose used in the experiment with the polyplexes (1 μg/mL DNA) was in the range of typical doses used in transfection experiments. The observed decrease in cell invasion with control RHB/DNA polyplexes was not statistically significant ($p > 0.05$). At the same time, the differences between RPA and RPA/DNA polyplexes vs. untreated controls were highly significant with $P<0.001$, based on non-parametric ANOVA analysis with Dunn's multiple comparison test. The slight decrease in the number of invaded cells with RHB treatment could also be attributed by higher toxicity of RHB compared with RPA. The membrane damage caused by the treatment with RHB may affect the motility of the cells and thus decrease their ability to invade through the extracellular matrix.

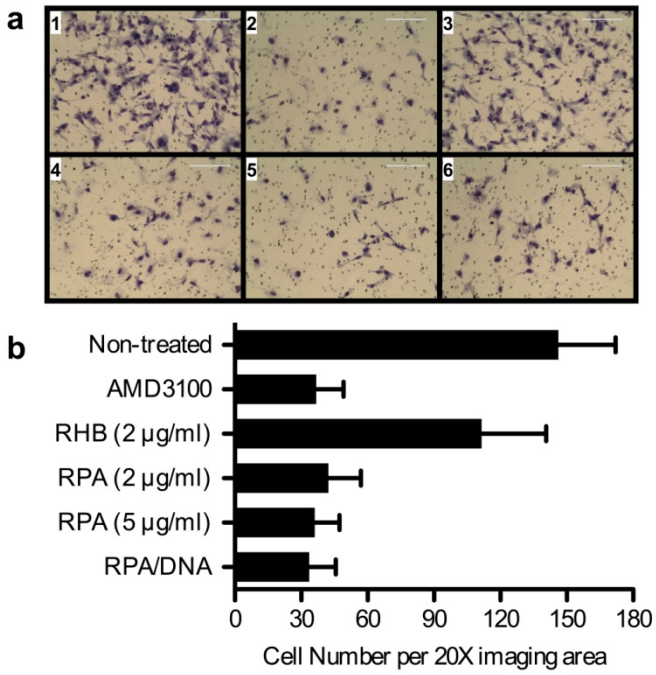

Figure 31. Inhibition of cancer cell invasion by RPA and RPA/DNA polyplexes. (a) Cell invasion assay with CXCR4+ U2OS cells treated with 1) no drug; 2) 0.24 µg/mL AMD3100.8HCl; 3) 2 µg/ml RHB.HCl; 4) 2 µg/ml RPA.HCl; 5) 5 µg/ml RPA.HCl and 6) RPA/DNA polyplexes (w/w 5, total RPA conc, 5 µg/ml). Cells were seeded in Matrigel-coated inserts and allowed to invade towards CXCL12-containing medium for 16 h before fixation and imaging. (b) Average number of invaded cells in 20× imaging area.

5.3.6 Transfection of RPA/DNA polyplexes

Having confirmed CXCR4 antagonism and inhibition of cancer cell invasion of the synthesized RPA, we then evaluated its gene delivery capability (Figure 32). A routine luciferase transfection experiment was conducted. RPA/DNA polyplexes exhibited high in vitro transfection efficiency that was comparable with that of control PEI/DNA polyplexes and RHB/DNA in B16F10 and U2OS cell lines at a DNA dose of 2.35 µg/mL. It is interesting that AMD3100 itself was able to mediate some transfection, especially in B16F10 cells when

compared with naked DNA only. As shown in Figure 28, the partial DNA condensation is the most likely reason for the observed transfection, which is nevertheless several orders of magnitude below transfection of the polymers.

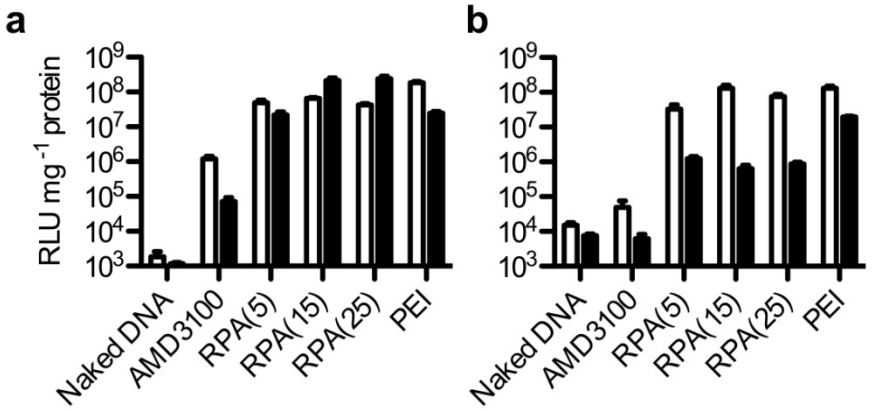

Figure 32. Transfection activity of RPA/DNA polyplexes prepared at w/w 5, 15 and 25 in the absence (white bars) and the presence (black bars) of 10% FBS in (a) B16F10 and (b) CXCR4+ U2OS cells. (Results are shown as mean luciferase expression in RLU/mg protein ± SD, n=3).

5.3.7 Simultaneous CXCR4 antagonism and gene delivery

CXCR4 antagonism by RPA does not require the polymer to be internalized, which is advantageous because no intracellular barriers need to be overcome (Wu, Liu et al. 2010). However, because the CXCR4 receptor is not internalized in the presence of an antagonist like RPA, binding of RPA/DNA to this receptor would be unproductive in mediating transfection. Polyplex transfection by CXCR4-mediated uptake was clearly unsuitable in experiments that attempted to use AMD3100 to target PEI polyplexes to CXCR4-overexpressing cells. The authors found no significant increase in transfection unless phorbol myristate acetate (PMA) was used to trigger CXCR4 receptor

endocytosis (Le Bon, Craynest et al. 2004). Here we show that RPA/DNA polyplexes use an alternative uptake pathway that does not require CXCR4. This is documented by the lack of signal from RPA/DNA polyplexes with fluorescently labeled DNA colocalized with the membrane-present CXCR4 receptor. As shown in Figure 33, after 3 h incubation with RPA/DNA polyplexes, the CXCR4+ U2OS cells were stimulated with hCXCL12 and the confocal image (taken in the middle of the Z-stack) shows more clearly that the GFP-CXCR4 receptors are mostly presented in the cell membrane. At the same time, labeled RPA/DNA polyplexes (red fluorescence) are shown internalized into the cells and notbound with the membrane-localized CXCR4 receptors. We thus hypothesize that the polyplexes are internalized through a different endocytic pathway that does not involve CXCR4.

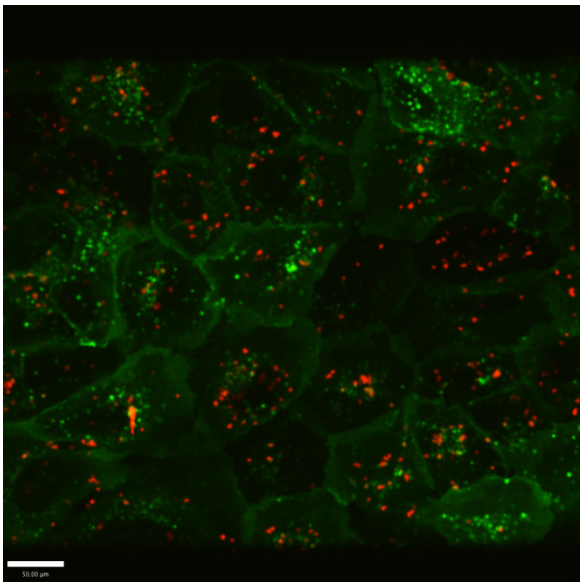

Figure 33. Intracellular distribution of RPA/DNA polyplexes in CXCR4+ U2OS cells (red fluorescence: CX-Rhodamine labeled plasmid DNA; green fluorescence: GFP-CXCR4 receptor).

To further study if CXCR4 inhibition affects the gene delivery function of

RPA/DNA polyplexes, AMD3100 was used to block the cell surface CXCR4 receptors before conducting transfection. No significant difference was observed in transfection efficiency in CXCR4+ U2OS cells either with or without CXCL12 simulation (Figure 34). The results suggest that the uptake of RPA/DNA polyplexes is not dependent on binding with CXCR4 receptors.

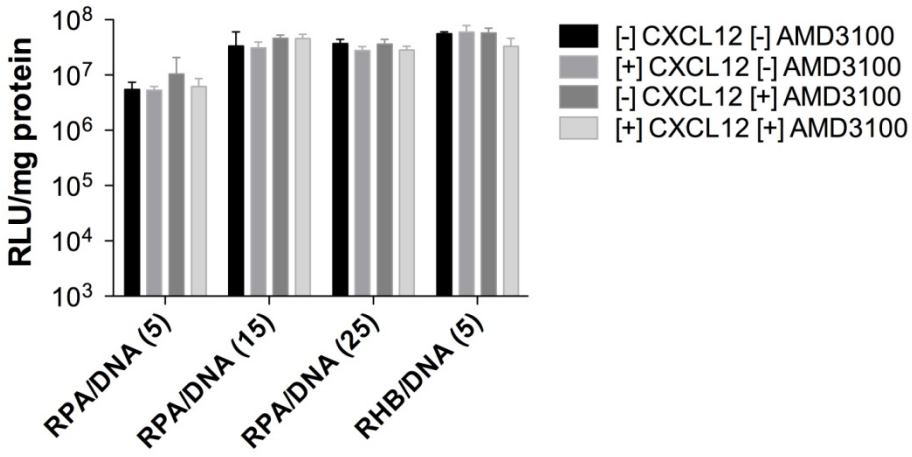

Figure 34. Effect of CXCR4 stimulation/inhibition on RPA/DNA transfection. CXCR4+ U2OS cells were pre-treated with 300 nM AMD3100 for 15 min before adding polyplexes prepared at different w/w ratios. The cells were then stimulated with 10 nM CXCL12 and co-incubated with the polyplexes during transfection.

It has been reported that CXCL12 and phorbol esters trigger CXCR4 internalization through entirely different uptake pathway (Signoret, Oldridge et al. 1997). AMD3100 only inhibits CXCL12-induced CXCR4 endocytosis, but does not affect phorbol ester-induced receptor internalization (Hatse, Princen et al. 2002). Here, CXCR4+ U2OS cells were treated with RPA/DNA polyplexes or AMD3100 before incubation with 100 ng/mL of phorbol 12-myristate 13-acetate (PMA) and the cells were imaged by fluorescence microscope (Figure 35). The

results show that internalization of CXCR4 receptor is not inhibited by RPA/DNA polyplexes similarly to AMD3100 when the cells are stimulated with phorbol myristate (PMA).

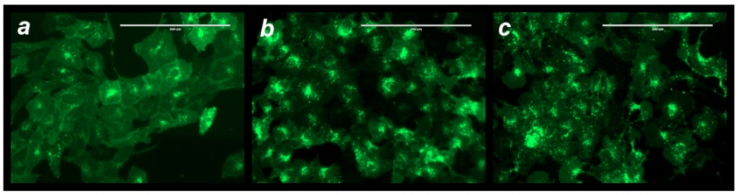

Figure 35. AMD3100 and RPA do not inhibit phorbol-stimulated CXCR4 internalization. CXCR4+ U2OS cells were treated with AMD3100.8HCl (0.24 µg/mL) and then stimulated with a) 10 nM CXCL12 or b) 100 ng/ml of phorbol myristate acetate. c) CXCR4+ U2OS cells were treated with RPA/DNA (w/w 5) polyplexes (i.e., 0.5 µg/mL RPA, 0.1 µg/mL DNA) and then stimulated with 100 ng/ml of phorbol myristate acetate.

To further confirm if CXCR4 is involved in the transfection process of the polyplexes, we evaluated the effect of PMA treatment on transfection activity of RPA/DNA polyplexes. The experiment was conducted using the same conditions as described above, except that the cells were co-incubated with polyplexes and 100 ng/mL of PMA in serum-free medium for 4 h. No cytotoxicity of PMA was observed under the used experimental conditions. The hypothesis was that PMA-induced CXCR4 internalization would improve cellular uptake of the polyplexes and that this would lead to improved transfection efficiency if polyplexes were internalized by CXCR4-dependent endocytic pathway. The results show that PMA did not enhance transfection of RPA polyplexes despite its ability to trigger internalization of the CXCR4 receptor by an alternative pathway from CXCL12 (Figure 36). This finding provides further support for the lack of involvement of the CXCR4 receptor in transfection activity of RPA/DNA.

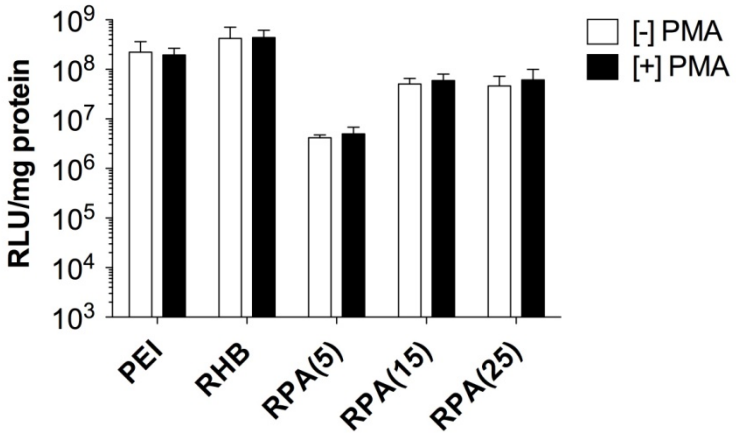

Figure 36. Effect of phorbol myristate (+/- PMA) treatment on transfection activity of RPA/DNA prepared at w/w 5, 15 and 25.

Importantly for practical utility of the dual-function polycations, we also show concurrent CXCR4 inhibition and transfection with RPA/DNA polyplexes (Figure 37). CXCR4+ U2OS cells were plated in black 96-well plate with optical bottom 24 h before the experiment at a seeding density of 8,000 cells per well. The cells were incubated with RPA/DNA polyplexes prepared at w/w 5, 10 and 15 (2.35 μg/mL DNA) or RHB/DNA polyplexes (negative control) prepared at w/w 5 in serum-free media. The polyplexes were removed after 4 h incubation and the cells were continued to grow in fresh complete culture media. The luciferase transfection was measured after 24 h. The CXCR4 antagonism was evaluated in the same cells at 0 h and 24 h after polyplex incubation by stimulating the cells with 10 nM hCXCL12. The results show that RPA/DNA polyplexes simultaneously inhibit CXCR4 (Figure 37a) and mediate effective transfection (Figure 37b). Additionally, RPA/DNA polyplexes maintain their CXCR4 inhibiting properties even after 24 hours (although the inhibition was not as complete as in

the early time point as judged by the reappearance of the punctate fluorescence distribution of the CXCR4 receptor at 24 h in Figure 37a). In contrast, the negative control (RHB/DNA polyplexes) shows no CXCR4 antagonism at any time point, while mediating similar transfection activity as RPA/DNA. These findings support our proposed mechanism of action in which the free RPA inhibits CXCR4 while the rest of the RPA/DNA polyplex formulation participates in transfection, most likely through nonspecific charge-mediated uptake.

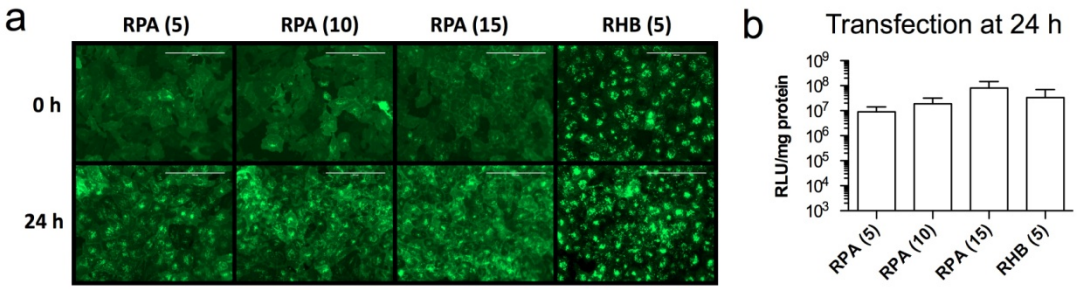

Figure 37. Simultaneous transfection and CXCR4 inhibition by RPA/DNA polyplexes in CXCR4+ U2OS cells. a) Cells treated with RPA/DNA polyplexes (RPA/DNA w/w = 5, 10 and 15) showed CXCR4 inhibition both at 0 h and, a weaker one, at 24 h after polyplex incubation. In contrast, RHB/DNA polyplexes (RHB(5)) showed no CXCR4 antagonism at any time. b) Simultaneously, RPA/DNA polyplexes exhibit similar transfection (luciferase expression) as control RHB polyplexes at 24 h after polyplex incubation.

5.4 Conclusions

In summary, we have described the preparation of a synthetic polycation that functions as a CXCR4 antagonist capable of blocking cancer cell invasion while simultaneously effectively delivering plasmid DNA and mediating transfection. Such dual-function delivery vectors can enhance antimetastatic efficacy of a variety of cancer gene therapy protocols.

REFERENCES

(2006). "One of three successfully treated CGD patients in a Swiss-German gene therapy trial died due to his underlying disease: A position statement from the European Society of Gene Therapy (ESGT)." J Gene Med **8**(12): 1435.

Aartsma-Rus, A. and G. J. van Ommen (2010). "Progress in therapeutic antisense applications for neuromuscular disorders." Eur J Hum Genet **18**(2): 146-153.

Akashi, T., K. Koizumi, et al. (2008). "Chemokine receptor CXCR4 expression and prognosis in patients with metastatic prostate cancer." Cancer Sci **99**(3): 539-542.

Al-Hajj, M., M. S. Wicha, et al. (2003). "Prospective identification of tumorigenic breast cancer cells." Proceedings of the National Academy of Sciences of the United States of America **100**(7): 3983-3988.

Alexandrova, R. (2009). "Experimental strategies in gene therapy of cancer." J BUON **14 Suppl 1**: S23-32.

Aravindan, L., K. A. Bicknell, et al. (2009). "Effect of acyl chain length on transfection efficiency and toxicity of polyethylenimine." Int J Pharm **378**(1-2): 201-210.

Arrigo, A. P. (1999). "Gene expression and the thiol redox state." Free Radical Biology and Medicine **27**(9-10): 936-944.

Aubry, S., F. Burlina, et al. (2009). "Cell-surface thiols affect cell entry of disulfide-conjugated peptides." FASEB Journal **23**(9): 2956-2967.

Austin, C. D., X. Wen, et al. (2005). "Oxidizing potential of endosomes and lysosomes limits intracellular cleavage of disulfide-based antibody-drug conjugates." Proceedings of the National Academy of Sciences of the United States of America **102**(50): 17987-17992.

Baker, A., M. Saltik, et al. (1997). "Polyethylenimine (PEI) is a simple, inexpensive and effective reagent for condensing and linking plasmid DNA to adenovirus for gene delivery." Gene Ther **4**(8): 773-782.

Bellomo, G., M. Vairetti, et al. (1992). "Demonstration of Nuclear Compartmentalization of Glutathione in Hepatocytes." Proceedings of the National Academy of Sciences of the United States of America **89**(10): 4412-4416.

Beloor, J., C. S. Choi, et al. (2012). "Arginine-engrafted biodegradable polymer for the systemic delivery of therapeutic siRNA." Biomaterials **33**(5): 1640-1650.

Bielinska, A., J. F. Kukowska-Latallo, et al. (1996). "Regulation of in vitro gene expression using antisense oligonucleotides or antisense expression plasmids transfected using starburst PAMAM dendrimers." Nucleic Acids Res **24**(11): 2176-2182.

Blacklock, J., Y. Z. You, et al. (2009). "Gene delivery in vitro and in vivo from bioreducible multilayered polyelectrolyte films of plasmid DNA." Biomaterials **30**(5): 939-950.

Blaese, R. M., K. W. Culver, et al. (1995). "T lymphocyte-directed gene therapy for ADA- SCID: initial trial results after 4 years." Science **270**(5235): 475-480.

Boden, D., O. Pusch, et al. (2004). "Enhanced gene silencing of HIV-1 specific siRNA using microRNA designed hairpins." Nucleic Acids Res **32**(3): 1154-1158.

Bokhari, M., R. J. Carnachan, et al. (2007). "Culture of HepG2 liver cells on three dimensional polystyrene scaffolds enhances cell structure and function during toxicological challenge." J Anat **211**(4): 567-576.

Bonehill, A., A. M. Van Nuffel, et al. (2009). "Single-step antigen loading and activation of dendritic cells by mRNA electroporation for the purpose of therapeutic vaccination in melanoma patients." Clin Cancer Res **15**(10): 3366-3375.

Borjesson, P. K., E. J. Postema, et al. (2003). "Phase I therapy study with (186)Re-labeled humanized monoclonal antibody BIWA 4 (bivatuzumab) in patients with head and neck squamous cell carcinoma." Clin Cancer Res **9**(10 Pt 2): 3961S-3972S.

Boswell, C. A., C. A. Regino, et al. (2009). "A novel side-bridged hybrid phosphonate/acetate pendant cyclam: synthesis, characterization, and 64Cu small animal PET imaging." Bioorg Med Chem **17**(2): 548-552.

Boussif, O., F. Lezoualc'h, et al. (1995). "A versatile vector for gene and oligonucleotide transfer into cells in culture and in vivo: polyethylenimine." Proc Natl Acad Sci U S A **92**(16): 7297-7301.

Braakman, I., J. Helenius, et al. (1992). "Manipulating disulfide bond formation and protein folding in the endoplasmic reticulum." Embo J **11**(5): 1717-1722.

Bridger, G. J., R. T. Skerlj, et al. (2010). "Synthesis and Structure−Activity Relationships of Azamacrocyclic C-X-C Chemokine Receptor 4 Antagonists: Analogues Containing a Single Azamacrocyclic Ring are Potent Inhibitors of T-Cell Tropic (X4) HIV-1 Replication." Journal of Medicinal Chemistry **53**(3): 1250-1260.

Brumbach, J. H., C. Lin, et al. (2010). "Mixtures of poly(triethylenetetramine/cystamine bisacrylamide) and poly(triethylenetetramine/cystamine bisacrylamide)-g-poly(ethylene glycol) for improved gene delivery." Bioconjug Chem **21**(10): 1753-1761.

Buehler, A., M. A. van Zandvoort, et al. (2006). "cNGR: a novel homing sequence for CD13/APN targeted molecular imaging of murine cardiac angiogenesis in vivo." Arterioscler Thromb Vasc Biol **26**(12): 2681-2687.

Bulpitt, P. and D. Aeschlimann (1999). "New strategy for chemical modification of hyaluronic acid: Preparation of functionalized derivatives and their use in the formation of novel biocompatible hydrogels." Journal of Biomedical Materials Research **47**(2): 152-169.

Burger, J. A. and T. J. Kipps (2006). "CXCR4: a key receptor in the crosstalk between tumor cells and their microenvironment." Blood **107**(5): 1761-1767.

Capecchi, M. R. (1980). "High efficiency transformation by direct microinjection of DNA into cultured mammalian cells." Cell **22**(2 Pt 2): 479-488.

Chan, J. H., S. Lim, et al. (2006). "Antisense oligonucleotides: from design to therapeutic application." Clin Exp Pharmacol Physiol **33**(5-6): 533-540.

Chang, L. and M. Karin (2001). "Mammalian MAP kinase signalling cascades." Nature **410**(6824): 37-40.

Check, E. (2003). "Harmful potential of viral vectors fuels doubts over gene therapy." Nature **423**(6940): 573-574.

Chen, C. P., J. S. Kim, et al. (2006). "Gene transfer with poly-melittin peptides." Bioconjugate Chemistry **17**(4): 1057-1062.

Chen, J., C. Wu, et al. (2009). "Bioreducible hyperbranched poly(amido amine)s for gene delivery." Biomacromolecules **10**(10): 2921-2927.

Chinni, S. R., S. Sivalogan, et al. (2006). "CXCL12/CXCR4 signaling activates Akt-1 and MMP-9 expression in prostate cancer cells: The role of bone microenvironment-associated CXCL12." Prostate **66**(1): 32-48.

Choi, K. Y., K. H. Min, et al. (2009). "Self-assembled hyaluronic acid nanoparticles as a potential drug carrier for cancer therapy: synthesis, characterization, and in vivo biodistribution." Journal of Materials Chemistry **19**(24): 4102-4107.

Choi, Y., T. Thomas, et al. (2005). "Synthesis and functional evaluation of DNA-assembled polyamidoamine dendrimer clusters for cancer cell-specific targeting." Chem Biol **12**(1): 35-43.

Christensen, L. V., C. W. Chang, et al. (2006). "Reducible poly(amido ethylenimine)s designed for triggered intracellular gene delivery." Bioconjug Chem **17**(5): 1233-1240.

Christensen, L. V., C. W. Chang, et al. (2006). "Reducible poly(amido ethylenimine)s designed for triggered intracellular gene delivery." Bioconjugate Chemistry **17**(5): 1233-1240.

Christensen, L. V., C. W. Chang, et al. (2007). "Reducible poly(amido ethylenediamine) for hypoxia-inducible VEGF delivery." J Control Release **118**(2): 254-261.

Collins, A. T., P. A. Berry, et al. (2005). "Prospective identification of tumorigenic prostate cancer stem cells." Cancer Research **65**(23): 10946-10951.

Collins, D. S., E. R. Unanue, et al. (1991). "Reduction of Disulfide Bonds within Lysosomes Is a Key Step in Antigen Processing." Journal of Immunology **147**(12): 4054-4059.

Collis, L., C. Hall, et al. (1998). "Rapid hyaluronan uptake is associated with enhanced motility: implications for an intracellular mode of action." FEBS Letters **440**(3): 444-449.

Colnot, D. R., G. J. Ossenkoppele, et al. (2002). "Reinfusion of unprocessed, granulocyte colony-stimulating factor-stimulated whole blood allows dose escalation of 186Relabeled chimeric monoclonal antibody U36 radioimmunotherapy in a phase I dose escalation study." Clin Cancer Res **8**(11): 3401-3406.

Colnot, D. R., J. C. Roos, et al. (2003). "Safety, biodistribution, pharmacokinetics, and immunogenicity of 99mTc-labeled humanized monoclonal antibody BIWA 4 (bivatuzumab) in patients with squamous cell carcinoma of the head and neck." Cancer Immunol Immunother **52**(9): 576-582.

Conry, R. M., A. F. LoBuglio, et al. (1995). "Characterization of a messenger RNA polynucleotide vaccine vector." Cancer Res **55**(7): 1397-1400.

Curnock, A. P., Y. Sotsios, et al. (2003). "Optimal chemotactic responses of leukemic T cells to stromal cell-derived factor-1 requires the activation of both class IA and IB phosphoinositide 3-kinases." J Immunol **170**(8): 4021-4030.

Dar, A., P. Goichberg, et al. (2005). "Chemokine receptor CXCR4-dependent internalization and resecretion of functional chemokine SDF-1 by bone marrow endothelial and stromal cells." Nat Immunol **6**(10): 1038-1046.

Davis, M. E. (2009). "The First Targeted Delivery of siRNA in Humans via a Self-Assembling, Cyclodextrin Polymer-Based Nanoparticle: From Concept to Clinic." Molecular Pharmaceutics **6**(3): 659-668.

De Clercq, E. (2003). "The bicyclam AMD3100 story." Nature Reviews. Drug Discovery **2**(7): 581-587.

Dean, D. A., D. D. Strong, et al. (2005). "Nuclear entry of nonviral vectors." Gene Ther **12**(11): 881-890.

Dessolin, J., P. Galea, et al. (1999). "New Bicyclam−AZT Conjugates: Design, Synthesis, Anti-HIV Evaluation, and Their Interaction with CXCR-4 Coreceptor." Journal of Medicinal Chemistry **42**(2): 229-241.

Di Guglielmo, G. M., C. Le Roy, et al. (2003). "Distinct endocytic pathways regulate TGF-beta receptor signalling and turnover." Nat Cell Biol **5**(5): 410-421.

Dias, N. and C. A. Stein (2002). "Antisense oligonucleotides: basic concepts and mechanisms." Mol Cancer Ther **1**(5): 347-355.

Dietrich, A., E. Tanczos, et al. (1997). "High CD44 surface expression on primary tumours of malignant melanoma correlates with increased metastatic risk and reduced survival." European Journal of Cancer **33**(6): 926-930.

Dominska, M. and D. M. Dykxhoorn (2010). "Breaking down the barriers: siRNA delivery and endosome escape." J Cell Sci **123**(Pt 8): 1183-1189.

Dong, Y., J. Li, et al. (2010). "Bisethylnorspermine lipopolyamine as potential delivery vector for combination drug/gene anticancer therapies." Pharm Res **27**(9): 1927-1938.

Donoghue, N. and P. J. Hogg (2002). "Characterization of redox-active proteins on cell surface." Methods Enzymol **348**: 76-86.

Donoghue, N. and P. J. Hogg (2002). "Characterization of redox-active proteins on cell surface." Methods in Enzymology **348**: 76-86.

Dorn, A. and S. Kippenberger (2008). "Clinical application of CpG-, non-CpG-, and antisense oligodeoxynucleotides as immunomodulators." Curr Opin Mol Ther **10**(1): 10-20.

Driessen, W. H. P., N. Fujii, et al. (2008). "Development of Peptide-targeted Lipoplexes to CXCR4-expressing Rat Glioma Cells and Rat Proliferating Endothelial Cells." Molecular Therapy **16**(3): 516-524.

Dwarki, V. J., R. W. Malone, et al. (1993). "Cationic liposome-mediated RNA transfection." Methods Enzymol **217**: 644-654.

Edelstein, M. L., M. R. Abedi, et al. (2007). "Gene therapy clinical trials worldwide to 2007--an update." J Gene Med **9**(10): 833-842.

Egorova, A., A. Kiselev, et al. (2009). "Chemokine-derived peptides as carriers for gene delivery to CXCR4 expressing cells." The Journal of Gene Medicine **11**(9): 772-781.

Eliaz, R. E., S. Nir, et al. (2004). "Determination and modeling of kinetics of cancer cell killing by doxorubicin and doxorubicin encapsulated in targeted liposomes." Cancer Research **64**(2): 711-718.

Eliaz, R. E. and F. C. Szoka, Jr. (2001). "Liposome-encapsulated Doxorubicin Targeted to CD44: A Strategy to Kill CD44-overexpressing Tumor Cells." Cancer Res **61**(6): 2592-2601.

Entwistle, J., C. L. Hall, et al. (1996). "Receptors: Regulators of signalling to the cytoskeleton." Journal of Cellular Biochemistry **61**(4): 569-577.

Faham, A., T. Herringson, et al. (2011). "pDNA-lipoplexes engrafted with flagellin-related peptide induce potent immunity and anti-tumour effects." Vaccine **29**(40): 6911-6919.

Feener, E. P., W. C. Shen, et al. (1990). "Cleavage of Disulfide Bonds in Endocytosed Macromolecules - a Processing Not Associated With Lysosomes or Endosomes." Journal of Biological Chemistry **265**(31): 18780-18785.

Felgner, P. L., T. R. Gadek, et al. (1987). "Lipofection: a highly efficient, lipid-mediated DNA-transfection procedure." Proc Natl Acad Sci U S A **84**(21): 7413-7417.

Fella, C., G. F. Walker, et al. (2008). "Amine-reactive pyridylhydrazone-based PEG reagents for pH-reversible PEI polyplex shielding." Eur J Pharm Sci **34**(4-5): 309-320.

Fernandis, A. Z., A. Prasad, et al. (2004). "Regulation of CXCR4-mediated chemotaxis and chemoinvasion of breast cancer cells." Oncogene **23**(1): 157-167.

Filippov, S. K., C. Konak, et al. (2010). "Effect of hydrophobic interactions on properties and stability of DNA-polyelectrolyte complexes." Langmuir **26**(7): 4999-5006.

Fire, A., S. Xu, et al. (1998). "Potent and specific genetic interference by double-stranded RNA in Caenorhabditis elegans." Nature **391**(6669): 806-811.

Fivaz, M., F. Vilbois, et al. (2002). "Differential sorting and fate of endocytosed GPI-anchored proteins." Embo J **21**(15): 3989-4000.

Florea, B. I., C. Meaney, et al. (2002). "Transfection efficiency and toxicity of polyethylenimine in differentiated Calu-3 and nondifferentiated COS-1 cell cultures." AAPS PharmSci **4**(3): E12.

Forster, R., E. Kremmer, et al. (1998). "Intracellular and surface expression of the HIV-1 coreceptor CXCR4/fusin on various leukocyte subsets: rapid internalization and recycling upon activation." J Immunol **160**(3): 1522-1531.

Gansbacher, B. (2002). "Policy statement on the social, ethical and public awareness issues in gene therapy." J Gene Med **4**(6): 687-691.

Gansbacher, B. (2003). "Report of a second serious adverse event in a clinical trial of gene therapy for X-linked severe combined immune deficiency (X-SCID). Position of the European Society of Gene Therapy (ESGT)." J Gene Med **5**(3): 261-262.

Geiger, R. C., C. D. Kaufman, et al. (2009). "Tubulin acetylation and histone deacetylase 6 activity in the lung under cyclic load." Am J Respir Cell Mol Biol **40**(1): 76-82.

Gilbert, H. F. (1990). "Molecular and cellular aspects of thiol-disulfide exchange." Adv Enzymol Relat Areas Mol Biol **63**: 69-172.

Gilbert, H. F. (1997). "Protein disulfide isomerase and assisted protein folding." Journal of Biological Chemistry **272**(47): 29399-29402.

Gilbert, H. F. (1997). "Protein disulfide isomerase and assisted protein folding." J Biol Chem **272**(47): 29399-29402.

Gilboa, E. and J. Vieweg (2004). "Cancer immunotherapy with mRNA-transfected dendritic cells." Immunol Rev **199**: 251-263.

Girotto, D., S. Urbani, et al. (2003). "Tissue-specific gene expression in chondrocytes grown on three-dimensional hyaluronic acid scaffolds." Biomaterials **24**(19): 3265-3275.

Goncalves, C., E. Mennesson, et al. (2004). "Macropinocytosis of polyplexes and recycling of plasmid via the clathrin-dependent pathway impair the

transfection efficiency of human hepatocarcinoma cells." Mol Ther **10**(2): 373-385.

Gosselin, M. A., W. Guo, et al. (2001). "Efficient gene transfer using reversibly cross-linked low molecular weight polyethylenimine." Bioconjug Chem **12**(6): 989-994.

Goyal, R., S. K. Tripathi, et al. (2012). "Linear PEI nanoparticles: efficient pDNA/siRNA carriers in vitro and in vivo." Nanomedicine **8**(2): 167-175.

Graessmann, M., J. Menne, et al. (1989). "Helper activity for gene expression, a novel function of the SV40 enhancer." Nucleic Acids Res **17**(16): 6603-6612.

Hanahan, D. and Robert A. Weinberg (2011). "Hallmarks of Cancer: The Next Generation." Cell **144**(5): 646-674.

Hansen, R. E., D. Roth, et al. (2009). "Quantifying the global cellular thiol-disulfide status." Proceedings of the National Academy of Sciences of the United States of America **106**(2): 422-427.

Hartmann, T. N., J. A. Burger, et al. (2005). "CXCR4 chemokine receptor and integrin signaling co-operate in mediating adhesion and chemoresistance in small cell lung cancer (SCLC) cells." Oncogene **24**(27): 4462-4471.

Harvey, J. R., P. Mellor, et al. (2007). "Inhibition of CXCR4-mediated breast cancer metastasis: a potential role for heparinoids?" Clin Cancer Res **13**(5): 1562-1570.

Hathcock, K. S., H. Hirano, et al. (1993). "CD44 EXPRESSION ON ACTIVATED B-CELLS - DIFFERENTIAL CAPACITY FOR CD44-DEPENDENT

BINDING TO HYALURONIC-ACID." Journal of Immunology **151**(12): 6712-6722.

Hatse, S., K. Princen, et al. (2002). "Chemokine receptor inhibition by AMD3100 is strictly confined to CXCR4." FEBS Letters **527**(1): 255-262.

Hatse, S., K. Princen, et al. (2002). "Chemokine receptor inhibition by AMD3100 is strictly confined to CXCR4." FEBS Lett **527**(1-3): 255-262.

He, L. and G. J. Hannon (2004). "MicroRNAs: small RNAs with a big role in gene regulation." Nat Rev Genet **5**(7): 522-531.

Hill, A., S. McFarlane, et al. (2006). "The emerging role of CD44 in regulating skeletal micrometastasis." Cancer Letters **237**(1): 1-9.

Hobbs, S. K., W. L. Monsky, et al. (1998). "Regulation of transport pathways in tumor vessels: Role of tumor type and microenvironment." Proceedings of the National Academy of Sciences of the United States of America **95**(8): 4607-4612.

Holter, D., A. Burgath, et al. (1997). "Degree of branching in hyperbranched polymers." Acta Polymerica **48**(1-2): 30-35.

Hong, C. Y., Y. Z. You, et al. (2007). "Thermal control over the topology of cleavable polymers: From linear to hyperbranched structures." Journal of the American Chemical Society **129**(17): 5354-+.

Hoon Jeong, J., L. V. Christensen, et al. (2007). "Reducible poly(amido ethylenimine) directed to enhance RNA interference." Biomaterials **28**(10): 1912-1917.

Hornof, M., M. de la Fuente, et al. (2008). "Low molecular weight hyaluronan shielding of DNA/PEI polyplexes facilitates CD44 receptor mediated uptake in human corneal epithelial cells." J Gene Med **10**(1): 70-80.

Hornof, M., M. de la Fuente, et al. (2008). "Low molecular weight hyaluronan shielding of DNA/PEI polyplexes facilitates CD44 receptor mediated uptake in human corneal epithelial cells." Journal of Gene Medicine **10**: 70-80.

Horton, H. M., P. A. Lalor, et al. (2008). "IL-2 plasmid electroporation: from preclinical studies to phase I clinical trial." Methods Mol Biol **423**: 361-372.

Huang, Q. D., W. J. Ou, et al. (2011). "Novel cationic lipids possessing protonated cyclen and imidazolium salt for gene delivery." Eur J Pharm Biopharm **78**(3): 326-335.

Huang, Q. D., J. Ren, et al. (2012). "Cationic lipids containing cyclen and ammonium moieties as gene delivery vectors." Chemical Biology & Drug Design **79**(6): 879-887.

Huang, Q. D., G. X. Zhong, et al. (2011). "Cyclen-based cationic lipids for highly efficient gene delivery towards tumor cells." Plos One **6**(8): e23134.

Hwang, C., H. F. Lodish, et al. (1995). "Measurement of glutathione redox state in cytosol and secretory pathway of cultured cells." Methods Enzymol **251**: 212-221.

Hwang, C., A. J. Sinskey, et al. (1992). "Oxidized redox state of glutathione in the endoplasmic reticulum." Science **257**(5076): 1496-1502.

Iida, T., T. Mori, et al. (2007). "Overall interaction of cytosolic proteins with the PEI/DNA complex." Journal of Controlled Release **118**(3): 364-369.

Ishihara, T., M. Goto, et al. (2009). "Intracellular delivery of siRNA by cell-penetrating peptides modified with cationic oligopeptides." Drug Deliv **16**(3): 153-159.

Ito, T., C. Yoshihara, et al. (2010). "DNA/polyethyleneimine/hyaluronic acid small complex particles and tumor suppression in mice." Biomaterials **31**(10): 2912-2918.

Jacobson, O., I. D. Weiss, et al. (2009). "64Cu-AMD3100--a novel imaging agent for targeting chemokine receptor CXCR4." Bioorg Med Chem **17**(4): 1486-1493.

Jain, S., L. W. McGinnes, et al. (2007). "Thiol/Disulfide Exchange Is Required for Membrane Fusion Directed by the Newcastle Disease Virus Fusion Protein." Journal of Virology **81**(5): 2328-2339.

Jarnjak-Jankovic, S., R. D. Pettersen, et al. (2005). "Evaluation of dendritic cells loaded with apoptotic cancer cells or expressing tumour mRNA as potential cancer vaccines against leukemia." BMC Cancer **5**: 20.

Jere, D., R. Arote, et al. (2009). "Bioreducible polymers for efficient gene and siRNA delivery." Biomed Mater **4**(2): 025020.

Jiang, G., K. Park, et al. (2008). "Hyaluronic acid-polyethyleneimine conjugate for target specific intracellular delivery of siRNA." Biopolymers **89**(7): 635-642.

Jiang, X. M., M. Fitzgerald, et al. (1999). "Redox control of exofacial protein thiols/disulfides by protein disulfide isomerase." J Biol Chem **274**(4): 2416-2423.

Jiang, X. M., M. Fitzgerald, et al. (1999). "Redox control of exofacial protein thiols/disulfides by protein disulfide isomerase." Journal of Biological Chemistry **274**(4): 2416-2423.

Jin, Z. H., T. Furukawa, et al. (2011). "Noninvasive visualization and quantification of tumor alphaVbeta3 integrin expression using a novel positron emission tomography probe, 64Cu-cyclam-RAFT-c(-RGDfK-)4." Nucl Med Biol **38**(4): 529-540.

Jones, D. P., J. L. Carlson, et al. (1998). "Glutathione measurement in human plasma. Evaluation of sample collection, storage and derivatization conditions for analysis of dansyl derivatives by HPLC." Clinica Chimica Acta **275**(2): 175-184.

Kaneda, Y. and Y. Tabata (2006). "Non-viral vectors for cancer therapy." Cancer Sci **97**(5): 348-354.

Katoh, S., Z. Zheng, et al. (1995). "GLYCOSYLATION OF CD44 NEGATIVELY REGULATES ITS RECOGNITION OF HYALURONAN." Journal of Experimental Medicine **182**(2): 419-429.

Kawabata, A., A. Baoum, et al. (2012). "Intratracheal administration of a nanoparticle-based therapy with the angiotensin II type 2 receptor gene attenuates lung cancer growth." Cancer Res **72**(8): 2057-2067.

Kayali, A. G., K. Van Gunst, et al. (2003). "The stromal cell-derived factor-1alpha/CXCR4 ligand-receptor axis is critical for progenitor survival and migration in the pancreas." J Cell Biol **163**(4): 859-869.

Khan, A., J. Greenman, et al. (2007). "Small molecule CXCR4 chemokine candidates receptor antagonists: Developing drug candidates." Current Medicinal Chemistry **14**(21): 2257-2277.

Khan, A., G. Nicholson, et al. (2009). "Binding Optimization through Coordination Chemistry: CXCR4 Chemokine Receptor Antagonists from Ultrarigid Metal Complexes." Journal of the American Chemical Society **131**(10): 3416-3417.

Kichler, A., J. S. Remy, et al. (1995). "Efficient Gene Delivery with Neutral Complexes of Lipospermine and Thiol-Reactive Phospholipids." Biochemical and Biophysical Research Communications **209**(2): 444-450.

Kim, S. H., J. H. Jeong, et al. (2009). "VEGF siRNA delivery system using arginine-grafted bioreducible poly(disulfide amine)." Mol Pharm **6**(3): 718-726.

Kim, S. H., J. H. Jeong, et al. (2008). "Cardiomyocyte-targeted siRNA delivery by prostaglandin E(2)-Fas siRNA polyplexes formulated with reducible poly(amido amine) for preventing cardiomyocyte apoptosis." Biomaterials **29**(33): 4439-4446.

Kim, T. I. and S. W. Kim (2011). "Bioreducible polymers for gene delivery." React Funct Polym **71**(3): 344-349.

Kim, T. I., M. Lee, et al. (2012). "Efficient GLP-1 gene delivery using two-step transcription amplification plasmid system with a secretion signal peptide and arginine-grafted bioreducible polymer." J Control Release **157**(2): 243-248.

Kim, T. I., M. Ou, et al. (2009). "Arginine-grafted bioreducible poly(disulfide amine) for gene delivery systems." Biomaterials **30**(4): 658-664.

Kim, Y., M. Tewari, et al. (2009). "Polymersome delivery of siRNA and antisense oligonucleotides." J Control Release **134**(2): 132-140.

Knorr, V., L. Allmendinger, et al. (2007). "An acetal-based PEGylation reagent for pH-sensitive shielding of DNA polyplexes." Bioconjug Chem **18**(4): 1218-1225.

Kohn, D. B. and B. Gansbacher (2003). "Letter to the editors of Nature from the American Society of Gene Therapy (ASGT) and the European Society of Gene Therapy (ESGT)." J Gene Med **5**(7): 641.

Koo, H., G. W. Jin, et al. (2010). "Biodegradable branched poly(ethylenimine sulfide) for gene delivery." Biomaterials **31**(5): 988-997.

Koppe, M., F. Schaijk, et al. (2004). "Safety, pharmacokinetics, immunogenicity, and biodistribution of (186)Re-labeled humanized monoclonal antibody BIWA 4 (Bivatuzumab) in patients with early-stage breast cancer." Cancer Biother Radiopharm **19**(6): 720-729.

Kosower, N. S. and E. M. Kosower (1978). "The glutathione status of cells." Int Rev Cytol **54**: 109-160.

Krieg, A. M., A. K. Yi, et al. (1995). "CpG motifs in bacterial DNA trigger direct B-cell activation." Nature **374**(6522): 546-549.

Kukowska-Latallo, J. F., A. U. Bielinska, et al. (1996). "Efficient transfer of genetic material into mammalian cells using Starburst polyamidoamine dendrimers." Proc Natl Acad Sci U S A **93**(10): 4897-4902.

Kulkarni, R. P., K. Castelino, et al. (2006). "Intracellular transport dynamics of endosomes containing DNA polyplexes along the microtubule network." Biophys J **90**(5): L42-44.

Kwon, E. J., J. M. Bergen, et al. (2008). "Application of an HIV gp41-derived peptide for enhanced intracellular trafficking of synthetic gene and siRNA delivery vehicles." Bioconjug Chem **19**(4): 920-927.

Lam, A. R., S. Bhattacharya, et al. (2010). "Importance of Receptor Flexibility in Binding of Cyclam Compounds to the Chemokine Receptor CXCR4." Journal of Chemical Information and Modeling **51**(1): 139-147.

Lash, L. H., D. A. Putt, et al. (2002). "Overexpression of a mitochondrial glutathione transporter protects NRK-52E cells from chemically induced apoptosis." Journal of the American Society of Nephrology **13**: 292A-292A.

Lavigne, M. D., S. S. Pennadam, et al. (2007). "Enhanced gene expression through temperature profile-induced variations in molecular architecture of thermoresponsive polymer vectors." J Gene Med **9**(1): 44-54.

Le Bon, B., N. V. Craynest, et al. (2004). "AMD3100 Conjugates as Components of Targeted Nonviral Gene Delivery Systems: Synthesis and in Vitro

Transfection Efficiency of CXCR4-Expressing Cells." Bioconjugate Chemistry **15**(2): 413-423.

Lee, E. R., J. Marshall, et al. (1996). "Detailed analysis of structures and formulations of cationic lipids for efficient gene transfer to the lung." Hum Gene Ther **7**(14): 1701-1717.

Lee, H., C. H. Ahn, et al. (2009). "Poly[lactic-co-(glycolic acid)]-Grafted Hyaluronic Acid Copolymer Micelle Nanoparticles for Target-Specific Delivery of Doxorubicin." Macromolecular Bioscience **9**(4): 336-342.

Lee, H., K. Lee, et al. (2008). "Hyaluronic acid-paclitaxel conjugate micelles: Synthesis, characterization, and antitumor activity." Bioconjugate Chemistry **19**(6): 1319-1325.

Lee, H., H. Mok, et al. (2007). "Target-specific intracellular delivery of siRNA using degradable hyaluronic acid nanogels." Journal of Controlled Release **119**(2): 245-252.

Lee, H. J., Y. T. Nguyen, et al. (2012). "MR traceable delivery of p53 tumor suppressor gene by PEI-functionalized superparamagnetic iron oxide nanoparticles." J Biomed Nanotechnol **8**(3): 361-371.

Lee, S. H., S. H. Choi, et al. (2008). "Thermally sensitive cationic polymer nanocapsules for specific cytosolic delivery and efficient gene silencing of siRNA: swelling induced physical disruption of endosome by cold shock." J Control Release **125**(1): 25-32.

Lee, Y., K. Jeon, et al. (2002). "MicroRNA maturation: stepwise processing and subcellular localization." EMBO J **21**(17): 4663-4670.

Lee, Y., H. Y. Nam, et al. (2012). "Human Erythropoietin Gene Delivery Using an Arginine-grafted Bioreducible Polymer System." Mol Ther **20**(7): 1360-1366.

Leopold, P. L., G. Kreitzer, et al. (2000). "Dynein- and microtubule-mediated translocation of adenovirus serotype 5 occurs after endosomal lysis." Hum Gene Ther **11**(1): 151-165.

Lesley, J., N. English, et al. (2000). "The role of the CD44 cytoplasmic and transmembrane domains in constitutive and inducible hyaluronan binding." European Journal of Immunology **30**(1): 245-253.

Lesley, J., V. C. Hascall, et al. (2000). "Hyaluronan binding by cell surface CD44." J Biol Chem **275**(35): 26967-26975.

Lesley, J., V. C. Hascall, et al. (2000). "Hyaluronan binding by cell surface CD44." Journal of Biological Chemistry **275**(35): 26967-26975.

Leung, K. (2004). 64Cu-1,4,8,11-Tetraazacyclotetradecane-regioselectively addressable functionalized template-[cyclo-(Arg-Gly-Asp-d-Phe-Lys)]4. Molecular Imaging and Contrast Agent Database (MICAD). Bethesda (MD).

Li, C. W., D. G. Heidt, et al. (2007). "Identification of pancreatic cancer stem cells." Cancer Research **67**(3): 1030-1037.

Li, J., D. S. Manickam, et al. (2012). "Effect of cell membrane thiols and reduction-triggered disassembly on transfection activity of bioreducible polyplexes." Eur J Pharm Sci **46**(3): 173-180.

Li, J., Y. Zhu, et al. (2012). "Dual-Function CXCR4 Antagonist Polyplexes To Deliver Gene Therapy and Inhibit Cancer Cell Invasion." Angew Chem Int Ed Engl.

Li, S., Y. Wang, et al. (2012). "Biodegradable cyclen-based linear and cross-linked polymers as non-viral gene vectors." Bioorg Med Chem **20**(4): 1380-1387.

Liang, Z., W. Zhan, et al. (2012). "Development of a Unique Small Molecule Modulator of CXCR4." PLoS One **7**(4): e34038.

Liang, Z. X., Y. H. Yoon, et al. (2005). "Silencing of CXCR4 blocks breast cancer metastasis." Cancer Research **65**(3): 967-971.

Lin, C., C. J. Blaauboer, et al. (2008). "Bioreducible poly(amido amine)s with oligoamine side chains: synthesis, characterization, and structural effects on gene delivery." J Control Release **126**(2): 166-174.

Lin, C., Z. Zhong, et al. (2006). "Linear poly(amido amine)s with secondary and tertiary amino groups and variable amounts of disulfide linkages: synthesis and in vitro gene transfer properties." Journal of Controlled Release **116**(2): 130-137.

Lin, C., Z. Zhong, et al. (2007). "Novel bioreducible poly(amido amine)s for highly efficient gene delivery." Bioconjug Chem **18**(1): 138-145.

Lin, C., Z. Zhong, et al. (2007). "Random and block copolymers of bioreducible poly(amido amine)s with high- and low-basicity amino groups: study of DNA condensation and buffer capacity on gene transfection." J Control Release **123**(1): 67-75.

Liu, F., Y. Song, et al. (1999). "Hydrodynamics-based transfection in animals by systemic administration of plasmid DNA." Gene Ther **6**(7): 1258-1266.

Liu, J. L., Q. P. Ma, et al. (2011). "Cationic lipids containing protonated cyclen and different hydrophobic groups linked by uracil-PNA monomer: synthesis and application for gene delivery." Eur J Med Chem **46**(9): 4133-4141.

Liu, Z., M. Zheng, et al. (2011). "Non-viral gene transfection in vitro using endosomal pH-sensitive reversibly hydrophobilized polyethylenimine." Biomaterials **32**(34): 9109-9119.

Lo, A. T., N. K. Salam, et al. (2011). "Polyamide-scorpion cyclam lexitropsins selectively bind AT-rich DNA independently of the nature of the coordinated metal." Plos One **6**(5): e17446.

Lo, H. W., C. P. Day, et al. (2005). "Cancer-specific gene therapy." Adv Genet **54**: 235-255.

Luker, K. E. and G. D. Luker (2006). "Functions of CXCL12 and CXCR4 in breast cancer." Cancer Lett **238**(1): 30-41.

Luo, J., B. D. Manning, et al. (2003). "Targeting the PI3K-Akt pathway in human cancer: rationale and promise." Cancer Cell **4**(4): 257-262.

Luo, Y. and G. D. Prestwich (1999). "Synthesis and Selective Cytotoxicity of a Hyaluronic Acid-Antitumor Bioconjugate." Bioconjugate Chemistry **10**(5): 755-763.

Luo, Y. and G. D. Prestwich (2001). "Hyaluronic acid-N-hydroxysuccinimide: a useful intermediate for bioconjugation." Bioconjug Chem **12**(6): 1085-1088.

Luo, Y., M. R. Ziebell, et al. (2000). "A hyaluronic acid-taxol antitumor bioconjugate targeted to cancer cells." Biomacromolecules **1**(2): 208-218.

Maeda, H., L. W. Seymour, et al. (1992). "Conjugates of anticancer agents and polymers: advantages of macromolecular therapeutics in vivo." Bioconjug Chem **3**(5): 351-362.

Mahato, R. I., M. Lee, et al. (2001). "Intratumoral delivery of p2CMVmIL-12 using water-soluble lipopolymers." Mol Ther **4**(2): 130-138.

Malek, A., O. Merkel, et al. (2009). "In vivo pharmacokinetics, tissue distribution and underlying mechanisms of various PEI(-PEG)/siRNA complexes." Toxicol Appl Pharmacol **236**(1): 97-108.

Malone, R. W., P. L. Felgner, et al. (1989). "Cationic liposome-mediated RNA transfection." Proc Natl Acad Sci U S A **86**(16): 6077-6081.

Manickam, D. S., H. S. Bisht, et al. (2005). "Influence of TAT-peptide polymerization on properties and transfection activity of TAT/DNA polyplexes." Journal of Controlled Release **102**(1): 293-306.

Manickam, D. S., A. Hirata, et al. (2008). "Overexpression of Bcl-2 as a proxy redox stimulus to enhance activity of non-viral redox-responsive delivery vectors." Biomaterials **29**(17): 2680-2688.

Manickam, D. S., J. Li, et al. (2010). "Effect of innate glutathione levels on activity of redox-responsive gene delivery vectors." J Control Release **141**(1): 77-84.

Manickam, D. S., J. Li, et al. (2010). "Effect of innate glutathione levels on activity of redox-responsive gene delivery vectors." Journal of Controlled Release **141**(1): 77-84.

Manickam, D. S. and D. Oupicky (2006). "Multiblock reducible copolypeptides containing histidine-rich and nuclear localization sequences for gene delivery." Bioconjug Chem **17**(6): 1395-1403.

Manickam, D. S. and D. Oupicky (2006). "Multiblock reducible copolypeptides containing histidine-rich and nuclear localization sequences for gene delivery." Bioconjugate Chemistry **17**(6): 1395-1403.

Markovic, I., T. S. Stantchev, et al. (2004). "Thiol/disulfide exchange is a prerequisite for CXCR4-tropic HIV-1 envelope-mediated T-cell fusion during viral entry." Blood **103**(5): 1586-1594.

Martinon, F., S. Krishnan, et al. (1993). "Induction of virus-specific cytotoxic T lymphocytes in vivo by liposome-entrapped mRNA." Eur J Immunol **23**(7): 1719-1722.

Marwick, C. (1998). "First "antisense" drug will treat CMV retinitis." JAMA **280**(10): 871.

Matsumura, Y. and D. Tarin (1992). "SIGNIFICANCE OF CD44 GENE-PRODUCTS FOR CANCER-DIAGNOSIS AND DISEASE EVALUATION." Lancet **340**(8827): 1053-1058.

Meister, A. and M. E. Anderson (1983). "Glutathione." Annual Review of Biochemistry **52**: 711-760.

Mersch-Sundermann, V., S. Knasmuller, et al. (2004). "Use of a human-derived liver cell line for the detection of cytoprotective, antigenotoxic and cogenotoxic agents." Toxicology **198**(1-3): 329-340.

Moghimi, S. M., P. Symonds, et al. (2005). "A two-stage poly(ethylenimine)-mediated cytotoxicity: implications for gene transfer/therapy." Mol Ther **11**(6): 990-995.

Morgan, R. A., M. E. Dudley, et al. (2006). "Cancer regression in patients after transfer of genetically engineered lymphocytes." Science **314**(5796): 126-129.

Mu, L. J., J. A. Kyte, et al. (2005). "Immunotherapy with allotumour mRNA-transfected dendritic cells in androgen-resistant prostate cancer patients." Br J Cancer **93**(7): 749-756.

Muller, A., B. Homey, et al. (2001). "Involvement of chemokine receptors in breast cancer metastasis." Nature **410**(6824): 50-56.

Murugesa, S., S. J. Shetty, et al. (2001). "A technetium-99m-labelled cyclam acid porphyrin (CAP) for tumour imaging." Appl Radiat Isot **55**(5): 641-646.

Nabel, G. J., E. G. Nabel, et al. (1993). "Direct gene transfer with DNA-liposome complexes in melanoma: expression, biologic activity, and lack of toxicity in humans." Proc Natl Acad Sci U S A **90**(23): 11307-11311.

Nam, H. Y., J. Kim, et al. (2011). "Cell penetrating peptide conjugated bioreducible polymer for siRNA delivery." Biomaterials **32**(22): 5213-5222.

Nam, H. Y., A. McGinn, et al. (2010). "Primary cardiomyocyte-targeted bioreducible polymer for efficient gene delivery to the myocardium." Biomaterials **31**(31): 8081-8087.

Namgung, R., J. H. Brumbach, et al. (2010). "Dual bio-responsive gene delivery via reducible poly(amido amine) and survivin-inducible plasmid DNA." Biotechnol Lett **32**(6): 755-764.

Namgung, R., J. H. Brumbach, et al. (2010). "Dual bio-responsive gene delivery via reducible poly(amido amine) and survivin-inducible plasmid DNA." Biotechnology Letters **32**(6): 755-764.

Naor, D., S. Nedvetzki, et al. (2002). "CD44 in cancer." Critical Reviews in Clinical Laboratory Sciences **39**(6): 527-579.

Naor, D., S. B. Wallach-Dayan, et al. (2008). "Involvement of CD44, a molecule with a thousand faces, in cancer dissemination." Seminars in Cancer Biology **18**(4): 260-267.

Nasevicius, A. and S. C. Ekker (2000). "Effective targeted gene 'knockdown' in zebrafish." Nat Genet **26**(2): 216-220.

Neu, M., O. Germershaus, et al. (2007). "Crosslinked nanocarriers based upon poly(ethylene imine) for systemic plasmid delivery: in vitro characterization and in vivo studies in mice." J Control Release **118**(3): 370-380.

Neu, M., O. Germershaus, et al. (2007). "Crosslinked nanocarriers based upon poly(ethylene imine) for systemic plasmid delivery: In vitro characterization and in vivo studies in mice." Journal of Controlled Release **118**(3): 370-380.

Neu, M., J. Sitterberg, et al. (2006). "Stabilized nanocarriers for plasmids based upon cross-linked poly(ethylene imine)." Biomacromolecules **7**(12): 3428-3438.

Nimmagadda, S., M. Pullambhatla, et al. (2010). "Molecular imaging of CXCR4 receptor expression in human cancer xenografts with [64Cu]AMD3100 positron emission tomography." Cancer Res **70**(10): 3935-3944.

Nlend Nlend, R., K. Meyer, et al. (2010). "Repair of pre-mRNA splicing: prospects for a therapy for spinal muscular atrophy." RNA Biol **7**(4): 430-440.

Ogris, M. and E. Wagner (2002). "Tumor-targeted gene transfer with DNA polyplexes." Somat Cell Mol Genet **27**(1-6): 85-95.

Oliveira, S., M. M. Fretz, et al. (2007). "Photochemical internalization enhances silencing of epidermal growth factor receptor through improved endosomal escape of siRNA." Biochim Biophys Acta **1768**(5): 1211-1217.

Oliveira, S., I. van Rooy, et al. (2007). "Fusogenic peptides enhance endosomal escape improving siRNA-induced silencing of oncogenes." Int J Pharm **331**(2): 211-214.

Orsini, M. J., J. L. Parent, et al. (1999). "Trafficking of the HIV coreceptor CXCR4. Role of arrestins and identification of residues in the c-terminal tail that mediate receptor internalization." J Biol Chem **274**(43): 31076-31086.

Ouhtit, A., Z. Y. A. Elmageed, et al. (2007). "In vivo evidence for the role of CD44s in promoting breast cancer metastasis to the liver." American Journal of Pathology **171**(6): 2033-2039.

Oupicky, D., C. Konak, et al. (2000). "DNA delivery systems based on complexes of DNA with synthetic polycations and their copolymers." J Control Release **65**(1-2): 149-171.

Paget, S. (1989). "The distribution of secondary growths in cancer of the breast. 1889." Cancer Metastasis Rev **8**(2): 98-101.

Paisey, S. J. and P. J. Sadler (2004). "Anti-viral cyclam macrocycles : rapid zinc uptake at physiological pH." Chem Commun (Camb)(3): 306-307.

Pan, W. H. and G. A. Clawson (2006). "Antisense applications for biological control." J Cell Biochem **98**(1): 14-35.

Peer, D. and R. Margalit (2004). "Loading mitomycin C inside long circulating hyaluronan targeted nano-liposomes increases its antitumor activity in three mice tumor models." International Journal of Cancer **108**(5): 780-789.

Peer, D. and R. Margalit (2004). "Tumor-targeted hyaluronan nanoliposomes increase the antitumor activity of liposomal doxorubicin in syngeneic and human xenograft mouse tumor models." Neoplasia **6**(4): 343-353.

Peng, S. B., V. Peek, et al. (2005). "Akt activation, but not extracellular signal-regulated kinase activation, is required for SDF-1alpha/CXCR4-mediated migration of epitheloid carcinoma cells." Mol Cancer Res **3**(4): 227-236.

Phan, U. T., B. Arunachalam, et al. (2000). "Gamma-interferon-inducible lysosomal thiol reductase (GILT) - Maturation, activity, and mechanism of action." Journal of Biological Chemistry **275**(34): 25907-25914.

Philpott, G. W., S. W. Schwarz, et al. (1995). "RadioimmunoPET: detection of colorectal carcinoma with positron-emitting copper-64-labeled monoclonal antibody." J Nucl Med **36**(10): 1818-1824.

Piest, M., C. Lin, et al. (2008). "Novel poly(amido amine)s with bioreducible disulfide linkages in their diamino-units: Structure effects and in vitro gene transfer properties." Journal of Controlled Release **130**(1): 38-45.

Ponsaerts, P., V. F. Van Tendeloo, et al. (2003). "Cancer immunotherapy using RNA-loaded dendritic cells." Clin Exp Immunol **134**(3): 378-384.

Pouyani, T. and G. D. Prestwich (1993). "Functionalized Derivatives of Hyaluronic-Acid (Ha) as Drug Carriers and as Novel Biomaterials." Faseb Journal **7**(7): A1260-A1260.

Pouyani, T. and G. D. Prestwich (1994). "Functionalized Derivatives of Hyaluronic Acid Oligosaccharides: Drug Carriers and Novel Biomaterials." Bioconjugate Chemistry **5**(4): 339-347.

Prestwich, G. D., D. M. Marecak, et al. (1998). "Controlled chemical modification of hyaluronic acid: synthesis, applications, and biodegradation of hydrazide derivatives." Journal of Controlled Release **53**(1-3): 93-103.

Prince, M. E., R. Sivanandan, et al. (2007). "Identification of a subpopulation of cells with cancer stem cell properties in head and neck squamous cell carcinoma." Proceedings of the National Academy of Sciences of the United States of America **104**(3): 973-978.

Qiu, J., G. W. Lil, et al. (2007). "Truncated TERT mRNA transfected dendritic cells evoke TERT specific antitumor response in vivo." Hepatogastroenterology **54**(75): 681-687.

Rahbek, U. L., K. A. Howard, et al. (2008). "Intracellular siRNA and precursor miRNA trafficking using bioresponsive copolypeptides." Journal of Gene Medicine **10**(1): 81-93.

Raper, S. E., N. Chirmule, et al. (2003). "Fatal systemic inflammatory response syndrome in a ornithine transcarbamylase deficient patient following adenoviral gene transfer." Mol Genet Metab **80**(1-2): 148-158.

Ratajczak, M. Z., J. A. Kant, et al. (1992). "In vivo treatment of human leukemia in a scid mouse model with c-myb antisense oligodeoxynucleotides." Proc Natl Acad Sci U S A **89**(24): 11823-11827.

Rayburn, E. R. and R. Zhang (2008). "Antisense, RNAi, and gene silencing strategies for therapy: mission possible or impossible?" Drug Discov Today **13**(11-12): 513-521.

Read, M. L., K. H. Bremner, et al. (2003). "Vectors based on reducible polycations facilitate intracellular release of nucleic acids." Journal of Gene Medicine **5**(3): 232-245.

Read, M. L., K. H. Bremner, et al. (2003). "Vectors based on reducible polycations facilitate intracellular release of nucleic acids." J Gene Med **5**(3): 232-245.

Read, M. L., A. Logan, et al. (2005). "Barriers to gene delivery using synthetic vectors." Adv Genet **53**: 19-46.

Read, M. L., S. Singh, et al. (2005). "A versatile reducible polycation-based system for efficient delivery of a broad range of nucleic acids." Nucleic Acids Research **33**(9): e86.

Read, M. L., S. Singh, et al. (2005). "A versatile reducible polycation-based system for efficient delivery of a broad range of nucleic acids." Nucleic Acids Res **33**(9): e86.

Rejman, J., A. Bragonzi, et al. (2005). "Role of clathrin- and caveolae-mediated endocytosis in gene transfer mediated by lipo- and polyplexes." Mol Ther **12**(3): 468-474.

Rejman, J., G. Tavernier, et al. (2010). "mRNA transfection of cervical carcinoma and mesenchymal stem cells mediated by cationic carriers." J Control Release **147**(3): 385-391.

Rhodes, L. V., S. P. Short, et al. (2011). "Cytokine Receptor CXCR4 Mediates Estrogen-Independent Tumorigenesis, Metastasis, and Resistance to Endocrine Therapy in Human Breast Cancer." Cancer Research **71**(2): 603-613.

Ritter, W., C. Plank, et al. (2003). "A novel transfecting peptide comprising a tetrameric nuclear localization sequence." J Mol Med (Berl) **81**(11): 708-717.

Rizzuto, G., M. Cappelletti, et al. (1999). "Efficient and regulated erythropoietin production by naked DNA injection and muscle electroporation." Proc Natl Acad Sci U S A **96**(11): 6417-6422.

Roesler, E., R. Weiss, et al. (2009). "Immunize and disappear-safety-optimized mRNA vaccination with a panel of 29 allergens." J Allergy Clin Immunol **124**(5): 1070-1077 e1071-1011.

Rols, M. P., C. Delteil, et al. (1998). "In vivo electrically mediated protein and gene transfer in murine melanoma." Nat Biotechnol **16**(2): 168-171.

Rosenkilde, M. M., L.-O. Gerlach, et al. (2007). "Molecular Mechanism of Action of Monocyclam Versus Bicyclam Non-peptide Antagonists in the CXCR4 Chemokine Receptor." Journal of Biological Chemistry **282**(37): 27354-27365.

Roy, K., H. Q. Mao, et al. (1999). "Oral gene delivery with chitosan--DNA nanoparticles generates immunologic protection in a murine model of peanut allergy." Nat Med **5**(4): 387-391.

Rupp, U., E. Schoendorf-Holland, et al. (2007). "Safety and pharmacokinetics of bivatuzumab mertansine in patients with CD44v6-positive metastatic breast cancer: final results of a phase I study." Anticancer Drugs **18**(4): 477-485.

Ryser, H. J., E. M. Levy, et al. (1994). "Inhibition of human immunodeficiency virus infection by agents that interfere with thiol-disulfide interchange upon virus-receptor interaction." Proceedings of the National Academy of Sciences of the United States of America **91**(10): 4559-4563.

Saeboe-Larssen, S., E. Fossberg, et al. (2002). "mRNA-based electrotransfection of human dendritic cells and induction of cytotoxic T

lymphocyte responses against the telomerase catalytic subunit (hTERT)." J Immunol Methods **259**(1-2): 191-203.

Saito, G., G. L. Amidon, et al. (2003). "Enhanced cytosolic delivery of plasmid DNA by a sulfhydryl-activatable listeriolysin O/protamine conjugate utilizing cellular reducing potential." Gene Therapy **10**(1): 72-83.

Sanjoh, M., S. Hiki, et al. (2010). "pDNA/poly(L-lysine) Polyplexes Functionalized with a pH-Sensitive Charge-Conversional Poly(aspartamide) Derivative for Controlled Gene Delivery to Human Umbilical Vein Endothelial Cells." Macromol Rapid Commun **31**(13): 1181-1186.

Sauter, A., C. Kloft, et al. (2007). "Pharmacokinetics, immunogenicity and safety of bivatuzumab mertansine, a novel CD44v6-targeting immunoconjugate, in patients with squamous cell carcinoma of the head and neck." Int J Oncol **30**(4): 927-935.

Schafer, F. Q. and G. R. Buettner (2001). "Redox environment of the cell as viewed through the redox state of the glutathione disulfide/glutathione couple." Free Radic Biol Med **30**(11): 1191-1212.

Schaffert, D., C. Troiber, et al. (2011). "Solid-Phase Synthesis of Sequence-Defined T-, i-, and U-Shape Polymers for pDNA and siRNA Delivery." Angewandte Chemie, International Edition in English **50**(38): 8986-8989.

Shen, W. C., H. J. Ryser, et al. (1985). "Disulfide spacer between methotrexate and poly(D-lysine). A probe for exploring the reductive process in endocytosis." J Biol Chem **260**(20): 10905-10908.

Sheridan, C., H. Kishimoto, et al. (2006). "CD44(+)/CD24(-) breast cancer cells exhibit enhanced invasive properties: an early step necessary for metastasis." Breast Cancer Research **8**(5).

Signoret, N., J. Oldridge, et al. (1997). "Phorbol esters and SDF-1 induce rapid endocytosis and down modulation of the chemokine receptor CXCR4." J Cell Biol **139**(3): 651-664.

Skelton, T. P., C. X. Zeng, et al. (1998). "Glycosylation provides both stimulatory and inhibitory effects on cell surface and soluble CD44 binding to hyaluronan." Journal of Cell Biology **140**(2): 431-446.

Smith, C. V., D. P. Jones, et al. (1996). "Compartmentation of glutathione: implications for the study of toxicity and disease." Toxicol Appl Pharmacol **140**(1): 1-12.

Soboll, S., S. Grundel, et al. (1995). "The content of glutathione and glutathione S-transferases and the glutathione peroxidase activity in rat liver nuclei determined by a non-aqueous technique of cell fractionation." Biochem J **311 (Pt 3)**: 889-894.

Sonawane, N. D., F. C. Szoka, Jr., et al. (2003). "Chloride accumulation and swelling in endosomes enhances DNA transfer by polyamine-DNA polyplexes." J Biol Chem **278**(45): 44826-44831.

Soundara Manickam, D., H. S. Bisht, et al. (2005). "Influence of TAT-peptide polymerization on properties and transfection activity of TAT/DNA polyplexes." J Control Release **102**(1): 293-306.

Soundara Manickam, D. and D. Oupicky (2006). "Polyplex gene delivery modulated by redox potential gradients." J Drug Target **14**(8): 519-526.

Stoff-Khalili, M. A., P. Dall, et al. (2006). "Gene therapy for carcinoma of the breast." Cancer Gene Ther **13**(7): 633-647.

Sun, X., J. Kim, et al. (2004). "In vivo evaluation of copper-64-labeled monooxo-tetraazamacrocyclic ligands." Nucl Med Biol **31**(8): 1051-1059.

Sun, X., M. Wuest, et al. (2002). "Radiolabeling and in vivo behavior of copper-64-labeled cross-bridged cyclam ligands." J Med Chem **45**(2): 469-477.

Sun, X., H. W. Zhang, et al. (2009). "Growth inhibition of the pulmonary metastatic tumors by systemic delivery of the p27 kip1 gene using lyophilized lipid-polycation-DNA complexes." J Gene Med **11**(6): 535-544.

Sun, Y. X., X. Zeng, et al. (2008). "The influence of RGD addition on the gene transfer characteristics of disulfide-containing polyethyleneimine/DNA complexes." Biomaterials **29**(32): 4356-4365.

Surace, C., S. Arpicco, et al. (2009). "Lipoplexes targeting the CD44 hyaluronic acid receptor for efficient transfection of breast cancer cells." Mol Pharm **6**(4): 1062-1073.

Surace, C., S. Arpicco, et al. (2009). "Lipoplexes Targeting the CD44 Hyaluronic Acid Receptor for Efficient Transfection of Breast Cancer Cells." Molecular Pharmaceutics **6**(4): 1062-1073.

Taichman, R. S., C. Cooper, et al. (2002). "Use of the stromal cell-derived factor-1/CXCR4 pathway in prostate cancer metastasis to bone." Cancer Res **62**(6): 1832-1837.

Tavernier, G., O. Andries, et al. (2011). "mRNA as gene therapeutic: how to control protein expression." J Control Release **150**(3): 238-247.

Tijink, B. M., J. Buter, et al. (2006). "A phase I dose escalation study with anti-CD44v6 bivatuzumab mertansine in patients with incurable squamous cell carcinoma of the head and neck or esophagus." Clin Cancer Res **12**(20 Pt 1): 6064-6072.

Tokatlian, T. and T. Segura (2010). "siRNA applications in nanomedicine." Wiley Interdiscip Rev Nanomed Nanobiotechnol **2**(3): 305-315.

Tsutsumi, T., F. Hirayama, et al. (2007). "Evaluation of polyamidoamine dendrimer/alpha-cyclodextrin conjugate (generation 3, G3) as a novel carrier for small interfering RNA (siRNA)." J Control Release **119**(3): 349-359.

Urban-Klein, B., S. Werth, et al. (2005). "RNAi-mediated gene-targeting through systemic application of polyethylenimine (PEI)-complexed siRNA in vivo." Gene Ther **12**(5): 461-466.

Van Tendeloo, V. F., P. Ponsaerts, et al. (2001). "Highly efficient gene delivery by mRNA electroporation in human hematopoietic cells: superiority to lipofection and passive pulsing of mRNA and to electroporation of plasmid cDNA for tumor antigen loading of dendritic cells." Blood **98**(1): 49-56.

Vercauteren, D., M. Piest, et al. (2011). "Flotillin-dependent endocytosis and a phagocytosis-like mechanism for cellular internalization of disulfide-based poly(amido amine)/DNA polyplexes." Biomaterials **32**(11): 3072-3084.

Vercauteren, D., M. Piest, et al. (2011). "Flotillin-dependent endocytosis and a phagocytosis-like mechanism for cellular internalization of disulfide-based poly(amido amine)/DNA polyplexes." Biomaterials **32**(11): 3072-3084.

Vlahakis, S. R., A. Villasis-Keever, et al. (2002). "G protein-coupled chemokine receptors induce both survival and apoptotic signaling pathways." J Immunol **169**(10): 5546-5554.

Wahllander, A., S. Soboll, et al. (1979). "Hepatic mitochondrial and cytosolic glutathione content and the subcellular distribution of GSH-S-transferases." FEBS Lett **97**(1): 138-140.

Wallace, T. A., R. L. Prueitt, et al. (2008). "Tumor immunobiological differences in prostate cancer between African-American and European-American men." Cancer Res **68**(3): 927-936.

Wan, L., Y. You, et al. (2009). "DNA Release Dynamics from Bioreducible Poly(amido amine) Polyplexes." Journal of Physical Chemistry B **113**(42): 13735-13741.

Wang, D., Y. Liu, et al. (2005). "Michael addition polymerizations of trifunctional amines with diacrylamides." Polymer **46**(10): 3507-3514.

Wang, Y., S. Gao, et al. (2006). "Co-delivery of drugs and DNA from cationic core-shell nanoparticles self-assembled from a biodegradable copolymer." Nat Mater **5**(10): 791-796.

Wang, Y., L. S. Wang, et al. (2007). "Synthesis and characterization of cationic micelles self-assembled from a biodegradable copolymer for gene delivery." Biomacromolecules **8**(3): 1028-1037.

Weide, B., C. Garbe, et al. (2008). "Plasmid DNA- and messenger RNA-based anti-cancer vaccination." Immunol Lett **115**(1): 33-42.

Wheeler, C. J., P. L. Felgner, et al. (1996). "A novel cationic lipid greatly enhances plasmid DNA delivery and expression in mouse lung." Proc Natl Acad Sci U S A **93**(21): 11454-11459.

Won, Y. W., S. M. Yoon, et al. (2011). "Poly(oligo-D-arginine) with internal disulfide linkages as a cytoplasm-sensitive carrier for siRNA delivery." Mol Ther **19**(2): 372-380.

Wong, S. Y., N. Sood, et al. (2009). "Combinatorial evaluation of cations, pH-sensitive and hydrophobic moieties for polymeric vector design." Mol Ther **17**(3): 480-490.

Wu, K., J. Liu, et al. (2010). "Drug-Free Macromolecular Therapeutics: Induction of Apoptosis by Coiled-Coil-Mediated Cross-Linking of Antigens on the Cell Surface." Angewandte Chemie International Edition **49**(8): 1451-1455.

Wu, X., N. H. Bishopric, et al. (1996). "Physical and functional sensitivity of zinc finger transcription factors to redox change." Mol Cell Biol **16**(3): 1035-1046.

Xiang, Y. Z., Z. H. Feng, et al. (2010). "Linear cyclen-based polyamine as a novel and efficient reagent in gene delivery." Organic & Biomolecular Chemistry **8**(3): 640-647.

Xu, Z., Z. Zhang, et al. (2010). "The characteristics and performance of a multifunctional nanoassembly system for the co-delivery of docetaxel and

iSur-pDNA in a mouse hepatocellular carcinoma model." Biomaterials **31**(5): 916-922.

Yamamoto, M. and D. T. Curiel (2005). "Cancer gene therapy." Technol Cancer Res Treat **4**(4): 315-330.

Yockman, J. W., A. Kastenmeier, et al. (2008). "Novel polymer carriers and gene constructs for treatment of myocardial ischemia and infarction." J Control Release **132**(3): 260-266.

Yockman, J. W., A. Maheshwari, et al. (2003). "Tumor regression by repeated intratumoral delivery of water soluble lipopolymers/p2CMVmIL-12 complexes." J Control Release **87**(1-3): 177-186.

Yoon, Y., Z. Liang, et al. (2007). "CXC Chemokine Receptor-4 Antagonist Blocks Both Growth of Primary Tumor and Metastasis of Head and Neck Cancer in Xenograft Mouse Models." Cancer Research **67**(15): 7518-7524.

You, Y. Z., D. S. Manickam, et al. (2007). "Reducible poly(2-dimethylaminoethyl methacrylate): synthesis, cytotoxicity, and gene delivery activity." Journal of Controlled Release **122**(3): 217-225.

You, Y. Z., D. S. Manickam, et al. (2007). "A versatile approach to reducible vinyl polymers via oxidation of telechelic polymers prepared by reversible addition fragmentation chain transfer polymerization." Biomacromolecules **8**(6): 2038-2044.

Yu, H., L. A. Babiuk, et al. (2007). "Immunity and protection by adoptive transfer of dendritic cells transfected with hepatitis C NS3/4A mRNA." Vaccine **25**(10): 1701-1711.

Zhang, H., A. Mitin, et al. (2009). "Efficient transfection of blood-brain barrier endothelial cells by lipoplexes and polyplexes in the presence of nuclear targeting NLS-PEG-acridine conjugates." Bioconjug Chem **20**(1): 120-128.

Zheng, M., Z. Zhong, et al. (2012). "Poly(ethylene oxide) Grafted with Short Polyethylenimine Gives DNA Polyplexes with Superior Colloidal Stability, Low Cytotoxicity and Potent In Vitro Gene Transfection Under Serum Conditions." Biomacromolecules.

Zhou, B., C. T. McGary, et al. (2003). "Purification and molecular identification of the human hyaluronan receptor for endocytosis." Glycobiology **13**(5): 339-349.

Zhou, Q. H., C. Wu, et al. (2009). "Evaluation of Pharmacokinetics of Bioreducible Gene Delivery Vectors by Real-time PCR." Pharm Res.

Zidovska, A., H. M. Evans, et al. (2009). "The role of cholesterol and structurally related molecules in enhancing transfection of cationic liposome-DNA complexes." J Phys Chem B **113**(15): 5208-5216.

Zou, S. M., P. Erbacher, et al. (2000). "Systemic linear polyethylenimine (L-PEI)-mediated gene delivery in the mouse." J Gene Med **2**(2): 128-134.

Zrazhevskiy, P., M. Sena, et al. (2010). "Designing multifunctional quantum dots for bioimaging, detection, and drug delivery." Chem Soc Rev **39**(11): 4326-4354.

ABSTRACT

MULTIFUNCTIONAL BIOREDUCIBLE NANOPARTICLES FOR GENE THERAPY

by

JING LI

December 2012

Advisor: Dr. David Oupický

Major: Pharmaceutical Sciences

Degree: Doctor of Philosophy

Gene therapy is a promising therapeutic strategy to treat diseases caused by single or multiple gene mutations. Non-viral gene delivery vectors exhibit many advantages over viral vectors, including enhanced safety, versatility in choosing different types of therapeutic nucleic acids, and ease of formulation. However, low transgene efficiency and lack of targeting ability remain major challenges. Bioreducible polyplexes (polyelectrolyte complexes of disulfide-containing polycations and nucleic acids) utilize the redox potential gradient existing between extracellular space and intracellular environment as a physiological stimulus to enhance delivery of therapeutic nucleic acids to the subcellular space. Bioreducible containing polyplexes undergo intracellular reduction mediated GSH, which results in fast disassembly of the polyplexes and degradation of the delivery vector, leading to increased transfection efficiency and decreased cytotoxicity.

In this dissertation, we first evaluated the effect of enhanced reductive disassembly on transfection activity of plasmid DNA and antisense oligonucleotide (AON) polyplexes using on a series of synthesized bioreducible poly(amido amine)s (PAA). We found that increasing the disulfide content in PAA increased susceptibility to reduction-triggered DNA and AON release from the polyplexes. However, increasing disulfide content in PAA resulted in increased DNA transfection only and had no effect on AON transfection. We discovered that plasma membrane protein thiols played a key role in the observed enhancement of DNA transfection.

We then explored the possibility of introducing targeting moiety (hyaluronic acid, HA) into the design and formulation of the bioreducible polyplexes to stability polyplexes and to achieve selective delivery to CD44 expressing cancers. Three different approaches to incorporate low- and medium-molecular-weight HA into the structure of bioreducible DNA polyplexes have been explored with the goal of improving steric stability and achieving CD44-selective uptake and transfection. Our results show that higher molecular weight HA is required for steric stabilization of the polyplexes while lower molecular weight HA was beneficial for targeted transfection activity. Further studies and development are needed to combine steric stabilization with efficient, CD44-selective transfection into a single formulation.

Our next goal was to develop multifunctional bioreducible polyplexes for combination gene therapy in a single formulation. We have developed a series of bioreducible polycationic copper chelators (RPC) based on 1,4,8,11-

tetraazacyclotetradecane (cyclam). We confirmed that the cyclam moieties in the polycations retained their ability to form complexes with Cu(II). The presence of disulfide bonds in the polycations resulted in substantially lower cytotoxicity than control 25 KDa PEI and both the Cu(II)-free and Cu(II) complexed polymers exhibited high transfection efficiency in vitro. This novel type of polycationic Cu(II) chelates represent promising nucleic acid delivery vectors with potential for PET imaging using 64Cu radioisotope. We further designed and developed a cyclam-based dual-function bioreducible polycations that function simultaneously as gene delivery vectors and as CXCR4 antagonists. We found that these dual-function polycations with their own pharmacological activity are able to prevent cancer cell invasion by inhibiting CXCL12 stimulated CXCR4 activation, while at the same time efficiently and safely delivers plasmid DNA into cancer cells.

AUTOBIOGRAPHICAL STATEMENT

Education

2003-2007 B. Eng. Pharmaceutical Engineering; Southeast University, Nanjing, China

2007-pres. Ph.D. Pharmaceutical Sciences; Wayne State University, Detroit, MI

Publications

1. D. S. Manickam, J. Li, D. A. Putt, Q. H. Zhou, C. Wu, L. H. Lash, D. Oupicky. Effect of innate glutathione levels on activity of redox-responsive gene delivery vectors. ***J. Controlled Rel.***, 2010, 141(1), 77-84.
2. Y. Dong, J. Li, C. Wu, D. Oupicky. Bisethylnorspermine lipopolyamine as potential delivery vector for combination drug/gene anticancer therapies. ***Pharm. Res.***, 2010, 27(9) 1927-38.
3. J. Li, D. S. Manickam, J. Chen, D. Oupicky. Effect of cell membrane thiols and reduction-triggered disassembly on transfection activity of bioreducible polyplexes. ***Eur. J. Pharm. Sci.***, 2012, 46(3), 173-180.
4. Y. Dong, Y. Zhu, J. Li, Q. Zhou, C. Wu, D. Oupicky. Synthesis of bisethylnorspermine lipid prodrug as gene delivery vector targeting polyamine metabolism in breast cancer. ***Mol. Pharm.***, 2012, 9(6), 1654-64.
5. Y. Zhu, J. Li, D. Oupický. Intracellular Delivery Considerations for RNAi Therapeutics. In RNA Interference from Biology to Therapeutics, K. A. Howard, Ed., Springer, New York, 2012 (in press).
6. J. Li, Y. Zhu, S. Hazeldine, C. Li, D. Oupicky. Dual-function CXCR4 Antagonist Polyplexes to Deliver Gene Therapy and Inhibit Cancer Cell Invasion. ***Angew. Chem., Int. Ed.***, 2012, (in press).
7. J. Li, Y. Zhu, S. Hazeldine, D. Oupicky. Cyclam-based Polymeric Copper Chelators for Gene Delivery and Potential PET Imaging. (submitted to ***Biomacromolecules*** in June, 2012)

Invention disclosures/patents

1. "Cyclam-based polymeric CXCR4 antagonists for delivery of therapeutic Nucleic Acids", D. Oupicky and J. Li (co-inventors), filed 10/14/2011, PCT application under preparation

Awards

2009 Thomas C. Rumble University Graduate Fellowship, Wayne State University

2010 Frank O. Taylor Pharmaceutical Sciences Scholarship, Wayne State University

2012 Second Place in Podium Presentations at 44th Pharmaceutics Graduate Student Research Meeting, Omaha, NE